Reduction of ICI Effect in MIMO-OFDM System Using Self-Cancellation with Convolution Coding and Space Frequency Block Code

by

Saifur Rahman Sabuj

Institute of Information and Communication Technology

BANGLADESH UNIVERSITY OF ENGINEERING AND TECHNOLOGY

January 2011

REFERENCES

[1] A short history of mobile generation: http://www.techpages.org/2010/03/1g-first-generation-of-mobile.html last access on 1st October 2010.

[2] Steer, M., "Beyond 3G," IEEE microwave magazine, pp. 76-82, 2007.

[3] A short history of GSM and total user: http://www.gsmworld.com last access on 1st October 2010.

[4] A short history of CDMA and total user: http://www.cdg.org last access on 1st October 2010.

[5] Ibrahim, J., "4G Features," Bechtel Telecommunications Technical Journal, vol. 1, no. 1, pp. 11-14, 2002.

[6] Cimini, L. J. and Jr., "Analysis and simulation of a digital mobile channel using orthogonal frequency division multiplexing," IEEE Trans. on Communications, vol. 33, pp. 665-675, 1985.

[7] Li, Y., Cimini, L. J. and Jr., "Bounds on the interchannel interference of OFDM in time-varying Impairments," IEEE Trans. on communications, vol. 49, no. 3, pp. 401-404, 2001.

[8] Sinha, N. B., Bera, R. and Mitra, M., "Capacity and V-BLAST techniques for MIMO wireless channel," Journal of Theoretical and Applied Information Technology, vol. 14, no. 1, 2010.

[9] Russell, M. and Stuber, G., "Interchannel interference analysis of OFDM in a mobile environment," IEEE Vehicular Technology Conf., pp. 820 – 824, 1995.

[10] Armstrong, J., Grant, P. M. and Povey, G., "Polynomial cancellation coding of OFDM to reduce intercarrier interference due to Doppler spread," IEEE Global Telecommunications Conference, vol. 5, pp. 2771- 2776, 1998.

[11] Zhao, Y. and Haggman, S. G., “Intercarrier interference self-cancellation scheme for OFDM mobile communication systems,” IEEE Trans. Commu., vol. 49, no. 7, pp. 1185-1191, 2001.

[12] Chen, B., “Maximum likelihood estimation of OFDM carrier frequency offset,” IEEE Signal Processing Letters, vol. 9, no. 4, pp. 123-126, 2002.

[13] Chizhik, Ling, D., J., Wolniansky, P.W., Valensuela, R. A., Costa, N. and Huber, K., “Multiple-input multiple-output measurements and modeling in Manhattan,” IEEE Journal on Selected Areas on Communications, vol. 21, no. 3, pp. 321-331, 2003.

[14] Tan, P. and Beaulieu, N.C, “A novel pulse-shaping for reduced ICI in OFDM systems,” IEEE Vehicular Technology Conference, vol. 1, pp 456-459, 2004.

[15] Ling, Chizhik, D., J., Samardzija, D. and Valenzuela, R. A., “Spatial and polarization characterization of MIMO channels in rural environment,” IEEE 61st Vehicular Technology Conference 2005, vol. 1, pp. 161-164, 2005.

[16] Ryu, H.- G., Li, Y. and Park, J.-S., “An Improved ICI reduction method in OFDM communication system,” IEEE Trans. Broadcasting, vol. 51, no. 7, pp 395-400, 2005.

[17] Li, Y.-S., Ryu, H.-G., Li, J.-W., Sun, D.-Y., Liu, H.-Y., Zhou, L. -J. and Wu, Y.,“ ICI compensation in MISO-OFDM system affected by frequency offset and phase noise,” Wireless Commun., Networking and Mobile Computing (WiCOM '08), pp. 1-5, 2008.

[18] Yusof, S. K. S. and Zamani, A. I. A, “Intercarrier interference self-cancellation for space time-frequency MIMO-OFDM system,” IEEE international RF and Microwave conference, pp 520-523, 2008.

[19] Idris, A., Dimyati, K. and Yusof, S.K.S., “Interference self-cancellation schemes for space time frequency block codes MIMO-OFDM system,” International Journal of Computer Science and Network, vol. 8 no. 9, pp. 139-148, 2008.

[20] Rappaport, T. S., “Wireless communications principles and practice”, Prentice Hall, 2nd Edition, 2002.

[21] Lee, W. C. Y., “Mobile cellular telecommunication systems”, McGraw Hill Publications, 1989.

[22] Steele, R. (ed.), “Mobile radio communication”, IEEE Press, 1992.

[23] Akram, M. S., *Pilot-based Channel Estimation in OFDM Systems*, M. Sc Thesis, Nokia and Informatics and Mathematical Modeling (IMM) at the Technical University of Denmark (DTU), 2007.

[24] A short history of channel transfer function: http://cnx.org/ content/ m15529/ latest/ last access on 1st October 2010.

[25] Zhang, Y., Cosmas, J. and Song, Y., “Future transmitter/receiver diversity schemes in broadcast wireless networks” IEEE Communications Magazine, pp. 120-127, 2006.

[26] Chang, R. W., “Synthesis of band-limited orthogonal signals for multichannel data,” Bell System Technical Journal, pp. 1775-1797, 1996.

[27] Saltzburg, B. R., “Performance of an efficient parallel data transmission systems,” IEEE Trans. on Comm. Tech., pp. 805-811, 1967.

[28] Bahai, A. R. S., Saltzberg, B. R and Ergen, M., “Multicarrier digital communications theory and applications of OFDM”, 2nd Edition, Springer Science, Boston, USA, 2004.

[29] Bingham, J. A. C., “Multicarrier modulation for data Transmission, an idea whose time has come”, IEEE Communications Magazine, vol. 28, no. 5, pp. 5-14, 1990.

[30] Husein, A. A. A., *Orthogonal frequency division multiplexing (OFDM)*, M. Sc Thesis, College of Mathematical Sciences & Information Technology, AHLIA University, 2009.

[31] A short description of convolution coding: http://home.netcom.com/ ~chip.f/viterbi/ algrthms.html last access on 1st October 2010.

[32] A short description of viterbi coding: http://home.netcom.com/~chip.f/viterbi/ algrthms2.html last access on 1st October 2010.

[33] Bolcskei, H. and Paulraj, A. J., “Space-frequency coded broadband OFDM systems,” IEEE Wireless Commun. and Netw. Conf. (WCNC), vol. 1, pp. 1-6, 2000.

[34] Tarokh, V., Seshadri, N. and Calderbank, A. R., “Space-time codes for high data rate wireless communications: performance criterion and code construction,” IEEE Trans. Inf. Theory, vol. 44, no. 2, pp. 744-765, 1998.

[35] Alamouti, S. M., “A simple transmit diversity technique for wireless communications,” IEEE Journal on Selected Areas in Communication, vol. 16, pp. 1451-1458, 1998.

[36] Fazel, K., and Kaiser, S., “Multi-carrier and spread spectrum systems: from OFDM and MC-CDMA to LTE and WiMAX”, 2nd Edition, John Wiley & Sons Ltd, UK, 2008.

[37] Brahmaji, T. A. R. K., *An efficient ICI Cancellation Technique for OFDM Communication Systems,* M. Sc Thesis, Department of Electrical Engineering, National Institute of Technology, Rourkela, 2009.

[38] Proakis, J. G., “Digital communications”, New York: McGraw-Hill, 1989.

[39] Shannon, C. E., “A mathematical theory of communication,” Bell System Technical Journal, vol. 27, pp. 379-423, 623-656, 1948.

[40] Foschini, C. E., “Layered space-time architecture for wireless communication in a fading environment when using multi-element antennas,” Bell Labs Tech Jour., vol. 1, no. 2, pp. 41-59, 1996.

[41] Foschini, G. J. and Gans, M. J., “On limits of wireless communications in a fading environment when using multiple antennas,” Journal of wireless personal communications, vol. 6, no. 3, pp. 311-335, 1998.

[42] Sinha, N. B., Bera, R. and Mitra, M., “Capacity and V-BLAST techniques for MIMO wireless channel” Journal of Theoretical and Applied Information Technology, vol. 14, no. 1, 2010.

[43] Saunders, S. R., “Antennas and propagation for wireless communication systems”, Wiley India Pvt. Ltd., 2nd edition, 2008.

[44] Tarkiainen, M. and Westman, T., “Predictive switched diversity for slow speed mobile terminals,” IEEE Vehicular Technology Conference, vol. 3, pp. 2042-2044, 1997.

[45] Lizhong, Z. T. D. N. C, “Diversity and multiplexing: a fundamental tradeoff in multiple-antenna channels,” IEEE Trans. on Info. Theory, vol. 49, no. 5, pp. 1073-1096, 2003.

[46] Tse, D. and Viswanath, P., “Fundamentals of wireless communication”, Cambridge University Press, 2005.

[47] Ahn, J. and Lee, H. S., “Frequency domain equalization of OFDM signal over frequency nonselective rayleigh fading channels,” Elect. Lett., vol. 29, no. 16, pp. 1476–1477, 1993.

[48] Muschallik, C., “Improving an OFDM reception using an adaptive nyquist windowing”, IEEE Trans. Consumer Electron., vol. 42, no. 3, pp. 259-269, 1996.

[49] Tan, P. and Beaulieu, N. C., “A novel pulse-shaping for reduced ICI in OFDM systems,” IEEE Vehicular Technology Conference, vol. 1, pp 456-459, 2004.

[50] Chen, B., “Maximum likelihood estimation of OFDM carrier frequency offset,” IEEE Signal Processing Letters, vol. 9, no. 4, pp. 123-126, 2002.

[51] Liang, Y., Luo, H., Xu, Y. and Huang, J., “Channel estimation based on extended Kalman filtering for MIMO-OFDM systems,”, Wireless Communications, Networking and Mobile Computing (WiCOM), pp. 1-4, 2006.

[52] Dwivedi, V. K. and Singh, G. “An efficient BER analysis of OFDM systems with ICI conjugate cancellation method,” PIERS Proceedings, Cambridge, USA, 2008.

Reduction of ICI Effect in MIMO-OFDM System Using Self-Cancellation with Convolution Coding and Space Frequency Block Code

by

Saifur Rahman Sabuj

MASTER OF SCIENCE IN INFORMATION AND COMMUNICATION TECHNOLOGY

Institute of Information and Communication Technology

BANGLADESH UNIVERSITY OF ENGINEERING AND TECHNOLOGY

January, 2011

The thesis titled **"Reduction of ICI Effect in MIMO-OFDM System Using Self-Cancellation with Convolution Coding and Space Frequency Block Code"** submitted by Saifur Rahman Sabuj, Roll no: M04083121P, session April 2008 has been accepted as satisfactory in partial fulfillment of the requirement for the degree of Master of Science in Information and Communication Technology on 29 January, 2011.

BOARD OF EXAMINERS

1.	Dr. Md. Saiful Islam Associate Professor Institute of Information and Communication Technology BUET, Dhaka- 1000	Chairman (Supervisor)
2.	Dr. S. M. Lutful Kabir Professor and Director Institute of Information and Communication Technology BUET, Dhaka- 1000	Member (Ex-officio)
3.	Dr. Md. Liakot Ali Associate Professor Institute of Information and Communication Technology BUET, Dhaka- 1000	Member
4.	Dr. Md. Mofazzal Hossain Associate Professor Chairperson Department of Electronics and Communications Engineering East West University (EWU) 43 Mohakhali C/A, Dhaka - 1212	Member (External)

CANDIDATE'S DECLARATION

It is hereby declared that this thesis or any part of it has not been submitted elsewhere for the award of any degree or diploma.

_____

Saifur Rahman Sabuj

DEDICATED TO MY PARENTS

CONTENTS

Title page	i
Board of Examiners	ii
Candidate's Declaration	iii
Dedication	iv
Table of Contents	v
List of Figures	ix
List of Tables	xii
List of Abbreviations	xiii
List of Symbols	xv
Acknowledgement	xvi
Abstract	xvii
1 Introduction	1-9
1.1 Introduction to Wireless Networks	1
1.2 Review of Previous Works and Observation	4
1.3 Motivation	8
1.4 Objective of the Thesis	8
1.5 Organization of the Thesis	9
2 Fundamentals of Wireless Communication, OFDM and MIMO	10-51
2.1 Propagation Characteristics of Wireless Channel	10
2.1.1 Multipath effects	11
2.1.2 Fading parameters	11
2.1.2.1 Delay spread	12

2.1.2.2 Coherence bandwidth 13
2.1.2.3 Doppler shift 13
2.1.2.4 Doppler spread 14
2.1.2.5 Coherence time 14
2.1.3 Types of small-scale fading 15
2.1.3.1 Fading effects due to multipath time delay spread 16
2.1.3.1.1 Flat fading 16
2.1.3.1.2 Frequency selective fading 18
2.1.3.2 Fading effects due to doppler spread 18
2.1.3.2.1 Fast fading 18
2.1.3.2.1 Slow fading 18
2.1.4 Rayleigh fading distribution 19
2.1.5 Rician fading distributions 19
2.2 Orthogonal Frequency Division Multiplexing (OFDM) 20
2.2.1 Evolution of OFDM 21
2.2.1.1 Frequency division multiplexing (FDM) 21
2.2.1.2 Multicarrier communication (MC) 21
2.2.2 Orthogonality 22
2.2.3 OFDM generation and reception 24
2.2.4 Modulation 25
2.2.4.1 Binary phase shift keying (BPSK) 25
2.2.4.2 Quadrature phase shift keying (QPSK) 25
2.2.5 Serial to parallel conversion 26
2.2.6 FFT and IFFT implementation 27
2.2.7 Channel coding 28
2.2.7.1 Convolution coding 28
2.2.7.1.1 Convolution encoder (rate ½, K=3) 28

2.2.7.1.2 Viterbi decoding 31
2.2.7.2 Space frequency block code (SFBC) 34
2.2.8 RF modulation 35
2.2.9 Inter symbol interference and inter carrier interference 35
2.2.10 Guard period and cyclic prefix 36
2.2.11 Additive white gaussian noise (AWGN) channel 37
2.2.12 Advantages of OFDM 38
2.2.13 Disadvantages of OFDM 41
2.3 Multiple Input Multiple Output (MIMO) 41
2.3.1 Four basic system models 41
2.3.2 Channel capacity 42
2.3.2.1 Capacity of SISO system 42
2.3.2.2 Capacity of SIMO system 44
2.3.2.3 Capacity of MISO system 45
2.3.2.4 Capacity of MIMO system 45
2.3.3 Spatial multiplexing 47
2.3.4 Antenna diversity combining techniques 47
2.3.4.1 Switched combining 48
2.3.4.2 Selection combining 48
2.3.4.3 Equal gain combining 49
2.3.4.4 Maximum ratio combining 50
2.3.5 Performance improvements in MIMO system 50

3 Data Conjugate and Channel Coding with Self-Cancellation 52-67
3.1 Self-Cancellation Scheme in MIMO-OFDM 52
3.2 Methods of ICI Reduction 52
3.3 System Model in 2x2 MIMO-OFDM 52

3.3.1 Original 2x2 MIMO-OFDM 55

3.3.2 Self-cancellation data conjugate (SCDC) in 2x2 MIMO-OFDM 58

3.3.3 Convolution coding in SCDC of 2x2 MIMO-OFDM 62

3.3.4 Space frequency block code (SFBC) in 2x2 MIMO-OFDM 62

4 Results and Discussion 68-81

4.1 Real and Imaginary Parts of ICI Coefficients 68

4.2 ICI Cancellation during Modulation and Demodulation 70

4.3 Effect of Frequency Offset/Phase Noise on ICI 72

4.4 Effect of Frequency Offset/Phase Noise on CIR 73

4.5 BER Performance of BPSK MIMO-OFDM System 75

4.6 BER Performance of QPSK MIMO-OFDM System 77

4.7 Comparison of BER Performance of QPSK, BPSK MIMO-OFDM System 78

4.8 Effect of Convolution Coding on MIMO-OFDM System 79

4.9 Comparison of CIR and E_b/N_0 with Published Results 81

5 Conclusion and Future Work 82-84

5.1 Conclusion 82

5.2 Future Work 83

Appendix Derivation of ICI coefficient 85

References 86-90

LIST OF FIGURES

Figure No.	Figure Name	Page No.
Fig. 2.1:	Radio propagation effects	10
Fig. 2.2:	Effect of multipath on a mobile station	11
Fig. 2.3:	Multipath delay spread	12
Fig. 2.4:	Illustration of Doppler effect	13
Fig. 2.5:	Relationship between the channel correlation and power density function	15
Fig. 2.6:	Types of small-scale fading	16
Fig. 2.7:	Relationships between the coherence bandwidth and signal bandwidth B_s	17
Fig. 2.8:	Fading illustration of small scale fading	19
Fig. 2.9:	Carrier signals in OFDM transmission	22
Fig. 2.10:	Frequency spectrum of OFDM transmission	23
Fig. 2.11:	Block diagram of OFDM system model (a) Transmitter (b) Receiver	24
Fig. 2.12:	BPSK bit-pattern	25
Fig. 2.13:	QPSK bit-pattern	26
Fig. 2.14:	Serial to parallel conversion	27
Fig. 2.15:	Convolution encoder (rate ½, K=3)	29
Fig. 2.16:	A message sequence with rate ½, K=3 as it goes through the encoder	30
Fig. 2.17:	Viterbi decoder decoded message bit	33
Fig. 2.18:	RF modulation of OFDM signals using analog technique	35
Fig. 2.19:	ICI effect	36
Fig. 2.20:	Guard period insertion in OFDM	37

Fig. 2.21:	Spectrum Efficiency of OFDM Compared to FDM	38
Fig. 2.22:	(a) The signal and the channel frequency response (b) A fading channel frequency response	39
Fig. 2.23:	Immunity of OFDM to frequency selective fading channel	40
Fig. 2.24:	Four basics model	42
Fig. 2.25:	Capacity of SISO System	42
Fig. 2.26:	Shanons capacity for SISO system	43
Fig. 2.27:	Capacity of SIMO system	44
Fig. 2.28:	Capacity of MISO System	45
Fig. 2.29:	Capacity of MIMO System	45
Fig. 2.30:	Channel capacity MIMO system	46
Fig. 2.31:	Switched combining for N_R antenna elements with only one receiver	48
Fig. 2.32:	Block diagram of selection combining for N_R antenna elements	49
Fig. 2.33:	Block diagram of equal gain combining for N_R antenna elements	49
Fig. 2.34:	Block diagram of maximum ratio combining for N_R antenna elements	50
Fig. 3.1:	Block diagram of SCDC method in 2x2 MIMO-OFDM system model (a) Transmitter (b) Receiver	53
Fig. 4.1:	(a) Plots of Real part of Q_{l-k}^{τ}	68
Fig. 4.1:	(b) Plots of Imaginary part of Q_{l-k}^{τ}	69
Fig. 4.1:	(c) Plots of Amplitude of Q_{l-k}^{τ}	69
Fig. 4.2:	Plots of ICI without SC and with SC in OFDM using DC	70
Fig. 4.3:	Plots of ICI without SC and with SC in 2x2 MIMO-OFDM without DC	70
Fig. 4.4:	Plots of ICI without SC and with SC in 2x2 MIMO-OFDM using DC	71
Fig. 4.5:	Plots of ICI without SC and with SC in 2x2 MIMO-OFDM using SFBC	71
Fig. 4.6:	Plots of ICI vs. normalized frequency offset	72

Fig. 4.7:	Plots of ICI vs. phase noise variance	73
Fig. 4.8:	Plots of CIR vs. normalized frequency offset	74
Fig. 4.9:	Plots of CIR vs. phase noise variance	74
Fig. 4.10:	Plots of bit error rate vs. E_b/N_0 at $\varepsilon = 0.1$	75
Fig. 4.11:	Plots of bit error rate vs. E_b/N_0 at $\varepsilon = 0.1$ or 0.2	76
Fig. 4.12:	Plots of bit error rate vs. E_b/N_0 at $\varepsilon = 0.1$	77
Fig. 4.13:	Plots of bit error rate vs. E_b/N_0 at $\varepsilon = 0.1$ or 0.2	78
Fig. 4.14:	Plots of bit error rate vs. E_b/N_0 at $\varepsilon = 0.1$	79
Fig. 4.15:	Plots of bit error rate vs. E_b/N_0 at $\varepsilon = 0.1$ using BPSK	80
Fig. 4.16:	Plots of bit error rate vs. E_b/N_0 at $\varepsilon = 0.1$ using QPSK	80
Fig. 4.17:	Plots of bit error rate vs. E_b/N_0 at $\varepsilon = 0.1$	81

LIST OF TABLES

Table 1.1:	Short history of wireless communications evolution	3
Table 2.1:	Mapping with SFBC and two transmit antennas	34
Table 4.1:	BER of different normalized frequency offset for E_b/N_0 = 15dB	76
Table 4.2:	BER of BPSK and QPSK at $\varepsilon = 0.1$ for E_b/N_0 = 15dB	78
Table 4.3:	Comparison of CIR and E_b/N_0 with published results	81

LIST OF ABBREVIATIONS

1G	First Generation
2G	Second Generation
3G	Third Generation
4G	Fourth Generation
ADC	Analog-to-Digital Converter
AMPS	Advanced Mobile Phone Service
AWGN	Additive White Gaussian Noise
BER	Bit Error Rate
BPSK	Binary phase shift keying
CC	Convolution coding
CDMA	Code Division Multiple Access
CPE	Common Phase Error
CIR	Carrier to Interference Ratio
DAC	Digital-to-Analog Converter
DAMPS	Digital Advanced Mobile Phone Service
EDGE	Enhanced Data Rate for GSM Evolution
FDMA	Frequency Division Multiple Access
FEC	Forward Error Correction
FFT	Fast Fourier Transform
GPRS	General Packet Radio Service
GSM	Global System for Mobile communications
HSCSD	High Speed Circuit Switched Data
ICI	Inter-Carrier Interference
IFFT	Inverse Fast Fourier Transform

ISI	Inter-symbol Interference
LOS	Line-of-Sight
MIMO	Multiple Input Multiple Output
MISO	Multiple input single output
MC	Multicarrier communication
MLE	Maximum Likelihood Estimator
NLOS	Nonline-of-Sight
NMT	Nordic Mobile Telephone
OFDM	Orthogonal Frequency Division Multiplexing
PCC	Polynomial Cancellation Coding
QoS	Quality of Service
QPSK	Quadrature Phase Shift Keying
SC	Self-Cancellation
SCDC	Self-Cancellation Data Conjugate
SFBC	Space Frequency Block Code
SIMO	Single Input Multiple Output
SISO	Single Input Single Output
SNR	Signal-to-Noise Ratio
TACS	Total Access Communications System

LIST OF SYMBOLS

B_C	Coherence bandwidth
σ_τ	Root mean square delay spread
f_m	Maximum value of doppler frequency
f_D	Doppler shift
T_C	Coherence time
B_S	Transmitted signal bandwidth
T_S	Symbol period
B_D	Doppler spread
σ^2	Average power of the received signal
C	Shannon limit on channel capacity
N	Total number of subcarriers
Δf^τ	Frequency offset
$\varphi^\tau(n)$	Phase noise
N_k	Complex additive white gaussian noise
Q_L^τ	ICI coefficient
σ_{DRS}^2	Desired received signal power
σ_{ICI}^2	ICI power
$E[\cdot]$	Expected value
$Q(\sqrt{\cdot})$	Q-function
ε_τ	Normalized frequency offset
E_b	Energy per bit
N_0	Spectral density coefficient

ACKNOWLEDGEMENTS

First of all, I would like to thank Almighty Allah for his mercy and charity. This thesis is the most significant accomplishment in my life and would have been impossible without the will and wish of the almighty and I am grateful to him.

Most of all, I would like to express my deepest gratitude to my supervisor, Dr. Md. Saiful Islam, Associate Professor, Institute of Information and Communication Technology (IICT), Bangladesh University of Engineering and Technology (BUET), for introducing me in the arena of wireless communication and for his continuous inspiration, guidance and invaluable support during this research work. Next, I would like to thank all the teachers and staffs of the IICT, BUET for their cordial help and assistance during my study period.

Finally, I would like to thank my parents for their continuous support, encouragement and sacrifice throughout the years and I will be obliged to them forever for all they have done.

ABSTRACT

New generation wireless communication systems require high data rate transmission in order to fulfill the requirements for on demand multimedia communication such as- audio, video, image and data. Orthogonal frequency division multiplexing (OFDM) is a multicarrier modulation technique for high data rate transmission of signals over wireless channel. OFDM converts a frequency selective fading channel into a collection of parallel flat fading sub channels but sensitive to frequency offset and phase noise. The carrier frequency offset and phase noise cause loss of orthogonality among subcarriers resulting to inter carrier interference (ICI). Antenna diversity and channel coding in OFDM system reduces the effect of ICI and improves the performance of the conventional system significantly. In this thesis work, analytical models have been developed to suppress ICI with the concept of self-cancellation data conjugate (SCDC) along with convolution coding and space frequency block code (SFBC) for 2x2 multiple input and multiple output (MIMO) OFDM system. Detailed mathematical derivation is carried out for common phase error, ICI, carrier to interference ratio (CIR) and bit error rate (BER) for both SCDC with convolution coding and SFBC. The performance of the proposed systems is evaluated through numerical simulation by varying different system parameters. Results show that while SFBC is used in the proposed system, CIR is increased about 4 dB and 24 dB in SCDC MIMO and conventional OFDM system respectively. The BER performances of SCDC with convolution coding and SFBC have improved about 3 dB and 1.2 dB respectively (at BER of 10^{-8}) in 2x2 MIMO-OFDM system than that of 2x1 multiple input single output OFDM system. Thus, it is observed both coding schemes suppress the ICI effect considerably but SCDC with convolution coding is more effective than SFBC method in 2x2 MIMO-OFDM system.

CHAPTER 1

INTRODUCTION

1.1 Introduction to Wireless Networks

Wireless communication is an emerging field, which has seen enormous growth around the world in the last several years and this enlargement is likely to continue. Wireless systems are ahead popularity because of their ease of use and mobility. Initially, wireless systems were mainly designed and developed to support voice. The next generation wireless systems have to be designed considering the need for higher data rate with quality of service (QoS) and multimedia services.

Wireless communications systems that have been deployed for a short time are the first generation, second generation and third generation. Fourth generation system is also currently under deployment, but continue to go forward. Each generation of mobile communications has been based on a dominant technology, which has significantly improved spectrum capacity. The key to the success of all new technological developments is standardization. This demand for higher capacity networks has led to the development of next generation telecommunications systems.

Most first generations (1G) systems were introduced in the mid 1980's. The cellular system was an analog transmission technique and the use of simple multiple access techniques such as frequency division multiple access (FDMA). The most successful standards were nordic mobile telephone (NMT), total access communications system (TACS) in Europe and the rest of the world and advanced mobile phone service (AMPS) in North America. Other standards were often developed and used only in one country such as C-Netz in West Germany and Radiocomm 200 in France [1]. Analog systems were primarily based on circuit switched technology and designed for voice, not data. They also suffered from a low user capacity and security problems due to the simple radio interface.

Second generation (2G) systems were introduced in the early 1990's and all use digital technology. This provided an increase in the user capacity of around three times. This was achieved by compressing the voice waveforms before transmission. There are four main standards for second-generation systems: global system for mobile (GSM) communications, digital advanced mobile phone service (DAMPS), code division multiple access (CDMA [IS-95]) and personal digital cellular (PDC) [2].

The most popular 2G wireless technology is known as GSM system, first implemented in 1991. GSM technology was developed in Europe. GSM technology is a combination of FDMA and time division multiple access (TDMA). GSM is now operating in about 212 countries and territories around the world. An estimated 4.3 billion users now operate over GSM systems [3]. PDC used TDMA-based technology in Japan. CDMA technology was developed in North America. CDMA uses spread spectrum technology to break up speech into small, digitized segments and encodes them to identify each call. CDMA systems have been implemented worldwide in about 119 countries and serve an estimated 522 million subscribers [4].

Generation 2.5 is a designation that broadly includes all advances upgrades for the second generation networks. 2.5G systems are based on the following technologies: high speed circuit switched data (HSCSD), general packet radio service (GPRS) and enhanced data rates for global/GSM evolution (EDGE).

HSCSD is circuit switched technology improves the data rates up to 57.6 kbps. GPRS allows data rates of 115 kbps and theoretically up to 160 kbps on the physical layer. The modulation type that is used in GPRS is the Gaussian minimum shift keying (GMSK). EDGE is capable of offering data rates of 384 kbps and theoretically up to 473.6 kbps. The modulation type of EDGE is the 8 phase shift keying (8-PSK)/GMSK. This is the key to increase spectrum efficiency and enhanced applications such as wireless Internet access e-mail and file transfers.

Third generation (3G) systems are an extension on the complexity of second generation systems and began roll out of services sometime after the year 2001. 3G networks (UMTS, cdma2000 1x EVDO, cdma2000 3x, TD-SCDMA, WCDMA, IMT-

2000 DECT) are the latest cellular networks. 3G systems are targeted to offer a wide variety of services such as telephony, teleconference, voice mail, video conference, voice band data, message broadcast navigation, location etc. The third-generation network will concentrate on the service quality, system capacity and personal and terminal mobility issues. 3G wireless system services up to 384 kbps in wide area applications and up to 2 Mbps for indoor applications. The system will be improved by using smaller cells and the reuse of frequency channels in a geographically.

Table 1.1: Short history of wireless communications evolution

Technology	1G	2G	2.5G	3G	4G
Design Began	1970	1980	1985	1990	2000
Implementation	1984	1991	1999	2002	2010
Services	Analog voice, synchronous data to 9.6 kbps	Digital voice, Short messages	Higher capacity, packetized data	Higher capacity, Broadband data up to 2Mbps	Higher capacity, completely IP oriented, multimedia data
Standards	AMPS, TACS, NMT etc.	TDMA, CDMA, GSM, PDC	GPRS, EDGE, 1xRTT	WCDMA, cdma2000	OFDM, UWB
Data Rate	1.9 kbps	14.4 kbps	384 kbps	2 Mbps	10 Mbps - 20 Mbps
Multiplexing	FDMA	TDMA, CDMA	TDMA, CDMA	CDMA	FDMA, TDMA, CDMA
Core Network	PSTN	PSTN	PSTN, Packet network	Packet Network	All-IP Networks

Fourth generation (4G) is intended to provide high speed, high capacity, low cost per bit, IP based services. The goal is to have data rates up to 20 Mbps. Most probable the 4G network would be a network which is a combination of different technologies for example a combination of WiMAX and WiFi, software defined radio (SDR) receivers, orthogonal frequency division multiplexing (OFDM), orthogonal frequency division multiple access (OFDMA), multiple input multiple output (MIMO) technologies. All of these delivery methods are typified by high rates of data transmission and packet-switched transmission protocols or a mix of packet and circuit switched networks [5].

OFDM is a multicarrier modulation technique for high data rate transmission of signals over wireless channels and converts a frequency selective fading channel into a collection of parallel flat fading sub channels [6, 7]. MIMO exploits spatial diversity by having several transmit and receive antenna. The MIMO systems offer very higher data rates in the same bandwidth compared with the single input single output (SISO) systems [8].

1.2 Review of Previous Works and Observation

The carrier frequency offset and phase noise cause loss of orthogonality among subcarriers and leads to inter carrier interference (ICI). Over the years, researchers have proposed various methods to combat the ICI. We have discussed some contribution of different authors related to ICI and its suppression in this section.

Russell *et al.* (1995) have analyzed the effect of inter carrier interference (ICI) and obtained exact expressions for the ICI of an OFDM signal caused by Doppler spread. With the initial assumption that the channel is known with a fixed number of paths for a sufficiently large number of subcarriers N, the ICI can be modeled as a Gaussian random process according to the central limit theorem. Antenna diversity and trellis coding method have examined for reducing ICI [9].

Armstrong *et al.* (1998) have proposed polynomial cancellation coding (PCC) method for OFDM in which the information to be transmitted is modulated onto weighted groups of subcarriers rather than onto individual subcarriers. It has shown that

PCC reduced substantially the sensitivity of OFDM to carrier frequency offset. PCC also reduced the ICI due to Doppler spread. Results are presented for a frequency non-selective *i.e.* flat fading channel, subject to classical Doppler spread. By using weighted pairs of subcarriers the ICI due to Doppler spread can be reduced by approximately 15 dB. By using weighted groups of three subcarriers a further 15 dB reduction in ICI can be achieved [10].

Zhao *et al.* (2001) proposed the effect of ICI in OFDM system with self-cancellation (SC) scheme. The scheme works in two very simple steps. At the transmitter side, one data symbol is modulated onto a group of adjacent subcarriers with a group of weighting coefficients. The weighting coefficients are designed so that the ICI can be minimized. At the receiver side, by linearly combining the received signals on these subcarriers with proposed coefficients, the residual ICI contained in the received signals can be further reduced. The carrier to interference ratio (CIR) can be increased by 15 and 30 dB when the group size is two or three respectively for a channel with a constant frequency offset. Although the redundant modulation causes a reduction in bandwidth efficiency, it can be compensated. Simulations show that OFDM systems using the proposed ICI SC scheme perform much better than standard systems while having the same bandwidth efficiency in multipath mobile radio channels with large Doppler frequencies [11].

Chen *et al.* (2002) looked into the frequency offset estimated statistically using maximum likelihood algorithm and then cancel at the receiver. This paper presents two maximum likelihood CFO estimation schemes, one in frequency domain and another in time-domain, both the presence of Doppler fading in wireless channels. The properties of the estimators are analyzed and simulation results showing the performance gain of the proposed estimators are better than the conventional schemes. Apart from improved accuracy, the time-domain maximum likelihood estimator (MLE) features significantly reduced complexity [12].

Chizhik *et al.* (2003) have conducted measurements on 2x2, 4x4 and 16x16 MIMO systems in an urban environment at Manhattan, New York. In the measurement campaigns, vertically and horizontally polarized slot antenna elements were used for

both the transmitter and receiver. At the receiver (a laptop was used as the receiver terminal), the antenna elements were spaced half-wavelength apart from each other to achieve low correlation and high capacity. System capacities of 5.5 bps/Hz, 10 bps/Hz and 35 bps/Hz were reported respectively 2x2, 4x4 and 16x16 MIMO systems at the 10 dB system SNR [13].

Tan *et al.* (2004) probed novel pulse shaped in OFDM system to reduce ICI due to frequency offset. Each carrier consists of a main lobe followed by a number of side lobes with reducing amplitude in OFDM spectrum. As long as orthogonality is maintained there is no interference among the carriers because at the peak of the every carrier, there exist a spectral null. At that point the component of all other carriers is zero. Hence the individual carrier is easily separated. When there is a frequency offset the orthogonality is lost because now the spectral null does not coincide to the peak of the individual carriers. So some power of the side lobes exists at the centre of the individual carriers which is called ICI power. The ICI power is go on increasing as the frequency offset increases. Now the purpose of pulse shaping is to reduce the side lobes. If we can reduce the side lobe significantly then the ICI power will also be reduced significantly. The results show that new pulse outperforms the rectangular pulse and raised-cosine pulse in ICI power reduction [14].

Ling *et al.* (2005) have measured on MIMO channels in the rural environment (Lucent Technologies). It was reported that the capacity in a 8x10 MIMO system was approximately eight times the corresponding capacity in a 1x1 SISO system and 3.2 times the corresponding capacity in a 1x10 single input multiple output (SIMO) system. The measurement also found that antenna arrays containing antennas of both horizontal and vertical polarizations could increase the capacity by approximately 50% [15].

Ryu *et al.* (2005) observed the effect of ICI produced by the phase noise of transceiver local oscillator. Bit error rate (BER) performance is degraded because the orthogonal properties between the subcarriers are broken down. In this paper, the number of subcarriers is chosen according to the consideration of the trade off between the amount of ICI and data rate of the system. ICI SC of mapping method introduced using data conjugate and data conversion in OFDM to reduce ICI effectively. Then the

system performance of the mapping method is compared with those of the original OFDM and the conventional data conversion method [16].

Li *et al.* (2008) proposed several ICI SC methods in the MISO-OFDM system. In this paper, to compensate integrated effect of frequency offset and phase noise and CPE, ICI and CIR are derived theoretically in MISO-OFDM system. As results, by choosing several ICI SC methods appropriately, considerable performance improvement can be achieved in the MISO-OFDM system which affected by frequency offset and phase noise. Finally, CIR and PAPR are compared in order to evaluate ICI minimization efficiency and PAPR characteristic [17].

Yusof *et al.* (2008) investigated SISO and MIMO-OFDM with SC in space time frequency (STF). This paper also presented data allocation of complex pair and reduced peak to average power ratio (PAPR). Simulations by comparing STF MIMO-OFDM with conventional OFDM showed an optimistic result especially at a high E_b/N_o. The BER performance of OFDM and MIMO-OFDM system has reduced ICI 5 dB (at BER= 0.16) and 5.62 dB (at BER= 0.03) respectively through simulation [18].

Idris *et al.* (2008) examined ICI reductions with SC of data conjugate method and data conversion method using space time frequency block codes (STFBC) that exploit spatial, time and frequency diversity designed in MIMO-OFDM system by simulation. The system developed is analyzed with CFO and compared in terms of BER performance. It can be seen from the simulation results that the system developed improved the BER performance with high diversity order and successfully reduce ICI effect [19].

From the above literatures review, we found that most of the research works have tried to reduce ICI by using different analytical expression or simulation methods in SISO/MISO/MIMO-OFDM system. Analytical work to reduce ICI using SC, antenna diversity, channel coding, frequency-domain equalization, time-domain windowing, MLE, PCC and pulse shaping is yet to be reported. There is no analytical expression of ICI, CIR and BER in 2x2 MIMO-OFDM system. So, it is essential to explore analytical model to eliminate the ICI using the self-cancellation data conjugate (SCDC) with

convolution coding and space frequency block code (SFBC) in 2x2 MIMO-OFDM systems.

1.3 Motivation

Since the advent of wireless communications, a great technological effort has been devoted to the exploitation of the huge bandwidth of wireless. The available bandwidth is scarce and expensive. Increasing the spectral efficiency is the answer for the rising demand of high data rate when the available bandwidth is limited. Multiple inputs and multiple outputs (MIMO) OFDM provides very good spectral efficiency. One of the main disadvantages of MIMO-OFDM is its sensitivity against carrier frequency offset and phase noise which causes intercarrier interference (ICI). Our main goal in this thesis is to suppress the ICI effect significantly in MIMO-OFDM system using self-cancellation with data conjugate and channel coding. Usually, analytical methods are faster than simulation and drastically reduce the computational time. Simulations are simpler but slower and appropriate techniques must be used to reduce the number of simulation required to get a satisfactory result. Accurate models are needed to describe the propagation and performance evaluation of system for the transmitted signal through a transmission media like wireless. Analytical models have been developed for 2x2 MIMO-OFDM system integrating the effect of phase noise and frequency offset. Analytical models are always very helpful for a deeper comprehension and overall view of the system can be understood and they require rigorous statistical analysis of both the phase noise and frequency offset behavior.

1.4 Objective of the Thesis

The goal of this research is to analyze and reduce ICI in 2x2 MIMO-OFDM wireless communication system. To meet the goal, the following objectives have been identified.

1. To develop an analytical model using QPSK modulation.
2. To derive expression for common phase error (CPE), ICI and CIR using self-cancellation data conjugate (SCDC) method with convolution coding (CC) and space frequency block coding (SFBC).
3. To analyze the effect of ICI in terms of BER.
4. To compare ICI, CIR and BER performance results with published results.

1.5 Organization of the Thesis

This thesis is organized in five chapters as follows:

Chapter-1 is an introductory chapter. It contains the different generation of wireless communication system, developments and technologies.

Chapter-2 presents three parts. Firstly, the propagation characteristics wireless channels are presented. It contains to radio propagation effects such as multipath, fading parameters classified into time delay spread fading and Doppler spread fading from the view of propagation terrain. The performance of any wireless communication systems is highly dependent on the propagation channel and so a detailed knowledge of radio propagation is important for optimization of wireless communications. Secondly, the basic concept of OFDM and its implementation are explained. We list the advantages and drawbacks of OFDM compared with a conventional single carrier transmission. Finally, this chapter covers the introduction to MIMO systems, channel capacity and diversity combining techniques in different environments.

Chapater-3 describes ICI reduction using SCDC, SCDC with convolution coding (CC) and SFBC scheme in 2x2 MIMO-OFDM system in detail. In this thesis we have analytically derived expression of CPE, ICI, CIR and BER in original, SCDC and SFBC of 2x2 MIMO-OFDM system.

Chapter-4 is all about the results and discussion on the curves obtained from MATLAB programmes for original, SCDC, SCDC with CC and SFBC in 2x2 MIMO-OFDM system. BPSK and QPSK modulation techniques are considered and compared with each other for their performances.

Chapter-5 presents the concluding remarks of all the chapters and highlights some possible promising avenues of further development.

CHAPTER 2

FUNDAMENTALS OF WIRELESS COMMUNICATION, OFDM AND MIMO

2. 1 Propagation Characteristics of Wireless Channel

Wireless transmission uses air or space for its transmission medium. The radio propagation is not as smooth as in wire transmission since the received signal is not only coming directly from the transmitter, but the combination of reflection, diffraction, and scattering of the transmitted signal [20]. It is interesting and rewarding to examine the effects of propagation to a radio signal since consequences determine data rate, range and reliability of the wireless system.

Reflection occurs when a propagating electromagnetic wave impinges on a surface where partial energy is reflected and the remaining is transmitted into the surface.

Diffraction occurs when the radio path between the transmitter and receiver is obstructed by a dense body, causing secondary waves to be formed behind the obstructing body.

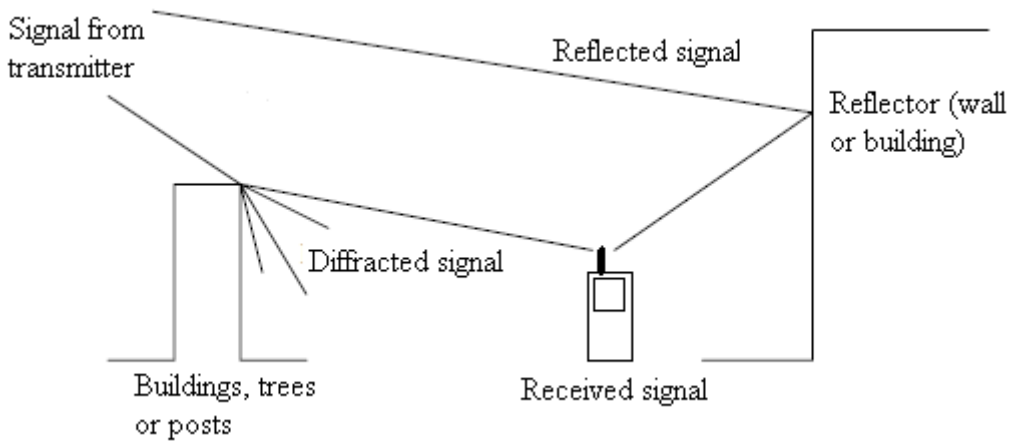

Fig 2.1: Radio propagation effects

Scattering occurs when a radio wave impinges on either a large rough surface or any surface, causing the reflected energy to spread out and scatter in all directions; consequently provides additional energy for the receiver which can receive more than one copies of the signal in multiple paths with different phases.

Shadowing of the signal can occur whenever there is an obstruction between the transmitter and receiver. It is generally caused by buildings and hills. It is the most important environmental attenuation factor.

2.1.1 Multipath effects

There are obstacles and reflectors in the wireless propagation channel, the transmitted signal arrivals at the receiver from various directions over a multiplicity of paths. Such a phenomenon is called multipath**.** It is an unpredictable set of reflections or direct waves each with its own degree of attenuation and delay. Multipath is usually described by

i) Line-of-sight (LOS): The direct connection between the transmitter (TX) and the receiver (RX).
ii) Non-line-of-sight (NLOS): The path arriving (to the receiver) after reflection from reflectors.

The illustration of LOS and NLOS is shown in Fig. 2.2.

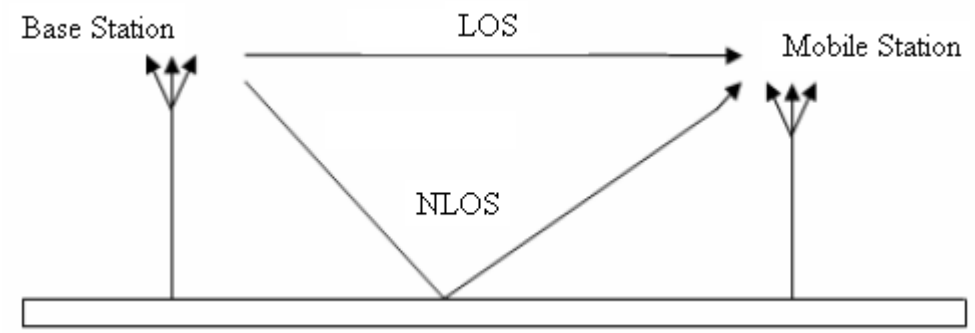

Fig. 2.2: Effect of multipath on a mobile station

2.1.2 Fading parameters

Fading is about loss of signal in wireless communication. In a received signal, fading is caused for the variation of the amplitude or relative phase, or both, one or more of the frequency components of the signal.

Three most important effects:

1. Rapid changes in signal strengths over small travel distances or short time periods.
2. Frequency of signals changes rapidly.
3. Multiple signals arrive different times. When added together at the antenna, signals are spread out in time. This can cause a smearing of the signal and interference between bits that are received.

2.1.2.1 Delay spread

The received radio signal from a transmitter consists of typically a direct signal, plus reflections off objects such as buildings, mountings, and other structures. The reflected signals arrive at a later time then the direct signal because of the extra path length, giving rise to a slightly different arrival times, spreading the received energy in time. Delay spread is the time spread between the arrival of the first and last significant multipath signal seen by the receiver.

In a digital system, the delay spread can lead to inter symbol interference (ISI). This is due to the delayed multipath signal overlapping with the following symbols. This can cause significant errors in high bit rate systems. Fig. 2.3 shows the effect of ISI due to delay spread on the received signal.

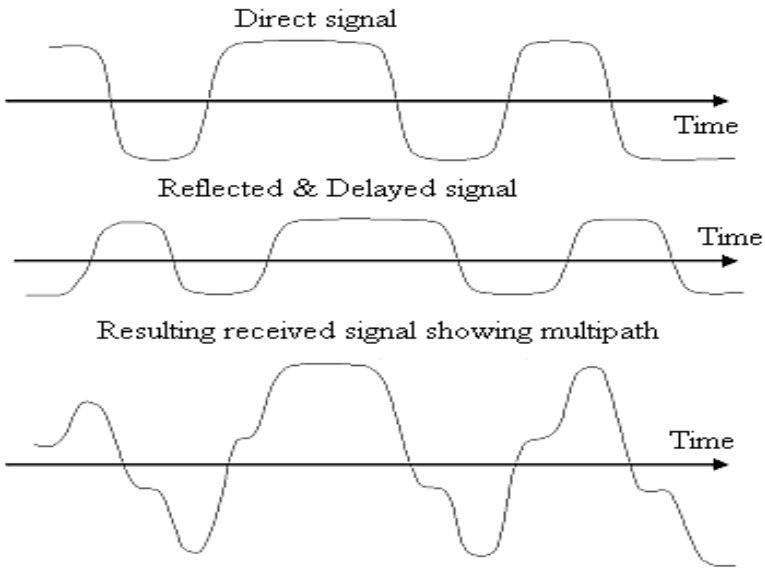

Fig. 2.3: Multipath delay spread

2.1.2.2 Coherence bandwidth

It is a statistical measure of the range of frequencies over which the channel can be considered to be flat (i.e., the channel passes all the spectral components with approximately equal gain and phase). If the coherence bandwidth is define bandwidth over which the frequency correlation function is above 0.9 and then the coherence bandwidth is approximately [21]

$$B_C \approx \frac{1}{50\sigma_\tau} \tag{2.1}$$

If the definition is relaxed so that the frequency correlation function is above 0.5 and then the coherence bandwidth is approximately

$$B_C \approx \frac{1}{5\sigma_\tau} \tag{2.2}$$

Where σ_τ is root mean square (RMS) delay spread.

2.1.2.3 Doppler shift

When a wave source and a receiver are moving relative to one another the frequency of the received signal will not be the same as the source. When they are moving toward each other the frequency of the received signal is higher then the source, and when they move away from the each other the frequency decreases. This is called the Doppler effect. This effect becomes important when developing mobile radio systems.

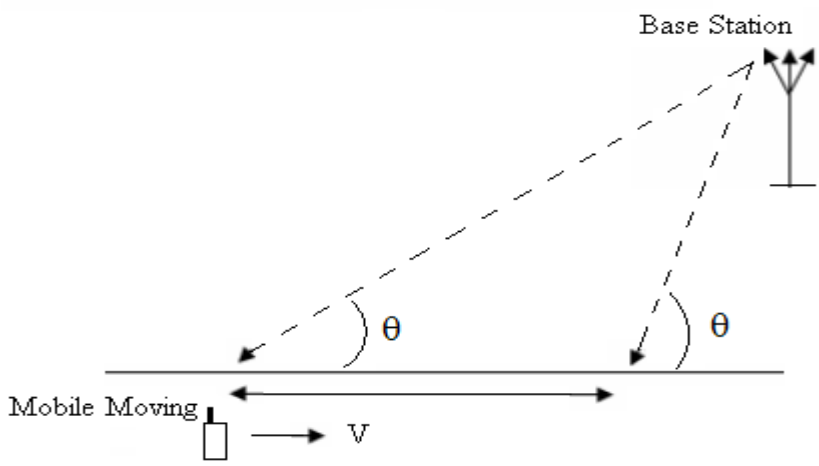

Fig. 2.4: Illustration of Doppler effect

The amount the frequency changes due to the Doppler effect depends on the relative motion between the source and receiver and on the speed of propagation of the wave. The Doppler shift in frequency can be written:

$$f_D = \frac{V}{\lambda}\cos\theta = f_m \cos\theta \tag{2.3}$$

The received signal frequency

$$f_r = f_c - f_m \cos\theta \tag{2.4}$$

When θ = 0° (mobile moving away from the transmitter)

$$f_r = f_c - f_m \tag{2.5}$$

When θ = 90° (mobile circling around)

$$f_r = f_c \tag{2.6}$$

When θ = 180° (mobile moving towards the transmitter)

$$f_r = f_c + f_m \tag{2.7}$$

Where, f_m = v/λ = maximum value of Doppler frequency

2.1.2.4 Doppler spread

Doppler spread is the measure of maximum broadening of the spectrum due to Doppler shift. When a pure sinusoidal tone of frequency f_c is transmitted, the received signal spectrum, called the Doppler spectrum, will have components in the range $f_c - f_m$ to $f_c + f_m$,where f_m is the Doppler shift. The amount of spectral broadening depends on f_m which is a function of the relative velocity of the mobile, and the angle θ between the direction of motion of the mobile and direction of arrival of the scattered waves. If the baseband signal bandwidth is much greater than B_D the effects of Doppler spread are negligible at the receiver.

2.1.2.5 Coherence time

Coherence time T_c is the time domain dual of Doppler spread and is used to characterize the time varying nature of the frequency dispersiveness of the channel in the time domain. The Doppler spread and coherence time are inversely proportional to one another.

$$T_C \approx \frac{1}{f_m} \tag{2.8}$$

If the coherence time is defined as the time over which the time correlation function is above 0.5, then the coherence time is approximately [22]

$$T_C \approx \frac{9}{16\pi f_m} \tag{2.9}$$

Where, f_m is the maximum Doppler shift. A popular rule of thumb for modern digital communication is to define the coherence time as the geometric mean of equations (2.8) and (2.9).

$$T_C = \sqrt{\frac{9}{16\pi f_m^2}} = \frac{0.423}{f_m} \tag{2.10}$$

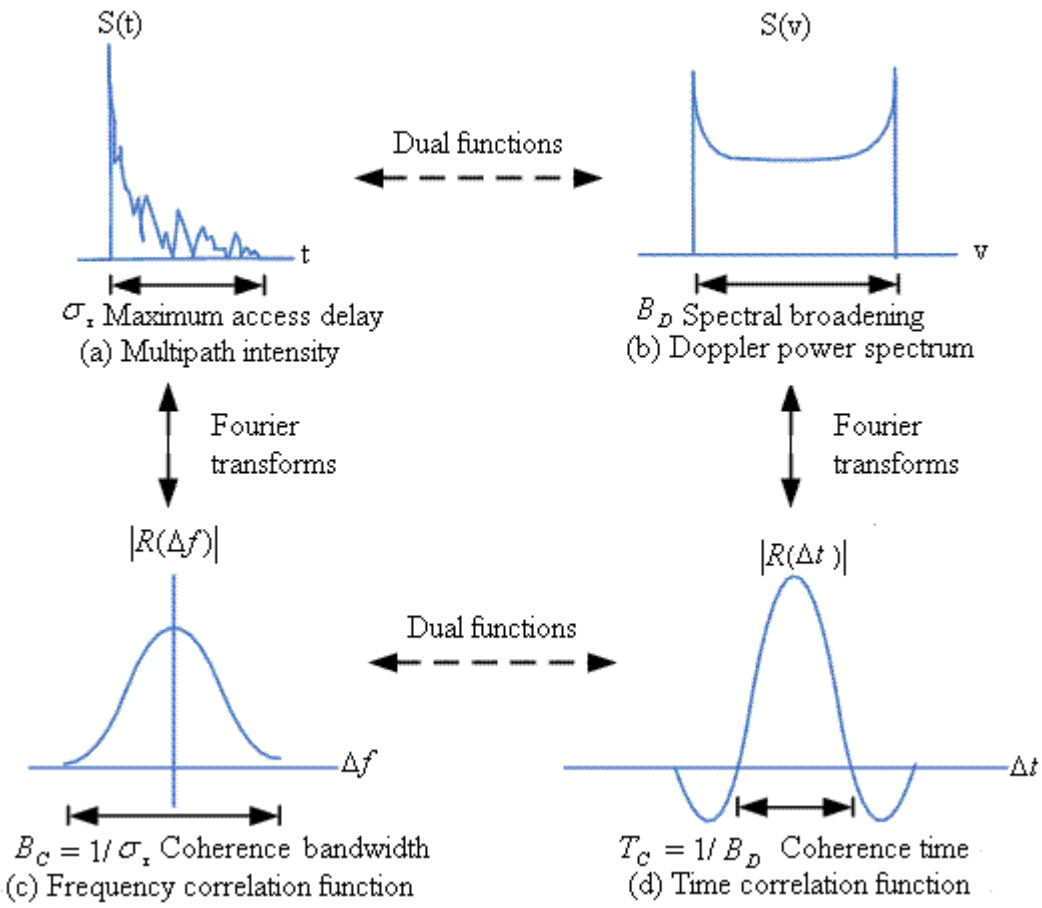

Fig. 2.5: Relationship between the channel correlation and power density function [23]

2.1.3 Types of small-scale fading

Depending on the relation between the signal parameters (such as bandwidth, symbol period etc.) and the channel parameters (such as RMS delay spread and Doppler spread), different transmitted signals will suffer different types of fading. The time dispersion and frequency dispersion mechanisms in a mobile radio channel lead to four

possible distinct effects, which are manifested depending on the nature of the transmitted signal, the channel and the velocity. While multipath delay spread leads to time dispersion and frequency selective fading, Doppler spread leads to frequency dispersion and time selective fading. The two propagation mechanisms are independent of one another. Fig. 2.6 shows a tree of the four different types of fading.

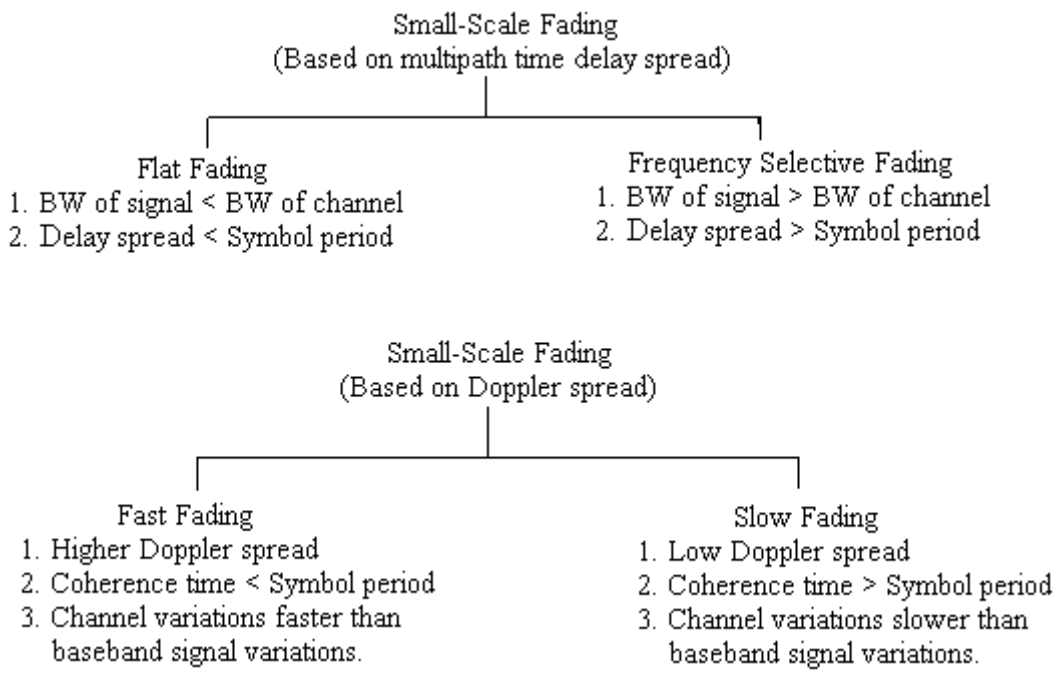

Fig. 2.6: Types of small-scale fading

2.1.3.1 Fading effects due to multipath time delay spread

Time dispersion due to multipath causes either flat or frequency selective fading.

2.1.3.1.1 Flat fading

The wireless channel is said to be flat fading if it has constant gain and linear phase response over a bandwidth which is greater than the bandwidth of the transmitted signal. In other words, flat fading occurs when the bandwidth of the transmitted signal (B_s) is smaller than the coherence bandwidth (B_c) of the channel.

$$\begin{aligned} B_S &<< B_C \\ T_S &>> \sigma_\tau \end{aligned} \tag{2.11}$$

Where T_s and σ_τ the symbol period and the RMS delay spread. The effect of flat fading channel can be seen as a decrease of the signal to noise (SNR) ratio. Since the signal is narrow with respect to the channel bandwidth, the flat fading channels are also known as amplitude varying channels or narrowband channels.

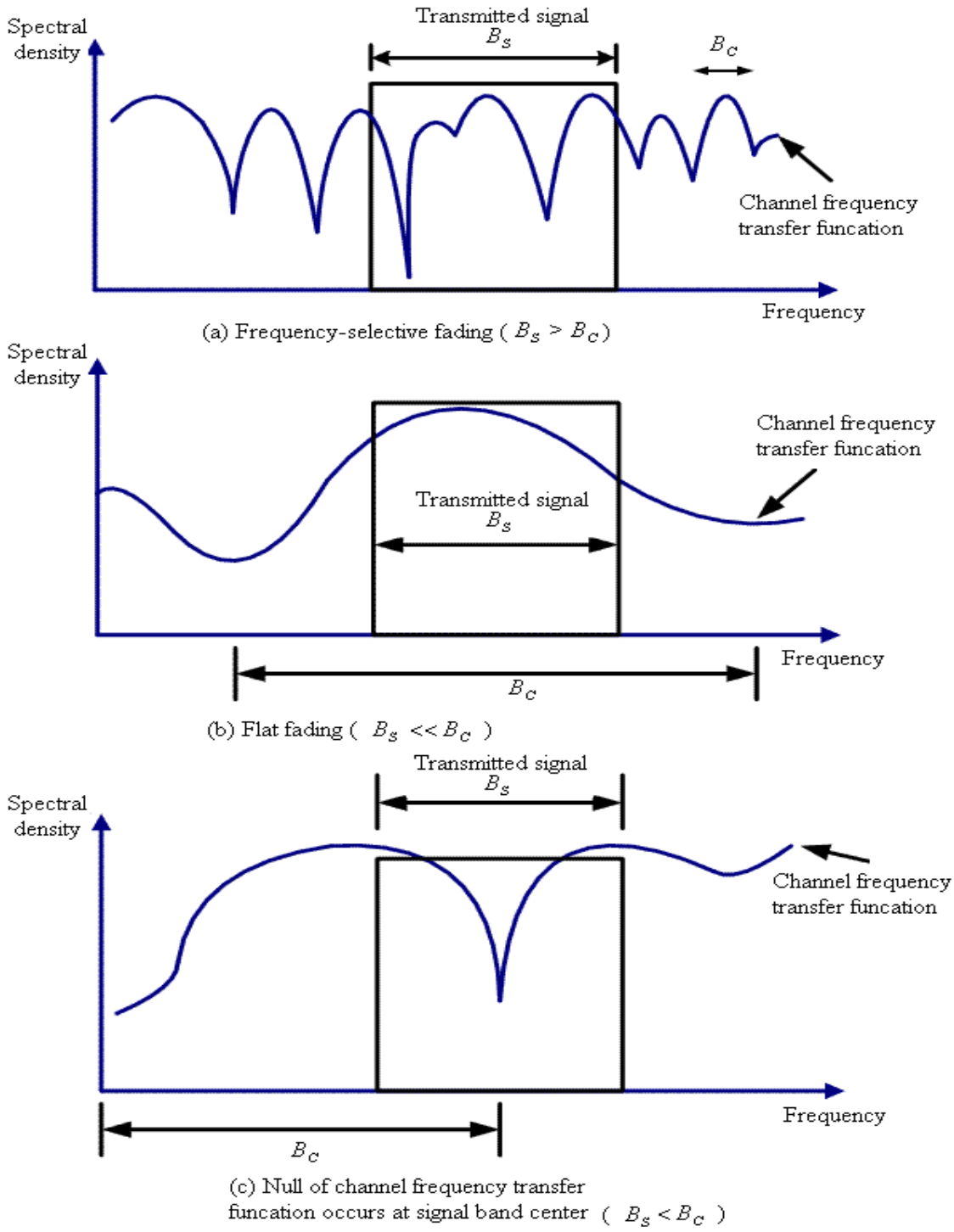

Fig. 2.7: Relationships between the coherence bandwidth and signal bandwidth B_s [24]

2.1.3.1.2 Frequency selective fading

A channel is said to be frequency selective if the signal bandwidth is greater than the coherence bandwidth of the channel. Overall symbol duration becomes more than the actual symbol duration. This phenomenon is called inter symbol interference (ISI).

$$\begin{aligned} B_S &> B_C \\ T_S &< \sigma_\tau \end{aligned} \tag{2.12}$$

A common rule of thumb is that a channel is flat fading if $T_S \geq 10\sigma_\tau$ and a channel is frequency selective if $T_S < 10\sigma_\tau$.

2.1.3.2 Fading effects due to doppler spread

The transmitted baseband signal changes rapidly as compared to the rate of change of the channel, a channel may be classified either as a fast fading or slow fading channel.

2.1.3.2.1 Fast fading

In a fast fading channel, the channel impulse response changes rapidly within the symbol duration, *i.e.* the coherence time of the channel is smaller that the symbol period of the transmitted signal.

$$\begin{aligned} B_S &< B_D \\ T_S &> T_C \end{aligned} \tag{2.13}$$

This causes frequency dispersion or time selective fading due to Doppler spreading. Fast fading is due to reflections of local objects and the motion of the objects relative to those objects.

2.1.3.2.2 Slow fading

In a slow fading channel, the channel impulse response changes at a rate much slower than the transmitted baseband signal. In this case, the channel may be assumed to be static over one or several reciprocal bandwidth intervals. In the frequency domain, this implies that the Doppler spread of the channel is much less, than the bandwidth of the base band signals.

$$B_S >> B_D$$
$$T_S << T_C \tag{2.14}$$

Over the years, some authors have confused the terms fast and slow fading with the terms large scale and small scale fading.

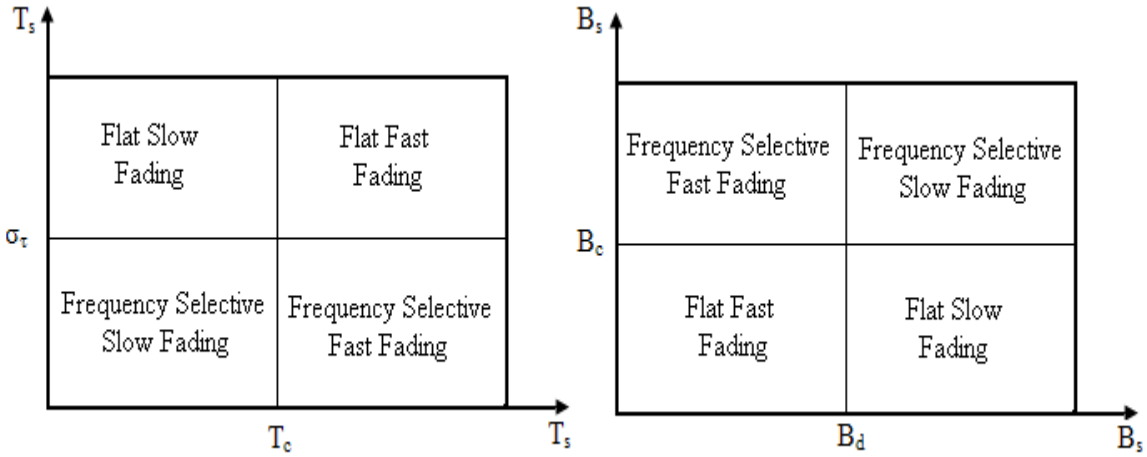

Fig. 2.8: Fading illustration of small scale fading

2.1.4 Rayleigh fading distribution

Constructive and destructive nature of multipath components in flat fading channels can be approximated by Rayleigh distribution if there is no line of sight which means when there is no direct path between transmitter and receiver [25]. The Rayleigh distribution is basically the magnitude of the sum of two equal independent orthogonal Gaussian random variables and the probability density function (pdf) given by

$$f(x) = \frac{x}{\sigma^2}\exp\left(\frac{-x^2}{2\sigma^2}\right) \quad \text{where } 0 \le x \le \infty \tag{2.15}$$

Where, σ^2 is the time-average power of the received signal.

2.1.5 Rician fading distributions

Direct path is normally the strongest component goes into deeper fade compared to the multipath components. There is line of sight. This kind of signal is approximated by Ricean distribution. As the dominating component run into more fade the signal characteristic goes from Rician to Rayleigh distribution. The Rician distribution has a pdf

$$f\left(x|v,\sigma\right)=\frac{x}{\sigma^2}\exp\left(\frac{-(x^2+v^2)}{2\sigma^2}\right)I_0(\frac{xv}{\sigma^2}) \tag{2.16}$$

Where, $I_0(z)$ is the modified Bessel function of the first kind with order zero. When $v = 0$, the distribution reduces to a Rayleigh distribution.

2.2 Orthogonal Frequency Division Multiplexing (OFDM)

The OFDM technology was first conceived in 1960s and 1970s, when Chang [26] published a paper on the synthesis of band limited orthogonal signals for multichannel data transmission. He presented a new principle of transmitting signals simultaneously over a bandlimited channel without the inter carrier interference (ICI) and the inter symbol interference (ISI). Right after Chang's publication of his paper, Saltzburg [27] demonstrated the performance of the efficient parallel data transmission systems in 1967. He concluded that “the strategy of designing an efficient parallel system should concentrate on reducing crosstalk between adjacent channels than on perfecting the individual channels themselves". His conclusion has been proven far sighted today in the digital baseband signal processing to battle the ICI.

The OFDM technology is widely used in two types of working environments, i.e., a wired environment and a wireless environment. When used to transmit signals through wires like twisted wire pairs and coaxial cables, it is usually called as digital multi-tone (DMT). OFDM is suitable a well-liked multicarrier modulation technique for transmission of wireless channels. It converts a frequency-selective fading channel into a collection of parallel flat fading sub channels, which greatly simplifies the structure of the receiver. The time domain waveform of the subcarriers are orthogonal, yet the signal spectral corresponding to different subcarriers overlap in frequency domain. Hence, the available bandwidth is utilized very efficiently in OFDM systems without causing the ICI. By combining multiple low data rate subcarriers, OFDM systems can provide a composite high data rate with long symbol duration. That helps to eliminate the ISI, which often occurs along with signals of short symbol duration in a multipath channel.

2.2.1 Evolution of OFDM

The evolution of OFDM can be divided into three parts [28]. There are consisting of frequency division multiplexing, multicarrier communication and orthogonal frequency division multiplexing.

2.2.1.1 Frequency division multiplexing (FDM)

The use of FDM goes back over a century, where more than one low rate signal, such as telegraph, telephone, was carried over a relatively wide bandwidth channel using different frequency channels to carry the information of different users. To facilitate separation of the signals at the receiver, the carrier frequencies were spaced sufficiently far apart so that the signal spectra did not overlap. Empty spectral regions between the signals assured that they could be separated with feasible filters. The resulting spectral efficiency was quite low.

2.2.1.2 Multicarrier communication (MC)

The theory of MC uses a form of FDM technologies but only between a single data source and a single data receiver [29]. As multicarrier communication was introduced, it enabled an increase in the overall capacity of communications, thereby increasing the overall throughput. MC is the concept of splitting a signal into a number of signals, modulating each of these new signals over its own frequency channel, multiplexing these different frequency channels together in an FDM manner; feeding the received signal via a receiving antenna into a demultiplexer that feeds the different frequency channels and combining the data output to form the received signal. In the multicarrier modulation, the carrier spacing is carefully selected so that each subcarrier is orthogonal to the other subcarriers. Orthogonality can be achieved by carefully selecting the subcarrier frequencies. Each modulated subcarrier is ‘orthogonal’ to all others which means that they do not interfere with each other.

2.2.2 Orthogonality

Signals are orthogonal if they are mutually independent of each other. Orthogonality is a property that allows multiple information signals to be transmitted perfectly over a common channel and detected without interference.

In time domain, it is given by,

$$\int_0^T x_i(t) \otimes x_j^*(t)dt = \begin{cases} 1, i = j \\ 0, i \neq j \end{cases} \tag{2.17}$$

and in frequency domain

$$\int_0^T X_i(f).X_j^*(f)df = \begin{cases} 1, i = j \\ 0, i \neq j \end{cases} \tag{2.18}$$

Two conditions must be satisfied for the orthogonality between the subcarriers.

1. Each subcarrier has exactly an integer number of cycles in the FFT interval.
2. The number of cycles between adjacent subcarriers differs by exactly one.

The signals are orthogonal if the integral value is zero over the interval [0 T], where T is the symbol period. Since the carriers are orthogonal to each other the nulls of one carrier coincides with the peak of another sub carrier.

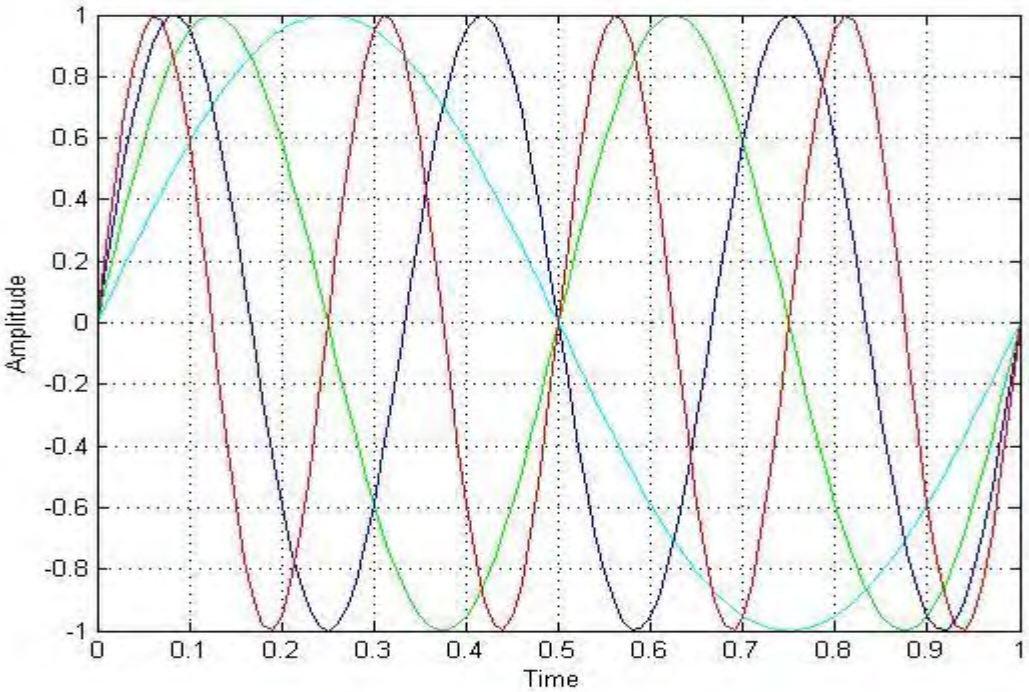

Fig. 2.9: Carrier signals in OFDM transmission

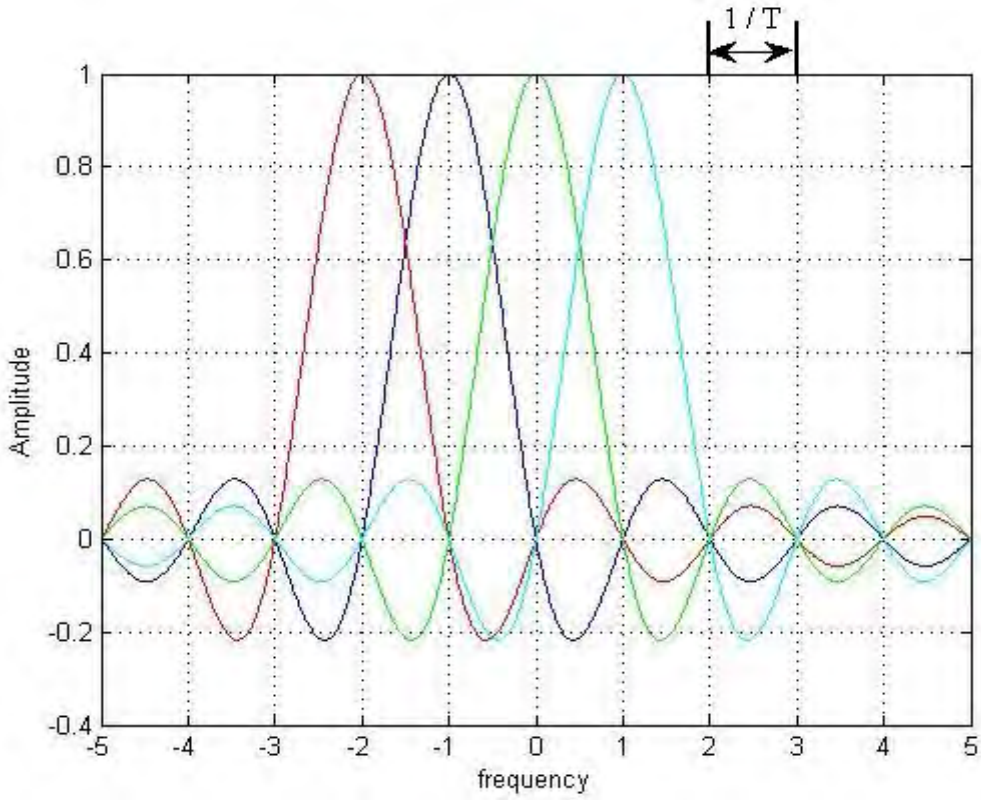

Fig. 2.10: Frequency spectrum of OFDM transmission

Fig. 2.9 shows the construction of an OFDM signal with four subcarriers. The baseband frequency of each subcarrier is chosen to be an integer multiple of the inverse symbol time, resulting in all subcarriers having an integer number of cycles per symbol. As a consequence the subcarriers are orthogonal to each other. In the frequency domain each OFDM subcarrier has a sinc (*sin(x)/x*) frequency response, as shown in Fig. 2.10. This is a result of the symbol time correspondent to the inverse of the carrier spacing. This symbol time corresponds to the inverse of the subcarrier spacing of *1/T* Hz. The *sinc* shape has a narrow main lobe, with many side lobes that decay slowly with the magnitude of the frequency difference away from the centre. Each carrier has a peak at the centre frequency and nulls evenly spaced with a frequency gap equal to the carrier spacing.

2.2.3 OFDM generation and reception

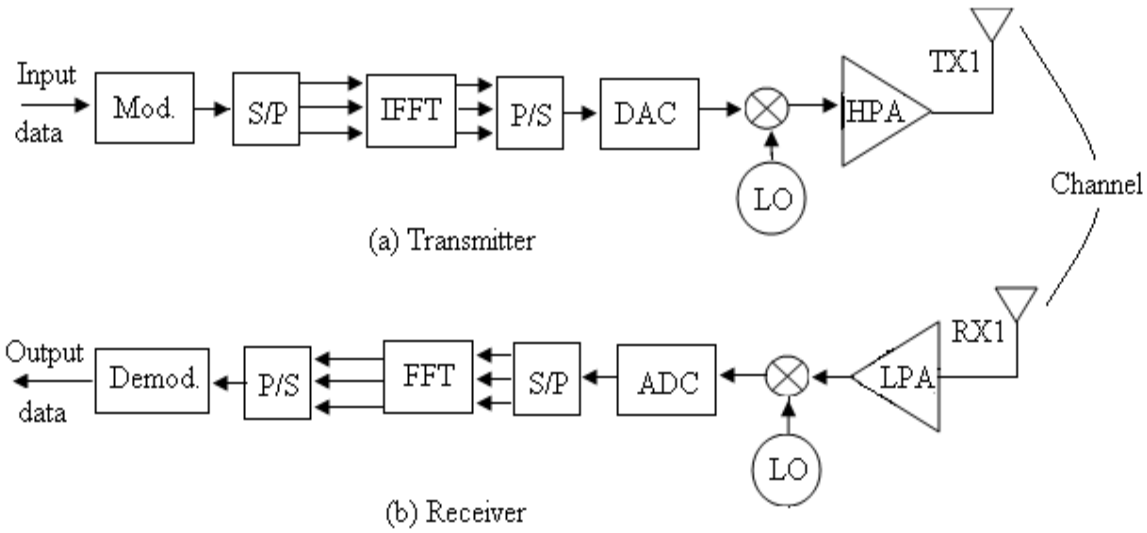

Fig. 2.11: Block diagram of OFDM system model (a) Transmitter (b) Receiver

The block diagram of a typical discrete-time baseband equivalent model of OFDM systems is shown in Fig. 2.11. As shown, input bits are first encoded by using suitable modulation technique like (BPSK, QPSK or M-QAM). The N symbols are transferred by the serial-to-parallel converter (S/P), in this stage duration of input bits is increased. After S/P converter, it then transforms this spectral representation of the data into the time domain using an Inverse Fast Fourier Transform (IFFT). After IFFT, the modulated symbols are serialized using a parallel-to-serial converter (P/S), then converted to analog via the digital-to-analog converter (DAC) and passing high power amplifier before being sent down to the channel. Then the signal is allowed to pass through additive white Gaussian noise (AWGN) channel. At the receiver side, the received symbols are passed low noise amplifier and converted from analog to digital using the analog-to-digital converter (ADC) and transferred by the S/P. In these parallel OFDM symbols, guard interval is removed and it is allowed to pass through fast fourier transform. Here the time domain OFDM symbols are converted into frequency domain. After this the low data rate parallel bit stream is converted into high data rate serial bit stream. Finally it is fed into signal demapper for demodulation purpose which is in form of binary.

2.2.4 Modulation

Modulation of a signal changes binary bits into an analog waveform. Modulation can be done by changing the amplitude, phase, and frequency of a sinusoidal carrier. There is several digital modulation techniques used for data transmission. A large number of modulation schemes are available allowing the number of bits transmitted per carrier. The number of bits that can be transferred using a single symbol corresponds to $\log_2(M)$, where M is the number of points in the constellation, thus 256-QAM transfers 8 bits per symbol. Increasing the number of points in the constellation does not change the bandwidth of the transmission, thus using a modulation scheme with a large number of constellation points, allows for improved spectral efficiency. For example 256-QAM has a spectral efficiency of 8 b/s/Hz and spectral efficiency 1 b/s/Hz for BPSK.

2.2.4.1 Binary phase shift keying (BPSK)

BPSK is the simplest form of phase shift keying (PSK). It uses two phases which are separated by 180°. It does not particularly matter exactly where the constellation points are positioned. They are shown on the real axis, at 0° and 180°. It is shown in Fig. 2.12.

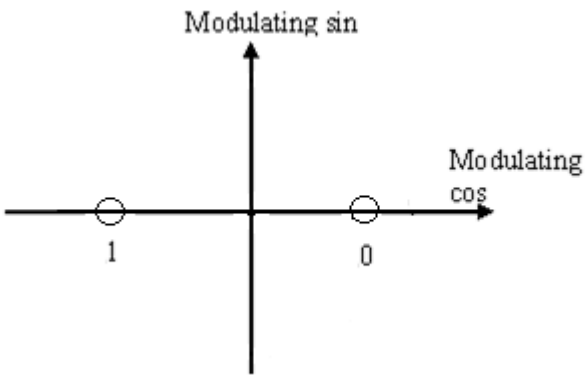

Bit	b_R
0	A
1	-A

Fig. 2.12: BPSK bit-pattern

2.2.4.2 Quadrature phase shift keying (QPSK)

QPSK is a method for transmitting digital information across an analog channel. Data bits are grouped into pairs and each pair is represented by a particular waveform, called a symbol. There are four possible combinations of data bits in a pair. QPSK creates four different symbols, one for each pair, by changing the I gain and Q

gain for the cosine and sine modulators. Four possible symbols of QPSK are shown in Fig. 2.13.

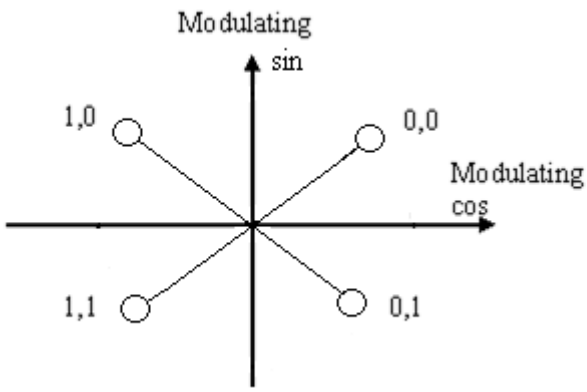

Bit1	Bit2	b_R	b_I
0	0	A	A
0	1	A	-A
1	0	-A	A
1	1	-A	-A

Fig. 2.13: QPSK bit-pattern

2.2.5 Serial to parallel conversion

Data to be transmitted is typically in the form of a serial data stream. In OFDM, serial to parallel conversion stage is considered to realize the concept of parallel data transmission.

Example for BPSK

input : x=[0,1,0,0,1,0,1,1,….]

The output will be a parallel: $x1$=[0] $x2$=[1] $x3$=[0] $x4$=[0] …..

Example for QPSK

input : x=[0,1,0,0,1,0,1,1,….]

The output will be a parallel : $x1$=[0,1] $x2$=[0,0] $x3$=[1,0] $x4$=[1,1] …..

In a conventional serial data system, the symbols are transmitted sequentially, with the frequency spectrum of each data symbol allowed to occupy the entire available bandwidth. When the data rate is sufficient high, symbol period is less that’s why several adjacent symbols may be completely distorted over frequency selective fading or multipath delay spread channel [30].

The spectrum of an individual data element normally occupies only a small part of available bandwidth. An entire channel bandwidth is divided into many narrow subchannels; each subchannel is longer symbol period and the frequency response over each individual sub channel is relatively flat.

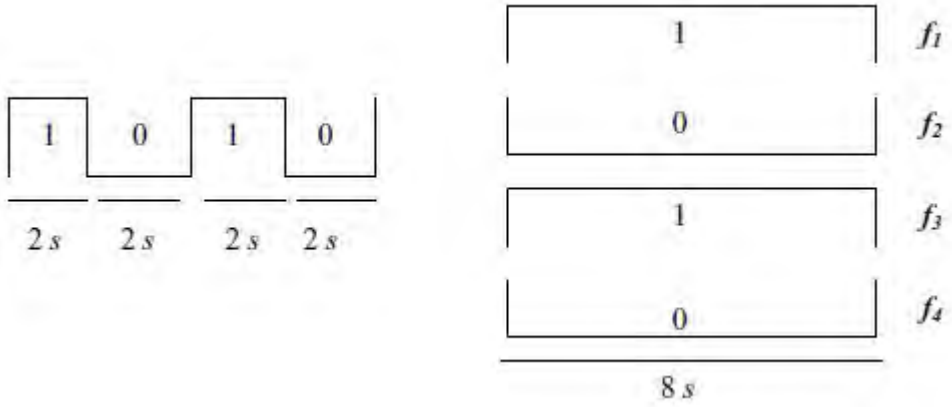

Fig. 2.14: Serial to parallel conversion

Suppose that this transmission takes eight seconds. Then, each piece of data in the left picture has duration of two second. On the other hand, OFDM would send the four pieces simultaneously as shown on the right. In this case, each piece of data has duration of eight seconds.

2.2.6 FFT and IFFT implementation

OFDM systems are implemented using a combination of fast fourier transform (FFT) and inverse fast fourier transform (IFFT) blocks that are mathematically equivalent versions of the DFT and IDFT. But we use FFT because of it's faster than a DFT and more efficient to implement. OFDM system treats the source symbols (e.g., the BPSK, QPSK or QAM symbols) at the transmitter as though they are in the frequency-domain. These symbols are used as the inputs to an IFFT block that brings the signal into the time-domain. The IFFT takes in N symbols at a time where N is the number of subcarriers in the system. Each of these N input symbols has a symbol period of T seconds. At the receiver, the OFDM message goes through the exact opposite operation in the fast fourier transform (FFT) to take from a time domain into the frequency domain. In practice, the baseband OFDM receiver performs the FFT of the receive message to recover the information that was originally sent.

The IFFT & FFT equations can be written as follows:

IFFT $X(k) = \frac{1}{N}\sum_{n=0}^{N-1} x(n)e^{j\frac{2\pi}{N}kn}$ k=0,1,2……N-1 (2.19)

FFT $x(n) = \frac{1}{N}\sum_{k-0}^{N-1} X(k)e^{-j\frac{2\pi}{N}kn}$ n=0,1,2……..N-1 (2.20)

2.2.7 Channel coding

To achieve satisfactory performance, coding is needed. High signal to noise ratio are required to achieve reasonable bit error rate in the presence of fading channel. Wireless systems use large constellation size to achieve high bit rates. Coding in this case is essential for achieving the highest possible rates in the presence of noise and interference. Proper coding is very important for wireless system.

2.2.7.1 Convolution coding

Convolution code is one of the most widely used channel coding in practical communication systems. Convolution code converts the entire data stream into one single codeword. It is a type of forward error correction (FEC) which its function is to improve the capacity of a channel by adding redundant information to the data being transmitted through the channel. Convolution codes are usually described using two parameters: the code rate (k/n) and the constraint length (K). The code rate is expressed as a ratio of the number of bits into the convolution encoder (k) to the number of channel symbols output by the convolution encoder (n) in a given encoder cycle. In practice, usually k=1 is chosen. K is the constraint length of the encoder where the encoder has K-1 memory elements [31].

The difference between convolution code and block code is that it has memory which is categorized by the constraint length (K). It does not need to segment the data stream into blocks of fixed size.

2.2.7.1.1 Convolution encoder (rate ½, K=3)

Convolution encoding data is accomplished using a shift registers and associated combinatorial logic that performs module-two addition. The combinatorial logic is often in the form of cascaded exclusive-or (XOR) gates. XOR gates are two

inputs and one output. For example, we consider 3 bit shift register where the first one takes the incoming data bit and the rest are the memory of the encoder.

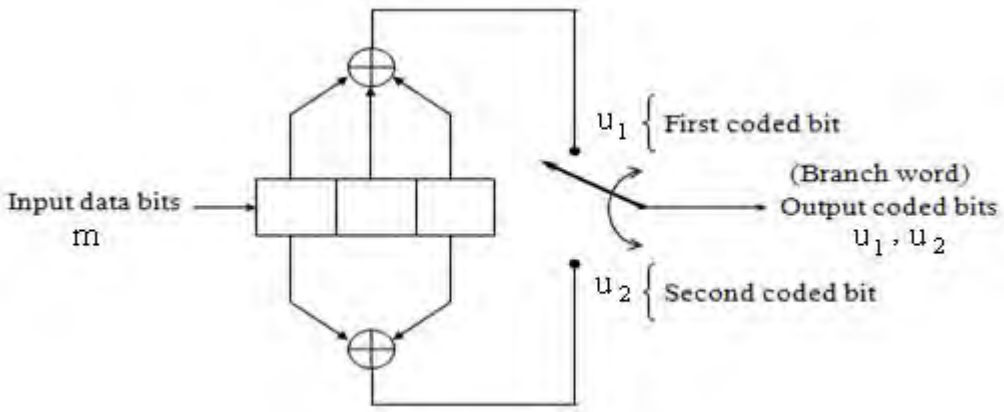

Fig. 2.15: Convolution encoder (rate ½, K=3)

Let the message sequence m=$(101)_2$. Initialize the memory before encoding the first bit (all-zero). Clear out the memory after encoding the last bit (all-zero).

Assume that the outputs of the flip-flops in the shift register are initially cleared, *i.e.* their outputs are zeroes. The first clock cycle makes the first input bit, a one, available to the encoder. The flip-flop outputs are both ones. The inputs to the modulo-two adders are all ones, so the output of the encoder is 11_2.

The second clock cycle makes the second input bit available to the encoder. The left-hand flip-flop clocks in the incoming input bit, which was a zero, and the right-hand flip-flop in the one bit (shifting from left hand to right hand). The inputs to the top modulo-two adder are 010_2, so the output is a one. The inputs to the bottom modulo-two adder are 00_2, so the output is also a one. So the encoder outputs 10_2 for the channel symbols.

The third clock cycle makes the third input bit (a one) available to the encoder. The inputs to the top modulo-two adder are 101_2, so the output is a zero. The inputs to the bottom modulo-two adder are 11_2, so the output is zero. So the encoder outputs 00_2 for the channel symbols and so on.

The circuit diagram is shown below the process:

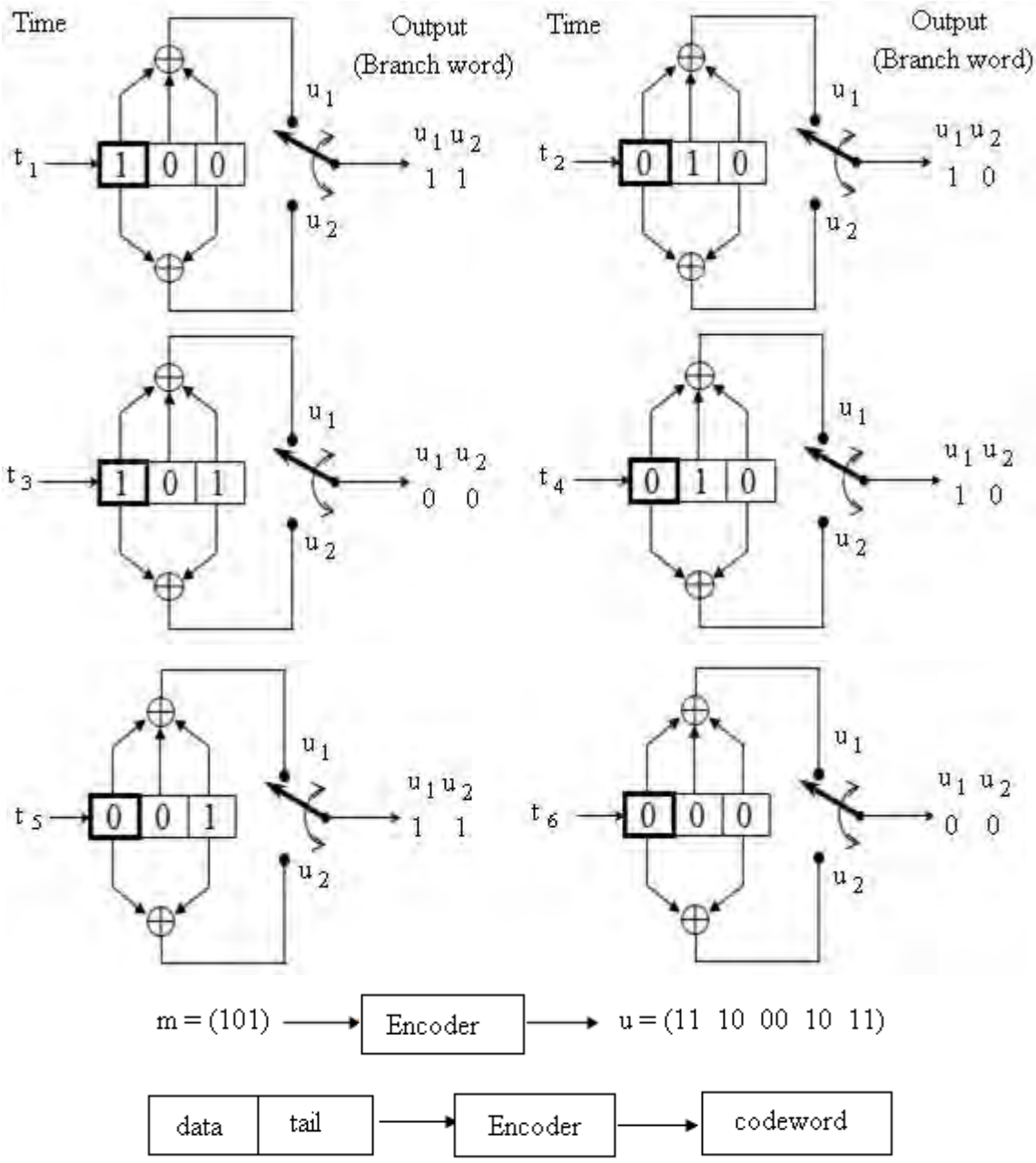

Fig. 2.16: A message sequence with rate ½, K=3 as it goes through the encoder

After all of the inputs have been presented to the encoder, the output sequence will be: 11 10 00 10 11_2.

2.2.7.1.2 Viterbi decoding

Viterbi decoding is one of two types of decoding algorithms used with convolution encoding. The other type is sequential decoding. Sequential decoding has the advantage that it can perform very well with long constraint length convolution codes, but it has a variable decoding time. Viterbi decoding has the advantage that it has a fixed decoding time. It is well suited to hardware decoder implementation. But its computational requirements grow exponentially as a function of the constraint length. Viterbi decoding is essentially performs the maximum likelihood decoding. It reduces the computational load by taking advantage of special structure in code trellis. The Viterbi decoder examines an entire received sequence of a given length. The decoder computes a metric for each path and makes a decision based on this metric. All paths are followed until two paths converge on one node. Then the path with the higher metric is kept and the one with lower metric is discarded. The paths selected are called the survivors [32].

The metric we are going to use Hamming distance between the received channel symbol pair and the possible channel symbol pairs. The Hamming distance is computed by simply counting how many bits are different between the received channel symbol pair and the possible channel symbol pairs. The results can only be zero, one, or two. The Hamming distance (or other metric) values we compute at each time instant for the paths between the states at the previous time instant and the states at the current time instant are called branch metrics. For the first time instant, we are going to save these results as "accumulated error metric" values, associated with states. For the second time instant on, the accumulated error metrics will be computed by adding the previous accumulated error metrics to the current branch metrics.

At t = 1, we received 11_2. The only possible channel symbol pairs we could have received are 00_2 and 11_2. The Hamming distance between 00_2 and 11_2 is two. The Hamming distance between 11_2 and 11_2 is zero. Therefore, the accumulated error metric value for the branch from state 00_2 to state 00_2 is two and the branch from state 00_2 to state 10_2 is zero. The accumulated error metric values for the other two states are undefined. The Fig. 2.17 below illustrates the results at t = 1.

At t=2, we compare the accumulated error metrics associated with each branch and discard the larger one of each pair of branches leading into a given state. If the members of a pair of accumulated error metrics going into a particular state are equal, we just save that value. The previous large accumulated error metric value is two. So we reject its path. Now we receive 10_2. The Hamming distance between 10_2 and 10_2 is zero. The Hamming distance between 10_2 and 01_2 is two. Therefore, the accumulated error metric value for the branch from state 10_2 to state 01_2 is zero and the branch from state 10_2 to state 11_2 is two. So we select the path from state 10_2 to state 01_2 and so on.

At t = 5, the path through the trellis corresponding to the actual message, shown in bold, is still associated with the smallest accumulated error metric. The Viterbi decoder exploits to recover the original message. We also get two extra flushing bits.

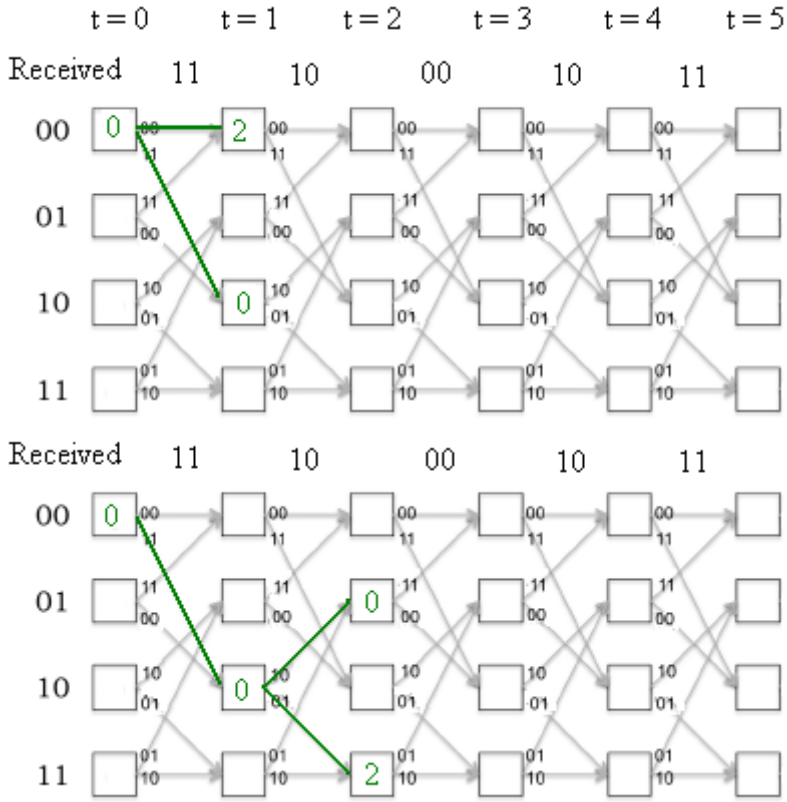

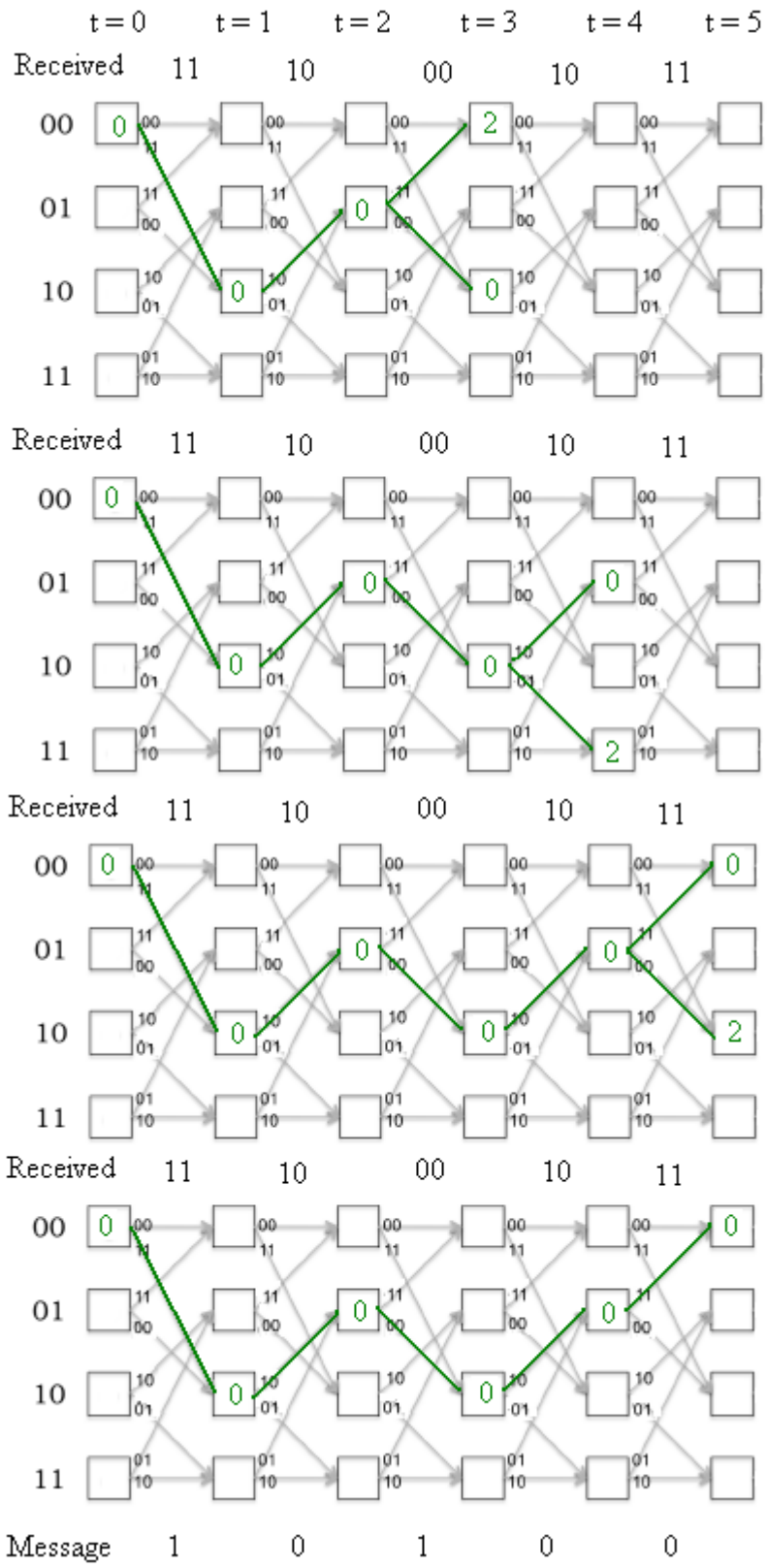

Fig. 2.17: Viterbi decoder decoded message bit

2.2.7.2 Space frequency block code (SFBC)

SFBC for OFDM systems with multiple transmit antennas, where coding is applied in the frequency domain (OFDM carriers) rather than in the time domain (OFDM symbols).

The domain of space-frequency coding was introduced in [33]. Space frequency coding basically extends the theory of space-time coding for narrowband flat fading channels to broadband time variant and frequency selective channels. The application of classical space-time coding techniques for narrowband flat fading channels to OFDM seems straightforward, since the individual subcarriers can be seen as independently flat fading channels. However, it was shown that the design criteria for space-frequency codes operating in the space-time. The frequency domain is different from classical space-time codes for narrowband fading channels as introduced in [34].

Alamouti space time block code [35] in the frequency domain (over two adjacent OFDM carriers), resulting in a space-frequency block coded system with two transmit antennas. Space diversity achieves a maximum diversity gain for two transmit antennas without rate loss. They have to be applied under the assumption that the channel coefficients remain constant for two subsequent symbol durations in order to guarantee the diversity gain.

The mapping scheme of the data symbols for SFBC with two transmit antennas is shown in Table 2.1.The mapping scheme for SFBC method in MIMO-OFDM will be applied such that on the first antenna the original data and negative second conjugate data will be transmitted, while the second antenna the conjugate original data and second data will be transmitted.

Table 2.1: Mapping with SFBC and two transmit antennas

At time i	Frequency k	Frequency k+1
Tx1	$S_k^{Tx1,(i)} = S_k^{(i)}$	$S_{k+1}^{Tx1,(i)} = -(S_{k+1}^{(i)})^*$
Tx2	$S_k^{Tx2,(i)} = S_{k+1}^{(i)}$	$S_{k+1}^{Tx2,(i)} = (S_k^{(i)})^*$

2.2.8 RF modulation

The output of the OFDM modulator generates a base band signal, which must be mixed up to the required transmission frequency. This can be implemented using analog techniques as shown in Fig. 2.18.

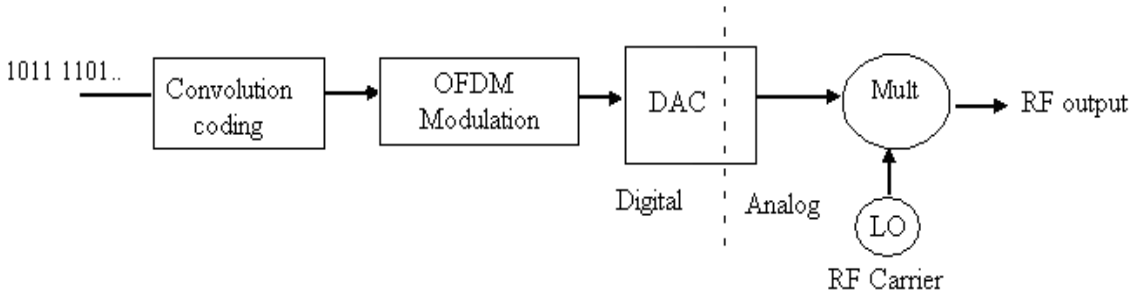

Fig. 2.18: RF modulation of OFDM signals using analog technique

2.2.9 Inter symbol interference and inter carrier interference

In a multipath environment, a transmitted symbol takes different times to reach the receiver through different propagation paths. The delay spread can cause ISI when adjacent data symbols overlap and interfere with each other due to different delays on different propagation paths [36]. The number of interfering symbols in a single-carrier modulated system is given by

$$N_{\text{ISI, single carrier}} = \tau_{\max}/T_d \tag{2.21}$$

For high data rate applications with very short symbol duration $T_d < \tau_{\max}$. If the duration of the transmitted symbol is significantly larger than the maximum delay $T_d >> \tau_{\max}$, the channel produces a negligible amount of ISI. This effect is exploited with multi-carrier transmission where the duration per transmitted symbol increases with the number of sub-carriers N_c and hence, the amount of ISI decreases. The number of interfering symbols in a multi-carrier modulated system is given by

$$N_{\text{ISI, multi carrier}} = \tau_{\max}/N_c T_d \tag{2.22}$$

The maximum Doppler spread in mobile radio applications using single-carrier modulation is typically much less than the distance between adjacent channels, such that the effect of interference on adjacent channels due to Doppler spread is not a problem for single-carrier modulated systems. For multi-carrier modulated systems, ICI caused by frequency offset and phase noise and degrades system performance. Rotation

of the constellation points caused by the phase noise may be observed in communication system. For the Doppler shift in the channel or the difference between the transmitter and receiver local oscillator frequencies, frequency offset occurs. The carrier frequency offset and phase noise breaks down the orthogonality among subcarriers and the signals transmitted on each carrier are not independent of each other, leading to ICI.

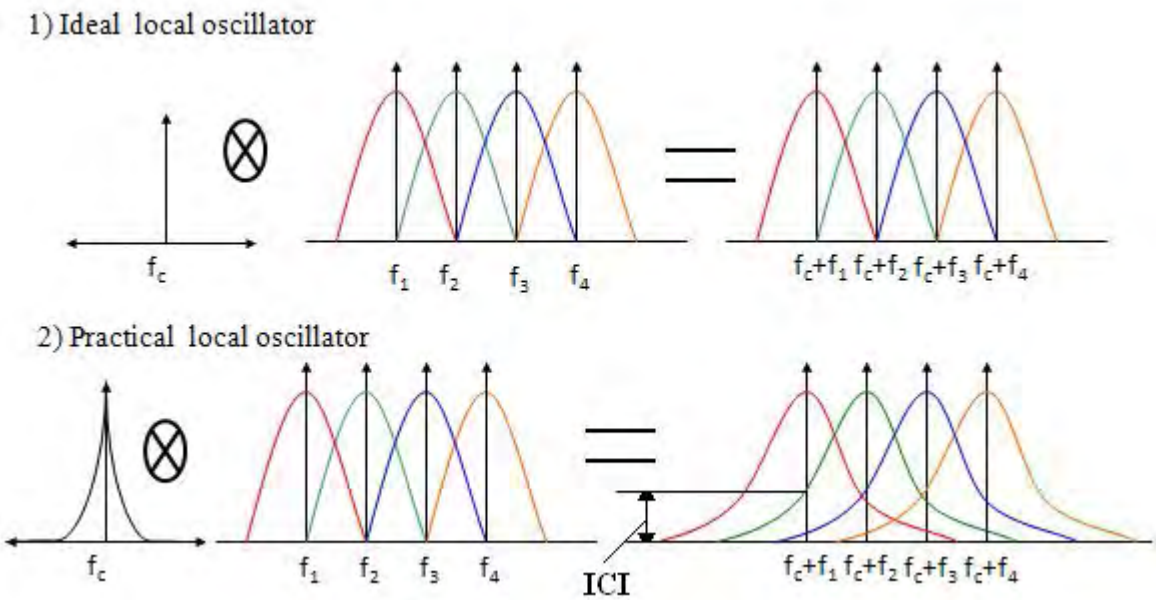

Fig. 2.19: ICI effect

2.2.10 Guard period and cyclic prefix

A cyclic prefix is a copy of the last part of the OFDM symbol that is pretended to the transmitted symbol remove at the receiver before the demodulation. To eliminate ICI, the OFDM symbol is cyclically extended in the guard interval. This guard period is a cyclic copy that extends the length of the symbol waveform. Fig. 2.20 shows the insertion of a guard period. The total length of the symbol is $T_S = T_g + T_{fft}$, where T_S is the total length of the symbol in samples, T_g is the length of the guard period in samples, and T_{fft} is the size of the IFFT used to generate the OFDM signal. In addition to protecting the OFDM from ISI, the guard period also provides protection against time-offset errors in the receiver.

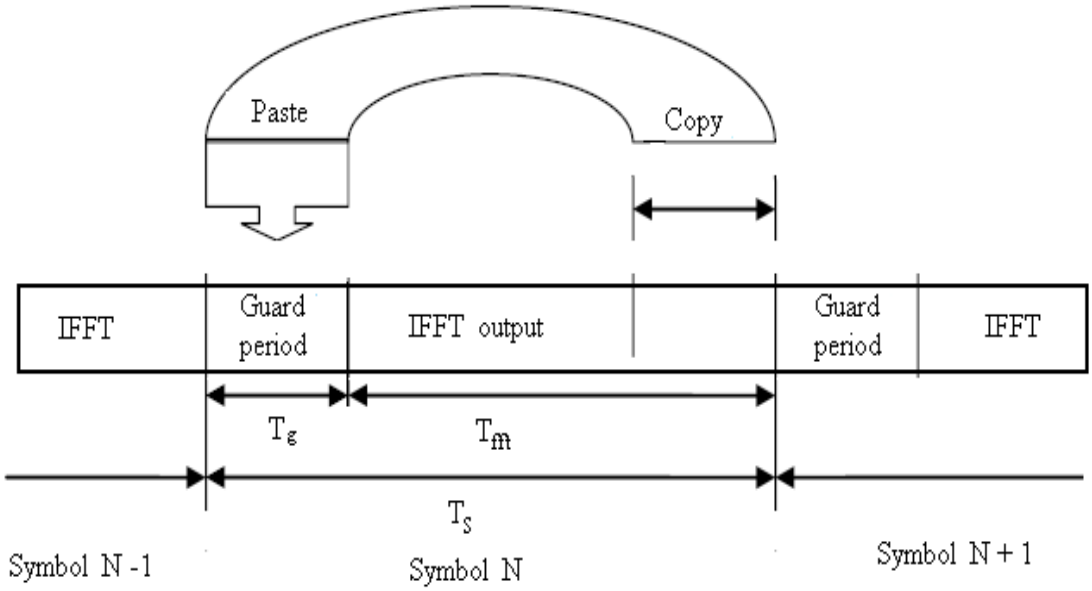

Fig. 2.20: Guard period insertion in OFDM

1. A Guard time is introduced at the end of each OFDM symbol in form of cyclic prefix to prevent ISI.
2. The Guard time is cyclically extended to avoid ICI - integer number of cycles in the symbol interval.
3. Guard Time > Multipath Delay Spread, to guarantee zero ISI and ICI.

2.2.11 Additive white gaussian noise (AWGN) channel

The AWGN channel is the simplest channel model used in most communication systems. Noise exists in all communications systems operating over an analog physical channel. The main sources are thermal background noise, antenna temperature, electrical noise in the receiver amplifiers and inter-cellular interference. In addition to this noise and other noise can also be generated internally to the communications system as a result of ISI, ICI, and inter modulation distortion. These sources of noise decrease the signal to noise ratio (SNR), ultimately limiting the spectral efficiency of the system.

2.2.12 Advantages of OFDM

OFDM has several advantages over single carrier modulation. Some of advantages are:

1. **High spectral efficiency:**

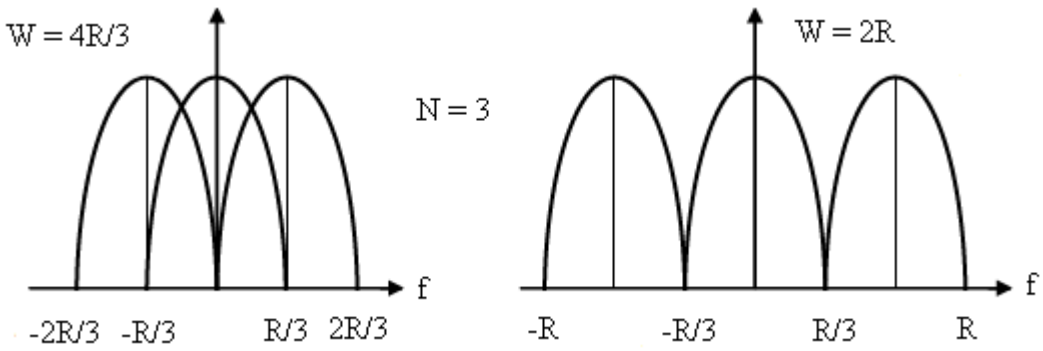

Fig. 2.21: Spectrum Efficiency of OFDM Compared to FDM

If the number of subcarriers is N and T_s is symbol duration, then total bandwidth required is $BW_{total} = \frac{(N+1)}{T_s}$

Since the transmission rate of each subchannel is $\frac{1}{T}$ symbols/sec. so, the total transmission rate of OFDM signal is $\frac{N}{T}$ symbol/sec.

Spectral efficiency of OFDM, $\eta_{OFDM} = \frac{Transmission \quad rate}{Bandwidth}$

$$= \frac{N/T}{(N+1)/T_s}$$

$$= (\frac{N}{N+1})(\frac{T_s}{T})$$

$$= (\frac{N}{N+1})(\frac{T_s}{T_s + T_g}) \qquad (2.23)$$

On the other hand, the bandwidth required for serial transmission of the same data is $BW_{total} = \frac{2N}{T_s}$

Spectral efficiency of FDM, $\eta_{FDM} = \dfrac{Transmission \quad rate}{Bandwidth}$

$$= \frac{1/T}{2N/T_s}$$

$$= (\frac{1}{2N})(\frac{T_s}{T})$$

$$= (\frac{1}{2N})(\frac{T_s}{T_s + T_g}) \tag{2.24}$$

So, OFDM achieves high spectral efficiency by allowing the subcarriers to overlap in the frequency domain.

2. Immunity to frequency selective fading channels:

In a multipath channel, the reflected signals are delayed. In the receiver side, reflected signals add to the main signal and cause either gains in the signal strength or loss (deep fade) in the signal strength. Deep fade means the signal is nearly wiped out [37].

In a channel where deep fades occurs at selected frequencies is called a frequency selective fading channel (Fig. 2.22) and those frequencies depends upon the environment. In a single carrier system the entire signal is lost during the fading intervals. But as in case of OFDM the signal consists of many subcarriers, so only few subcarriers are affected during the fading intervals (Fig. 2.23) and hence a very small percentage of the signal is lost which can be easily recovered by proper coding and interleaving.

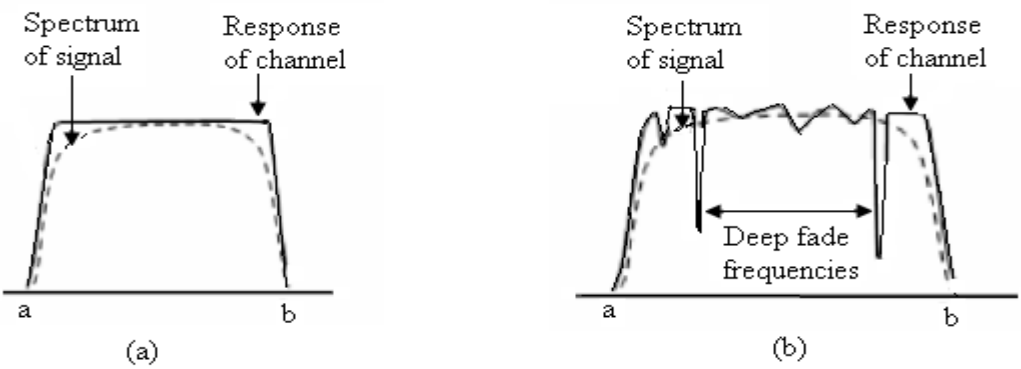

Fig. 2.22: (a) The signal and the channel frequency response (b) A fading channel frequency response

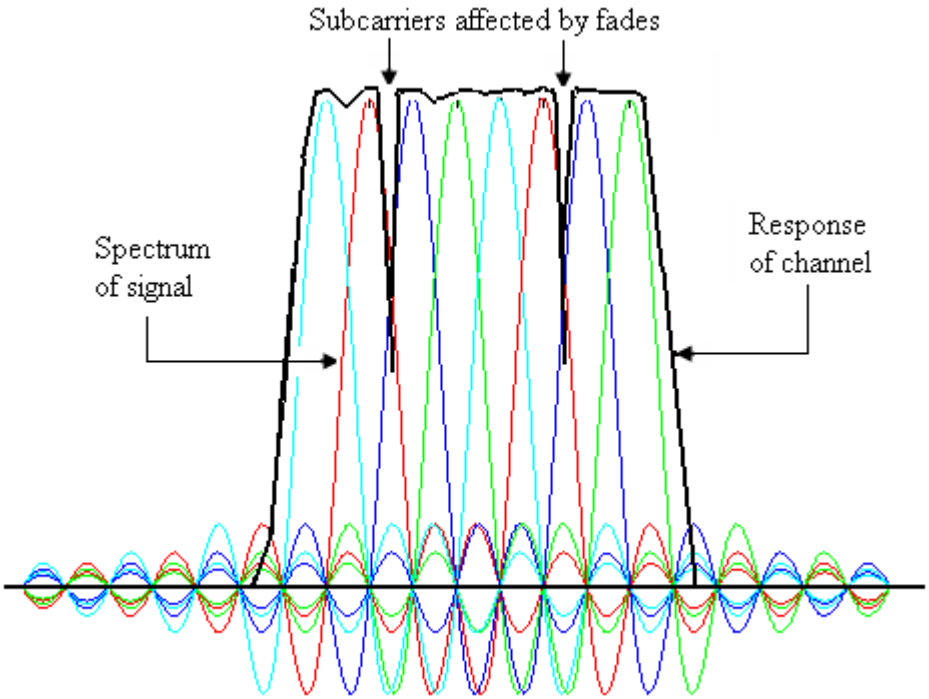

Fig. 2.23: Immunity of OFDM to frequency selective fading channel

3. Multipath delay spread tolerance:

OFDM is highly immune to multipath delay spread that causes ISI in wireless channels. Since the symbol duration is made larger (by converting a high data rate signal into N low rate signals), the effect of delay spread is reduced by the same factor. Also by introducing the concepts of guard time and cyclic extension, the effects of ISI and ICI are removed completely.

4. Decrease complexity:

The key difference between single carrier modulation and OFDM is FFT vs equalizer. Complexity of 64 point radix 4 FFT in IEEE 802.11a needs $3*N*(\log_2 N-2)/8$ = 96 million real multiplications per second. While 16 tap Gmsk equilizer at 24MHz means 2*1*624 = 768 million real multiplications per second.

5. Efficient Modulation and Demodulation:

Modulation and Demodulation of the subcarriers is done using IFFT and FFT methods respectively, which are computationally efficient.

2.2.13 Disadvantages of OFDM

Disadvantages of OFDM systems are:

1. Sensitive to frequency offsets, timing errors and phase noise
2. Relatively higher peak to average power ratio (PAPR) compared to single carrier system, which tends to reduce the power efficiency of the RF amplifier.

2.3 Multiple Input Multiple Output (MIMO)

In a conventional mobile wireless communication system, there is only one antenna at both transmitter and receiver. This system which is called the single input single output (SISO) antenna system suffers a bottleneck in terms of capacity due to the Shannon-Nyquist criterion [38, 39]. Future wireless mobile services demand much higher data bit-rate transmission. In order to increase the capacity of the SISO systems to meet such demand, the bandwidth and transmission power have to be increased significantly. Fortunately, recent developments have shown that using multiple input multiple output (MIMO) systems increase the capacity in wireless communication substantially without increasing the transmission power and bandwidth [40, 41]. The MIMO systems offer very higher data rates in the same bandwidth as compared to the SISO systems. In the MIMO systems, multiple antenna elements are required at both transmitter and receiver.

2.3.1 Four basic system models

There are four basic system models exist that are used in wireless communication system. These are:

i) Single input single output (SISO) is a radio system where neither the transmitter nor receiver has multiple antennas.

ii) Single input multiple output (SIMO) is a degenerate case when the transmitter has a single antenna.

iii) Multiple input single output (MISO) is a degenerate case when the receiver has a single antenna.

iv) Multiple input multiple output (MIMO) is a radio system where the transmitter and receiver have multiple antennas.

Fig. 2.24 shows the four basic wireless system models.

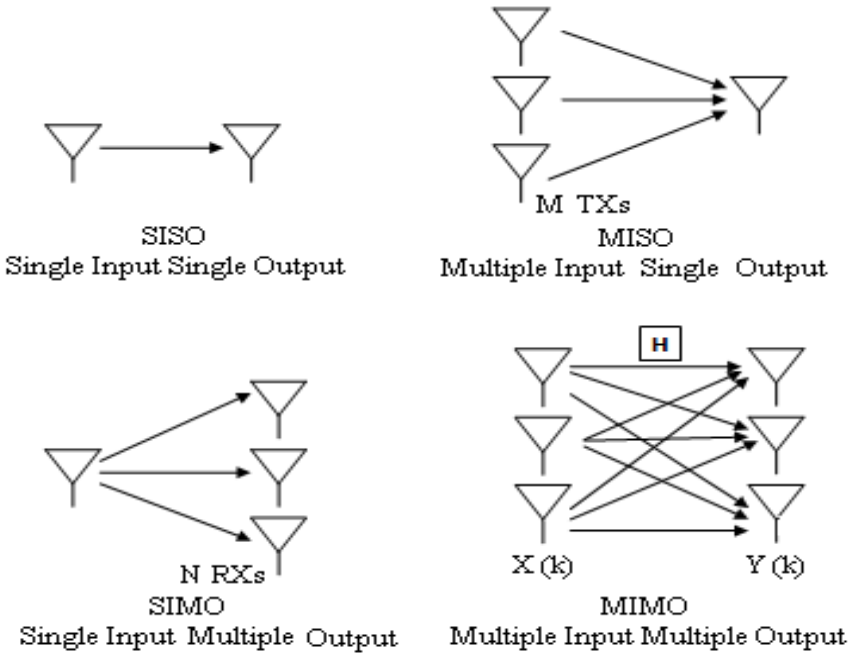

Fig. 2.24: Four basics model

2.3.2 Channel capacity

Channel capacity is the maximum information rate that can be transmitted and received with arbitrarily low probability of error at the receiver. A common representation of the channel capacity is within a unit bandwidth of the channel and can be expressed in bps/Hz. This representation is also known as spectral (bandwidth) efficiency.

2.3.2.1 Capacity of SISO system

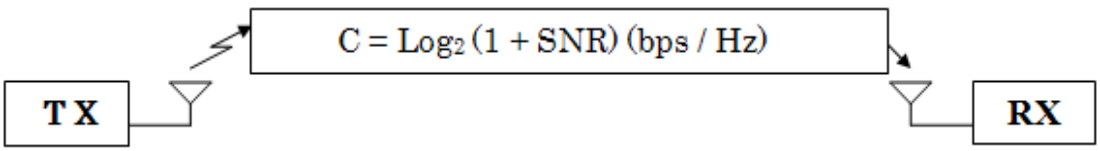

Fig. 2.25: Capacity of SISO System

According to Shannon capacity of wireless channels, from Fig. 2.25 a single channel corrupted by an AWGN, the capacity is:

$$C_{Shannon} = B.\log_2[1+SNR](bps/Hz) \tag{2.25}$$

where, C is the Shannon limit on channel capacity, SNR is signal-to-noise ratio, B is bandwidth of channel.

In the practical case of time varying and randomly fading wireless channel, the capacity can be written as:

$$C_{Shannon} = B.\log_2[1+SNR.|H|^2](bps/Hz) \tag{2.26}$$

where, H is the 1x1 unit-power complex matrix Gaussian amplitude of the channel. Moreover, it has been noticed that the capacity is very small due to fading events.

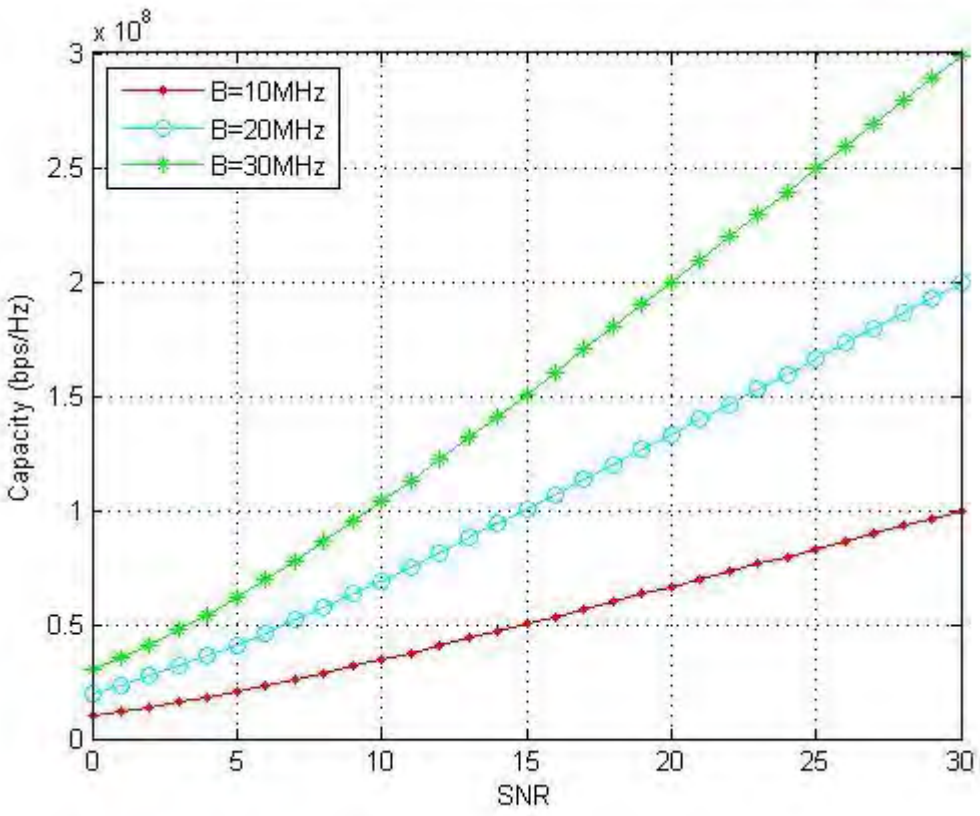

Fig. 2.26: Shanons capacity for SISO system

From the above expression it is clear that theoretically capacity increases as the bandwidth is increased which is shown in Fig. 2.26.

2.3.2.2 Capacity of SIMO system

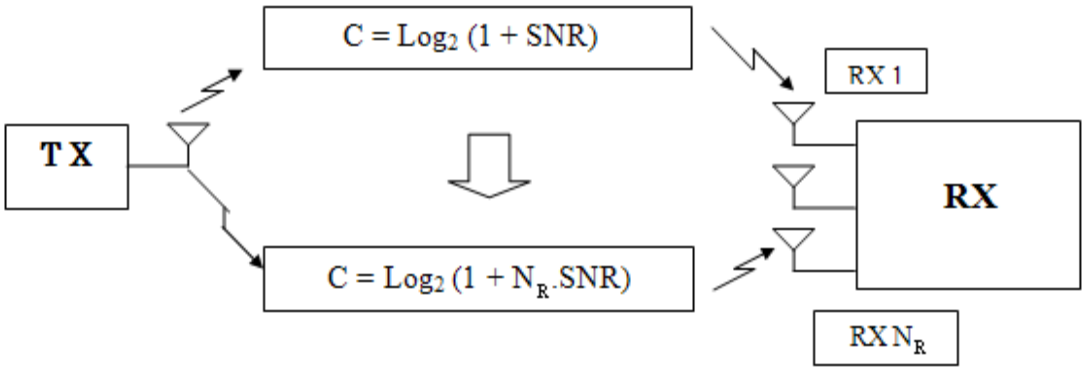

Fig. 2.27: Capacity of SIMO system

From Fig. 2.27, we have N_R antennas at receiver and only one at transmitter. If the signals received on these antennas have on same amplitude, then they can be added coherently to produce N increase in the signal power. On the other hand, there are N sets of noise that are added incoherently and result in N fold increase in the noise power. Hence, there is an overall increase in the SNR [42].

$$SNR \approx \frac{N_R^{\ 2}.Signal\ \ power}{N_R.Noise\ \ power} = N_R.SNR \tag{2.27}$$

So the capacity of SIMO channel is:

$$C_{SIMO} = B.\log_2[1 + N_R.SNR](bps/Hz) \tag{2.28}$$

The capacity of SIMO system in the practical case of time-varying and randomly fading wireless channel is:

$$C_{SIMO} = B.\log_2[1 + SNR.HH^*](bps/Hz) \tag{2.29}$$

where H is $1xN_R$ channel vector and ( )* is the transpose conjugate.

2.3.2.3 Capacity of MISO system

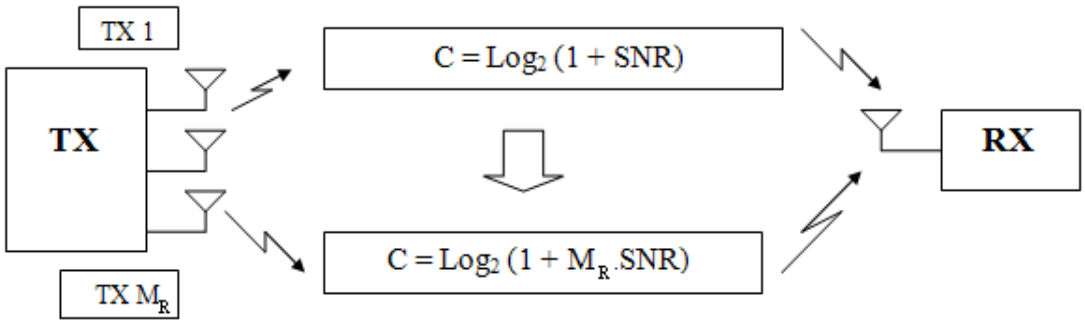

Fig. 2.28: Capacity of MISO System

Form Fig. 2.28, we have M_R antennas at transmitter and only one at receiver. As same as the case of the SIMO system, we have capacity of MISO system

$$C_{MISO} = B.\log_2[1 + M_R.SNR](bps/Hz) \tag{2.30}$$

In the practical case of time-varying and randomly fading wireless channel, it is shown that the capacity of M_R x 1 MISO system is:

$$C_{MISO} = B.\log_2[1 + SNR.HH^*](bps/Hz) \tag{2.31}$$

Compared with SISO system, the capacity of SIMO and MISO system shows improvement. The increase in capacity is due to the spatial diversity which reduces fading and SNR improvement. However, the SNR improvement is limited, since the SNR is increasing inside the log function.

2.3.2.4 Capacity of MIMO system

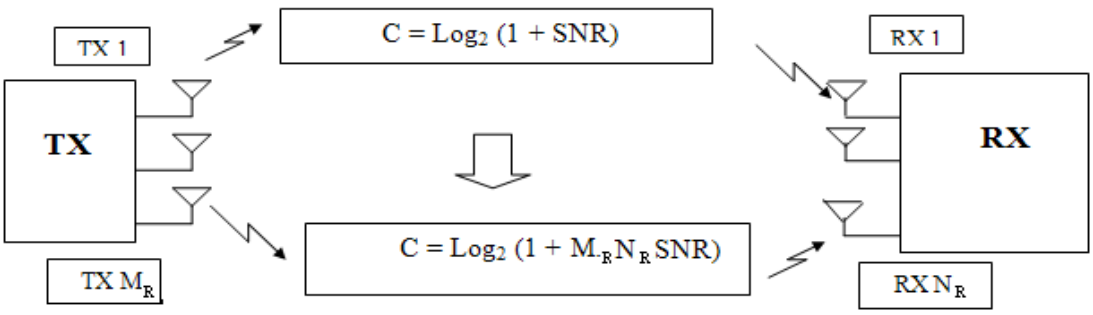

Fig. 2.29: Capacity of MIMO System

For the MIMO system, we have M_R antennas at transmitter and N_R antennas at receiver in Fig. 2.29.

In this case, the MIMO system can be view in effect as a combination of the SIMO and MISO channels. As same as the case in **2.3.2.2** and **2.3.2.3**, we have:

$$SNR \approx \frac{N_R^{\ 2}.M_R^{\ 2}.Signal\ \ power}{N_R.M_R.Noise\ \ power} = N_R.M_R.SNR \tag{2.32}$$

So the capacity of MIMO channels in this case is:

$$C_{MIMO} = B.\log_2[1 + M_R.N_R.SNR](bps/Hz) \tag{2.33}$$

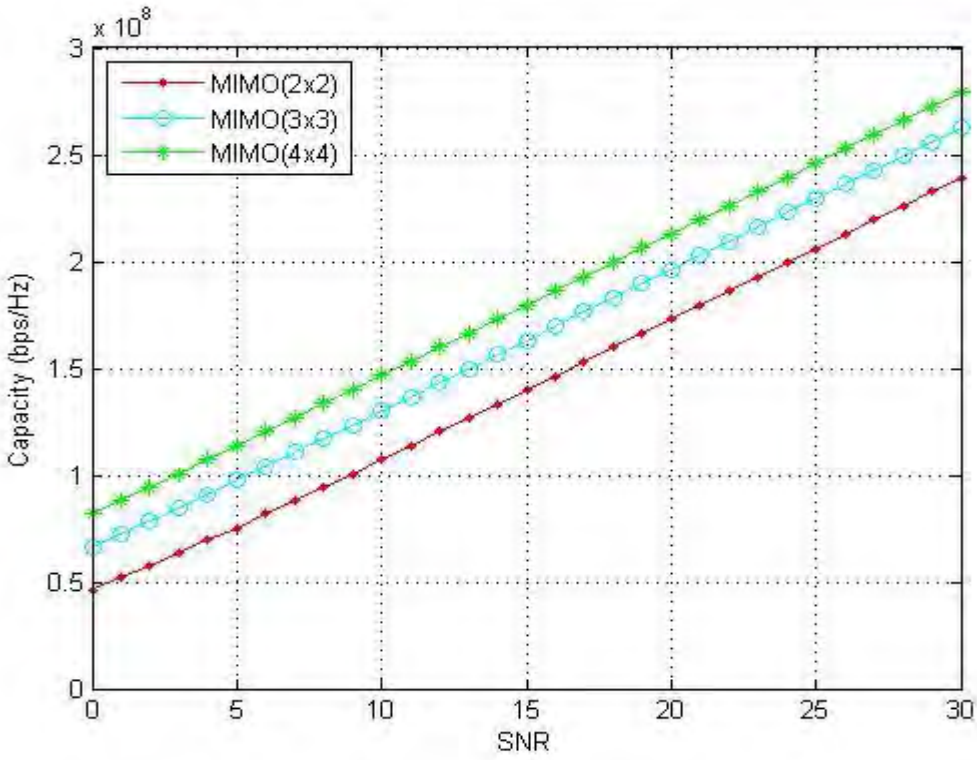

Fig. 2.30: Channel capacity MIMO system

In Fig. 2.30, the channel capacity is increasing when number of transmitter and receiver are increasing. Thus, we can see that the channel capacity for the MIMO systems is higher than that of SIMO and MISO system. But in this case, the capacity is increasing inside the log function. This means that trying to increase the data rate by simply transmitting more power is extremely costly.

Thus, we can get linear increase in capacity of the MIMO channels with respect to the number of transmitting antennas. So, the key principle at work here is that it is more beneficial to transmit data using many different low-powered channels than using one single, high-powered channel.

2.3.3 Spatial multiplexing

Spatial multiplexing requires MIMO antenna configuration. In spatial multiplexing, a high rate signal is split into multiple lower rate streams and each stream is transmitted from a different transmit antenna in the same frequency channel. If these signals arrive at the receiver antenna array with sufficiently different spatial signatures, the receiver can separate these streams. Spatial multiplexing is a very powerful technique for increasing channel capacity at higher signal to noise ratio (SNR). The maximum number of spatial streams is limited by the lesser in the number of antennas at the transmitter or receiver. Spatial multiplexing can be used with or without transmit channel knowledge.

2.3.4 Antenna diversity combining techniques

Diversity is a measure of reliability of a link. In multiple antenna systems, there is a path between each transmit and receive antenna. If each of the paths is independently faded, then we can obtain independently faded replicas of data symbols by sending them through different paths. Then we can use these independently faded replicas to improve our reception. Diversity can also be thought of as the number of independent fading coefficients in the channel. In a system with n_t transmit, n_r receive antennas, assuming the channel is Rayleigh faded, the maximum diversity gain is $n_t n_r$, the number of independent fading coefficients in the channel. In other words, the fastest error probability can decay with SNR is $SNR^{-n_t n_r}$.

There are five categories of diversities, *i.e.* frequency diversity, time diversity, spatial diversity, pattern diversity and polarization diversity. Amongst the five diversities, only the spatial, pattern and polarization diversity techniques are categorized as antenna diversity.

There are four different types of diversity combining techniques. They are discussed in detail below [43].

2.3.4.1 Switched combining

The switched combining technique requires only one receiver radio between the N_R branches as shown in Fig. 2.31. The receiver is switched to other branches when the SNR on the current branch is lower than a predefined threshold. Whereby, other combining techniques require N_R receivers to monitor the received instantaneous signals level of every branch when there are N_R element antennas. Due to size restrictions, battery life and complexity, the switched combining technique is presently implemented in mobile terminals with diversity antennas [44]. The optimum performance that a switched combiner can achieve is similar to that of a selection combiner.

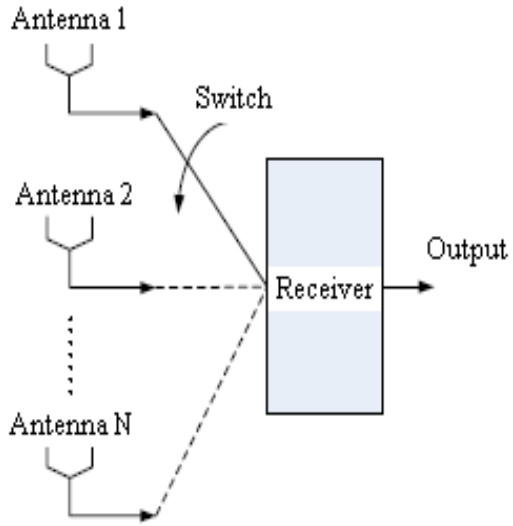

Fig. 2.31: Switched combining for N_R antenna elements with only one receiver

2.3.4.2 Selection combining

The selection combining technique is similar to the switched combining technique except that N_R receivers are required to monitor instantaneous SNR at all branches. The branch with the highest SNR is selected as the output signal.

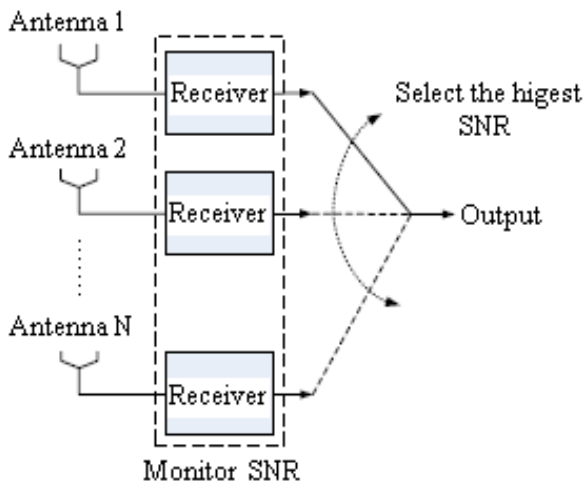

Fig. 2.32: Block diagram of selection combining for N_R antenna elements

2.3.4.3 Equal gain combining

Both switched and selection combining techniques use the signal from one of the branches as the output signal. In order to improve SNR at the output, the signals from all branches are combined to the output signal. However, the signal from each branch is not in-phase. Therefore, each branch must be multiplied by a complex phasor having a phase $-\theta_i$, where θ_i is the phase of the channel corresponding to branch i (*i.e.* co-phased) as shown in Fig. 2.33. When this is achieved, all signals will have zero phase and are combined coherently.

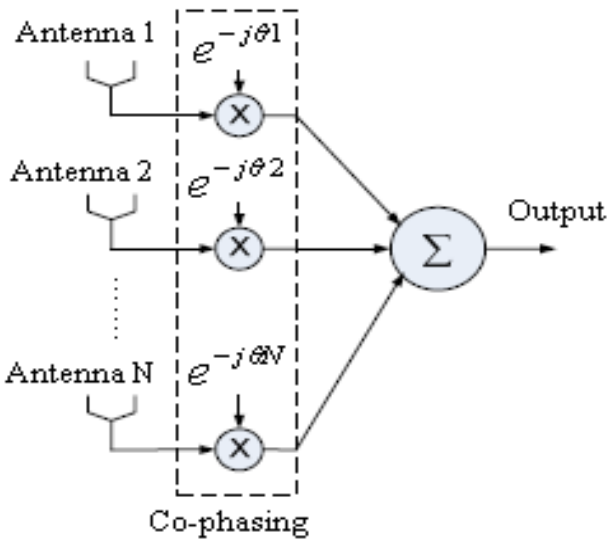

Fig. 2.33: Block diagram of equal gain combining for N_R antenna elements

2.3.4.4 Maximum ratio combining

In the equal gain combining technique, all the branches may not have a similar SNR. Sometimes one of the branches has a much lower SNR than the other branches and this will reduce the overall SNR to a lower value at the output. In order to maximize the SNR at the output, each branch is applied with a weight, W_i before all the signals are combined coherently as shown in Fig. 2.34. In order to maximize the SNR at the output, a branch with a higher SNR will be given a higher weighting.

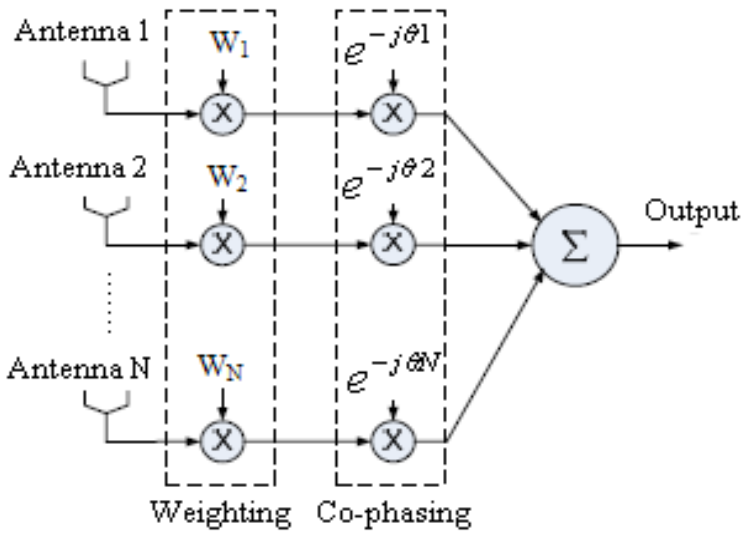

Fig. 2.34: Block diagram of maximum ratio combining for N_R antenna elements

2.3.5 Performance improvements in MIMO system

As defined in [45], spatial multiplexing gain r and diversity gain d as

$$\lim_{SNR\to\infty} \frac{R(SNR)}{\log SNR} = r \tag{2.34}$$

$$\lim_{SNR\to\infty} \frac{P_e(SNR)}{\log SNR} = -d \tag{2.35}$$

Then average error probability decays in SNR. That is $P_e(SNR) = SNR^{-d}$. According to the above definition, rate R = r log SNR. It is shown in [46] that for the Rayleigh fading MIMO channel with n_t transmit, n_r receive antennas, the high SNR outage probability at rate R = r log SNR is given by

$$P_{outage} \approx SNR^{-(n_t-r)(n_r-r)} \quad \text{for integer } r = 0, 1, \ldots, \min(n_r, n_t) \tag{2.36}$$

When operating at a multiplexing gain of r, the maximum diversity gain we can get $(n_t - r)(n_r - r)$. Multiple antennas increase the range and the coverage; as a result more areas can be covered with minimum base stations. It also reduces the transmitting power.

CHAPTER 3

DATA CONJUGATE AND CHANNEL CODING WITH SELF-CANCELLATION

3.1 Self-Cancellation Scheme in MIMO-OFDM

OFDM is a multicarrier modulation technique which is used in both wired and wireless communication. By combining multiple low data rate subcarriers, OFDM system can provide a composite high data rate with long symbol duration and high spectral efficiency. Antenna diversity has been applied to OFDM system. That is called MIMO-OFDM system to improve the performance of the conventional system.

In this thesis, we have established analytical models to reduce the ICI using self-cancellation data conjugate (SCDC) with convolution coding (CC) and space frequency block code (SFBC) in 2x2 MIMO-OFDM system integrating the effect of phase noise and frequency offset. The performance of the system in the presence of frequency offset and phase noise has been evaluated in terms of ICI, CIR and BER.

3.2 Methods of ICI Reduction

Over the years, researchers have proposed various methods to combat the ICI in OFDM systems. The existing approaches that have been developed to reduce ICI can be categorized as frequency-domain equalization [47], time-domain windowing [48], self-cancellation (SC) scheme, pulse shaping [49], maximum likelihood (ML) estimation [50], extended Kalman filtering (EKF) [51] etc. SC is very effective, good for lower modulation and frequency offsets. It is easy to software and hardware implementation.

3.3 System Model in 2x2 MIMO-OFDM

The block diagram of a typical discrete-time baseband equivalent model of 2x2 MIMO-OFDM systems is shown in Fig. 3.1. As shown, input bits are first encoded by using suitable modulation technique like - BPSK, QPSK or M-QAM. The N symbols

are transferred by the serial-to-parallel converter (S/P) and in this stage duration of input bits is increased. After S/P converter, the data symbols are remapped. The mapping scheme for data conjugate method in MIMO-OFDM is applied such that on the first antenna the original data is transmitted and the second antenna the conjugate data is transmitted. Both antenna, the modulated symbols are serialized using a parallel-to-serial converter (P/S), then converted to analog via the digital-to-analog converter (DAC) and passing through high power amplifier before being sent down to the channel. At the receiver side, the received symbols are passed through low noise amplifier and converted from analog to digital using the analog-to-digital converter (ADC) and transferred by the S/P both antenna.

The original signal can be recovered from the simple relation of $Z_k^{'} = Y_k^1 + Y_k^{2^*}$. Here, Y_k^1 and Y_k^2 are the first antenna and second antenna kth subcarrier data. Finally, the information data can be found through the detection process. In SFBC method, the original signal can be recovered from the simple relation of $Z_k^{'} = Y_k^1 + Y_{k+1}^{2^*}$. Here, Y_{k+1}^2 is the second antenna (k+1)th subcarrier data. Here, the cyclic prefix is not considered for the ease of analysis.

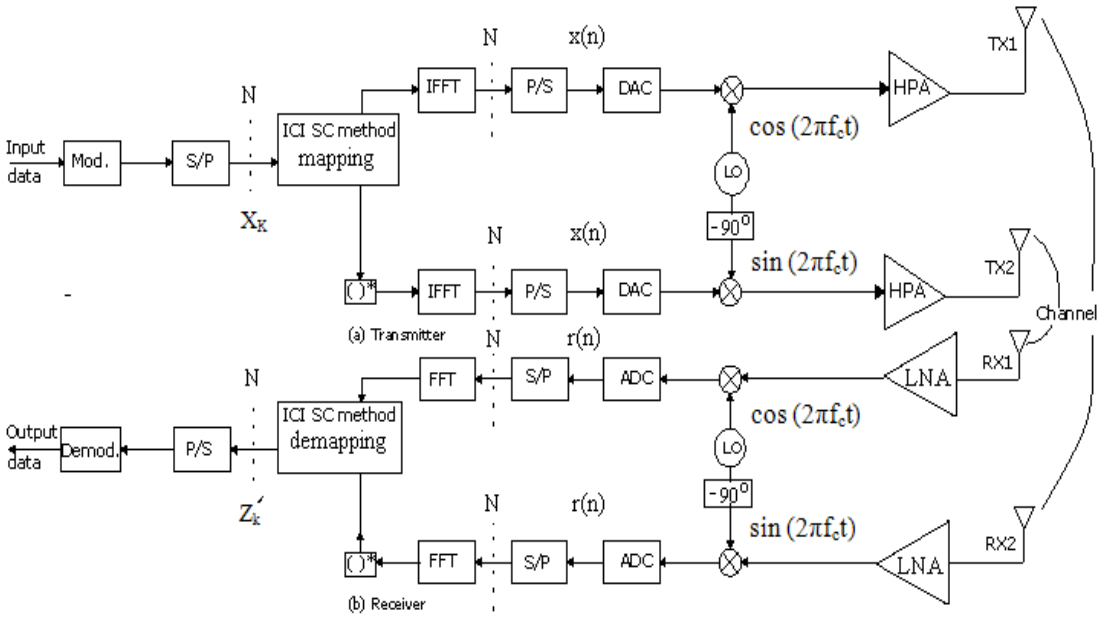

Fig. 3.1: Block diagram of SCDC method in 2x2 MIMO-OFDM system model (a) Transmitter (b) Receiver

The complex baseband MIMO-OFDM signal after IFFT at the transmitter,

$$x^{t}(n) = \sum_{k=0}^{N-1} X_k^t e^{j(\frac{2\pi}{N})kn} \qquad \text{for } 0 \le n \le N\text{-}1 \qquad (3.1)$$

$$t = 1 \text{ or } 2$$

where, $j = \sqrt{-1}$, N is the total number of subcarriers, t means transmitter antenna number, x_k^t is data symbol for kth subcarrier.

Received signal is affected by phase noise and frequency offset. So, it can be expressed as,

$$r^{\tau}(n) = \{\sum_{t=1}^{2}[x^t(n) \otimes h^t(n) + w(n)]\} e^{j[2\pi\Delta f^{\tau} t + \varphi^{\tau}(n)]}$$

$$\tau = 1 \text{ or } 2 \qquad (3.2)$$

where, Δf^{τ} and $\varphi^{\tau}(n)$ are frequency offset and phase noise. τ means received antenna number. *x(n), h(n), w(n), r(n)* are transmitted signal, channel impulse response, complex Gaussian noise and received signal respectively.

The FFT of the received signal can be expressed as,

$$Y_k^{\tau} = \frac{1}{N}\sum_{n=0}^{N-1} r^{\tau}(n) e^{-j[\frac{2\pi}{N}]kn}$$

$$= \frac{1}{N}\sum_{n=0}^{N-1}[\sum_{t=1}^{2}\sum_{l=0}^{N-1}(X_l^t H_l^t e^{j[\frac{2\pi}{N}]\ln})e^{j[\frac{2\pi}{N}]\varepsilon^{\tau} n + \varphi^{\tau}(n)]}]e^{-j[\frac{2\pi}{N}]kn}$$

$$= \frac{1}{N}\sum_{n=0}^{N-1}\sum_{t=1}^{2}\sum_{l=0}^{N-1} X_l^t H_l^t e^{j[(\frac{2\pi}{N})(l-k+\varepsilon^{\tau})n + \varphi^{\tau}(n)]} + N_k$$

$$= \sum_{t=1}^{2}\sum_{l=0}^{N-1} X_l^t H_l^t Q_{l-k}^{\tau} + N_k \qquad (3.3)$$

where, Y_k , X_l and H_l are the frequency domain expression of *r(n), x(n), h(n)* . N_k is the complex AWGN. Here, ε is the normalized frequency offset and is given by $\Delta f^{\tau} T$. Δf is the frequency difference between the transmitted and received carrier frequencies and *T* is the subcarrier symbol period. Q_L^{τ} is defined as follows,

$$Q_L^{\tau} = \frac{1}{N}\sum_{n=0}^{N-1} e^{j[(\frac{2\pi}{N})(L+\varepsilon^{\tau})n + \varphi^{\tau}(n)]}$$

$$= \exp[\{j2\pi(L+\varepsilon^{\tau}) + \varphi^{\tau}\}(1/2 - 1/2N)]\frac{\sin\{2\pi(L+\varepsilon^{\tau}) + \varphi^{\tau}\}/2]}{N.\sin[\{2\pi(L+\varepsilon^{\tau}) + \varphi^{\tau}\}/2N]} \qquad (3.4)$$

The expression of equation (3.4) is given in Appendix - A. Using phase noise linear approximation method, suppose $\varphi^{\tau}[n]$ is so small that $e^{j\varphi^{\tau}[n]}$ can be approximated into $1+j\varphi^{\tau}[n]$. So, Q_L^{τ} can be defined as,

$$Q_L^{\tau} = \frac{1}{N}\sum_{n=0}^{N-1} e^{j[(\frac{2\pi}{N})(L+\varepsilon^{\tau})n]}(1+j\varphi^{\tau}(n))$$

$$= \exp[\{j2\pi(L+\varepsilon^{\tau})\}(1/2-1/2N)]\frac{\sin\{2\pi(L+\varepsilon^{\tau})/2]}{N.\sin[\{2\pi(L+\varepsilon^{\tau})\}/2N]}(1+\frac{1}{N}\sum_{n=0}^{N-1} j\varphi^{\tau}(n))$$

$$= \exp[\{j\pi(L+\varepsilon^{\tau})\}(1-1/N)]\frac{\sin\{\pi(L+\varepsilon^{\tau})]}{N.\sin[\{\pi(L+\varepsilon^{\tau})\}/N]}\{1+\frac{1}{N}\sum_{n=0}^{N-1} j\varphi^{\tau}(n)\} \qquad (3.5)$$

Frequency offset and phase noise is analyzed independently and channels have similar flat frequency response in two paths such as $H_l^1 = H_l^2 = 1$. In this thesis, all received signal Y_k^{τ} equation after FFT block at the receiver side in given block diagram. For the simplicity of system performance analysis, we assume that $Q_L^{\tau,t} = Q_L^{\tau}$. Transmitted signal is supposed to have zero mean and statistically independence.

Generally, influenced by frequency offset and random phase noise signal of 2x2 MIMO-OFDM at the receiving end become corrupted. It involves two kinds of components. One component is its own subcarrier signal corrupted by common phase error (CPE), and the other is ICI from adjacent subcarrier signals. ICI is the summation of the other subcarrier signals multiplied by some complex number resulting from frequency offset and average phase noise with spectral shift.

3.3.1 Original 2x2 MIMO-OFDM

In original 2x2 MIMO-OFDM, both antennas transmit the same signal as the form of $X_l^1 = X_l^2 = X_k$ the kth subcarrier signal is expressed as,

$$Y_k^{\tau} = \frac{1}{N}\sum_{n=0}^{N-1} r^{\tau}[n]e^{-j\frac{2\pi}{N}kn}$$

$$= \sum_{t=1}^{2}\sum_{l=0}^{N-1} X_l^t \cdot H_l^t \cdot Q_{l-k}^{\tau} + N_k \qquad (3.6)$$

The received signal at the receiver 1 (RX1) can be expressed as,

$$Y_k^1 = \sum_{l=0}^{N-1} X_l^1 \cdot H_l^1 \cdot Q_{l-k}^1 + \sum_{l=0}^{N-1} X_l^2 \cdot H_l^2 \cdot Q_{l-k}^1 + N_{1k}$$

$$= X_k.H_k^1.Q_0^1 + \sum_{l=0,l\neq k}^{N-1} X_l^1.H_l^1.Q_{l-k}^1 + X_k.H_k^2.Q_0^1 + \sum_{l=0,l\neq k}^{N-1} X_l^2.H_l^2.Q_{l-k}^1 + N_{1k}$$

$$= X_k\{H_k^1.Q_0^1 + H_k^2.Q_0^1\} + \sum_{l=0,l\neq k}^{N-1}\{X_l^1.H_l^1.Q_{l-k}^1 + X_l^2.H_l^2.Q_{l-k}^1\} + N_{1k}$$

$$= X_k + X_k\{H_k^1.Q_0^1 + H_k^2.Q_0^1 - 1\} + \sum_{l=0,l\neq k}^{N-1}\{X_l^1.H_l^1.Q_{l-k}^1 + X_l^2.H_l^2.Q_{l-k}^1\} + N_{1k} \quad (3.7)$$

Similarly, the received signal at the receiver 2 (RX2) can be expressed as,

$$Y_k^2 = \sum_{l=0}^{N-1} X_l^1 \cdot H_l^1 \cdot Q_{l-k}^2 + \sum_{l=0}^{N-1} X_l^2 \cdot H_l^2 \cdot Q_{l-k}^2 + N_{2k}$$

$$= X_k + X_k\{H_k^1.Q_0^2 + H_k^2.Q_0^2 - 1\} + \sum_{l=0,l\neq k}^{N-1}\{X_l^1.H_l^1.Q_{l-k}^2 + X_l^2.H_l^2.Q_{l-k}^2\} + N_{2k}$$

(3.8)

Final signal are achieved as follows,

$$Z_k^{'} = Y_k^1 + Y_k^2$$

$$= 2X_k + X_k\{H_k^1.(Q_0^1 + Q_0^2) + H_k^2.(Q_0^1 + Q_0^2) - 2\}$$

$$+ \sum_{l=0,l\neq k}^{N-1}\{X_l^1.H_l^1.Q_{l-k}^1 + X_l^1.H_l^1.Q_{l-k}^2\} + \sum_{l=0,l\neq k}^{N-1}\{X_l^2.H_l^2.Q_{l-k}^1 + X_l^2.H_l^2.Q_{l-k}^2\} + N_k$$

$$= 2X_k + 2X_k\{(Q_0^1 + Q_0^2) - 1\} + \sum_{l=0,l\neq k}^{N-1}\{(X_l^1 + X_l^2).Q_{l-k}^1 + (X_l^1 + X_l^2).Q_{l-k}^2\} + N_k$$

(3.9)

All subcarriers are rotated by the same angle simultaneously. Usually CPE affects all the subchannels equally. The CPE signal is generated by the signal of *k*th subcarrier. Let us assume, *l=k.* So, CPE component is expressed as,

$$CPE = 2X_k\{(Q_0^1 + Q_0^2) - 1\} \quad (3.10)$$

ICI is corrupted by adjacent subcarrier signal and which is caused by the loss of

orthogonality of the subcarriers. Let us assume, $l \neq k$. So, ICI component is expressed as,

$$ICI = \sum_{l=0,l\neq k}^{N-1} (X_l^1 + X_l^2).Q_{l-k}^1 + (X_l^1 + X_l^2).Q_{l-k}^2 \tag{3.11}$$

CIR is the ratio of power in an RF carrier to the interference power in the channel. In this particular case, the CIR ratio is the signal power of *k*th subcarrier to the ICI power in the channel. So, the expression of CIR is given by,

$$CIR = \frac{Signal\ \ power}{ICI\ \ power}$$

$$= \frac{2[|Q_0^1|^2 + |Q_0^2|^2]}{2\sum_{l=0,l\neq k}^{N-1} |Q_{l-k}^1|^2 + |Q_{l-k}^2|^2} \qquad [\because X_l^1 = X_l^2 = X_k]$$

$$= \frac{[|Q_0^1|^2 + |Q_0^2|^2]}{\sum_{l=1}^{N-1} |Q_l^1|^2 + |Q_l^2|^2} \tag{3.12}$$

In order to evaluate the statistical properties [52]

$$E\left[|H_l^1|^2\right] = E\left[|H_l^2|^2\right] = 1 \text{ and}$$

$$E\left[|X_l^1|^2\right] = E\left[|X_l^2|^2\right] = |X|^2 \tag{3.13}$$

The desired received signal power can be represented by

$$\sigma_{DRS}^2 = E[|X_k|^2].E[|H_k^1|^2].|Q_0^1|^2 + E[|X_k|^2].E[|H_k^2|^2].|Q_0^1|^2$$

$$+ E[|X_k|^2].E[|H_k^1|^2].|Q_0^2|^2 + E[|X_k|^2].E[|H_k^2|^2].|Q_0^2|^2\}$$

$$= 2\{|X|^2.|Q_0^1|^2 + |X|^2.|Q_0^2|^2\}$$

$$= 2|X|^2\{|Q_0^1|^2 + |Q_0^2|^2\} \tag{3.14}$$

Hence, the ICI power is

$$\sigma_{ICI}^2 = E\left[|I_{ICI}|^2\right]$$

$$= \sum_{l=0,l\neq k}^{N-1} E[|X_l^1|^2].E[|H_l^1|^2].|Q_{l-k}^1|^2 + \sum_{l=0,l\neq k}^{N-1} E[|X_l^2|^2].E[|H_l^2|^2].|Q_{l-k}^1|^2$$

$$+\sum_{l=0,l\neq k}^{N-1} E[|X_l^1|^2].E[|H_l^1|^2].|Q_{l-k}^2|^2 + \sum_{l=0,l\neq k}^{N-1} E[|X_l^2|^2].E[|H_l^2|^2].|Q_{l-k}^2|^2$$

$$= 2\sum_{l=1}^{N-1} |X|^2.|Q_l^1|^2 + |X|^2.|Q_l^2|^2$$

$$= 2\sum_{l=1}^{N-1} |X|^2.\{|Q_l^1|^2 + |Q_l^2|^2\} \tag{3.15}$$

BER of quadrature phase shift keying (QPSK) modulated 2x2 MIMO-OFDM system is given,

$$BER = \frac{1}{2}Q\ (\sqrt{\frac{\sigma_{DRS}^2}{N_0 + \sigma_{ICI}^2}})$$

$$= \frac{1}{2}Q\ (\sqrt{\frac{2.|X|^2.\{|Q_0^1|^2 + |Q_0^2|^2\}}{N_0 + 2\sum_{l=1}^{N-1}|X|^2.\{|Q_l^1|^2 + |Q_l^2|^2\}}})$$

$$= \frac{1}{2}Q\ (\sqrt{\frac{2.\frac{|X|^2}{N_0}.\{|Q_0^1|^2 + |Q_0^2|^2\}}{1 + 2\sum_{l=1}^{N-1}\frac{|X|^2}{N_0}.\{|Q_l^1|^2 + |Q_l^2|^2\}}})$$

$$= \frac{1}{2}Q\ (\sqrt{\frac{2.\frac{E_b}{N_0}.\{|Q_0^1|^2 + |Q_0^2|^2\}}{1 + 2\sum_{l=1}^{N-1}\frac{E_b}{N_0}.\{|Q_l^1|^2 + |Q_l^2|^2\}}}) \tag{3.16}$$

3.3.2 Self-cancellation data conjugate (SCDC) in 2x2 MIMO-OFDM

From the Fig. 3.1, the SCDC signals are remapped as the form of $X_l^1 = X_k, X_l^2 = X_k^*$

The received signal at RX1 can be expressed as:

$$Y_k^1 = \sum_{l=0}^{N-1} X_l^1 \cdot H_l^1 \cdot Q_{l-k}^1 + \sum_{l=0}^{N-1} X_l^2 \cdot H_l^2 \cdot Q_{l-k}^1 + N_{1k}$$

$$= X_k.H_k^1.Q_0^1 + \sum_{l=0,l\neq k}^{N-1} X_l^1.H_l^1.Q_{l-k}^1 + X_k^*.H_k^2.Q_0^1 + \sum_{l=0,l\neq k}^{N-1} X_l^2.H_l^2.Q_{l-k}^1 + N_{1k}$$

(3.17)

Similarly, the received signal at RX2 can be expressed as:

$$Y_k^2 = \sum_{l=0}^{N-1} X_l^1 \cdot H_l^1 \cdot Q_{l-k}^2 + \sum_{l=0}^{N-1} X_l^2 \cdot H_l^2 \cdot Q_{l-k}^2 + N_{2k}$$

$$= X_k.H_k^1.Q_0^2 + \sum_{l=0,l\neq k}^{N-1} X_l^1.H_l^1.Q_{l-k}^2 + X_k^*.H_k^2.Q_0^2 + \sum_{l=0,l\neq k}^{N-1} X_l^2.H_l^2.Q_{l-k}^2 + N_{2k} \tag{3.18}$$

In the receiver, the final decision variable $Z_k^{'}$ of the kth symbol is found by

$$Z_k^{'} = Y_k^1 + Y_k^{2^*}$$

$$= X_k.H_k^1.Q_0^1 + \sum_{l=0,l\neq k}^{N-1} X_l^1.H_l^1.Q_{l-k}^1 + X_k^*.H_k^2.Q_0^1 + \sum_{l=0,l\neq k}^{N-1} X_l^2.H_l^2.Q_{l-k}^1 + X_k^*.(H_k^1)^*.Q_0^{1*}$$

$$+ \sum_{l=0,l\neq k}^{N-1} (X_l^1)^*.(H_l^1)^*.Q_{l-k}^{2*} + X_k.(H_k^2)^*.Q_0^{2*} + \sum_{l=0,l\neq k}^{N-1} (X_l^2)^*.(H_l^2)^*.Q_{l-k}^{2*} + N_k$$

$$= X_k.(H_k^1.Q_0^1 + (H_k^2)^*.Q_0^{2*}) + X_k^*.(H_k^2.Q_0^1 + (H_k^1)^*.Q_0^{2*})$$

$$+ \sum_{l=0,l\neq k}^{N-1} \{X_l^1.H_l^1.Q_{l-k}^1 + (X_l^1)^*.(H_l^1)^*.Q_{l-k}^{2*}\}$$

$$+ \sum_{l=0,l\neq k}^{N-1} \{X_l^2.H_l^2.Q_{l-k}^1 + (X_l^2)^*.(H_l^2)^*.Q_{l-k}^{2*}\} + N_k \tag{3.19}$$

Now, we consider two different situations based on the value of normalized frequency offset, ε_τ.

(i) Condition 1: Normalized frequency offset is not zero.

When $\varepsilon_\tau = \Delta f^\tau T \neq 0$, equation (3.19) can be written as,

$$Z_k^{'} = X_k + X_k.(H_k^1.Q_0^1 + (H_k^2)^*.Q_0^{2*} - 1) + X_k^*.(H_k^2.Q_0^1 + (H_k^1)^*.Q_0^{2*}) + \sum_{l=0,l\neq k}^{N-1} X_l^1.H_l^1.Q_{l-k}^1 + (X_l^1)^*.(H_l^1)^*.Q_{l-k}^{2*}$$

$$+ \sum_{l=0,l\neq k}^{N-1} X_l^2.H_l^2.Q_{l-k}^1 + (X_l^2)^*.(H_l^2)^*.Q_{l-k}^{2*} + N_k$$

$$= X_k + X_k.(Q_0^1 + Q_0^{2*} - 1) + X_k^*.(Q_0^1 + Q_0^{2*}) + \sum_{l=0,l\neq k}^{N-1} X_l^1.Q_{l-k}^1 + (X_l^1)^*.Q_{l-k}^{2*}$$

$$+ \sum_{l=0,l\neq k}^{N-1} X_l^2.Q_{l-k}^1 + (X_l^2)^*.Q_{l-k}^{2*} + N_k \tag{3.20}$$

CPE component is expressed as,

$$CPE = X_k.(Q_0^1 + Q_0^{2*} - 1) \tag{3.21}$$

ICI component is expressed as,

$$ICI = \sum_{l=0,l\neq k}^{N-1} X_l^1.Q_{l-k}^1 + (X_l^1)^*.Q_{l-k}^{2*} + \sum_{l=0,l\neq k}^{N-1} X_l^2.Q_{l-k}^1 + (X_l^2)^*.Q_{l-k}^{2*} \tag{3.22}$$

CIR is expressed as,

$$CIR = \frac{Signal\ \ power}{ICI\ \ power}$$

$$= \frac{\left|Q_0^1 + Q_0^{2*}\right|^2 + \left|Q_0^1 + Q_0^{2*}\right|^2}{2\sum_{l=0,l\neq k}^{N-1}\left|Q_{l-k}^1\right|^2 + \left|Q_{l-k}^{2*}\right|^2} \qquad [\because X_l^1 = X_k, X_l^2 = X_k^*]$$

$$= \frac{\left|Q_0^1 + Q_0^{2*}\right|^2}{\sum_{l=1}^{N-1}\left|Q_l^1\right|^2 + \left|Q_l^{2*}\right|^2} \tag{3.23}$$

(ii) Condition 2: Normalized frequency offset is zero.

When $\varepsilon_\tau = \Delta f^\tau T = 0$, equation (3.19) can be written as,

$$Z_k^{'} = 2X_k + 2X_k^* + \sum_{l=0,l\neq k}^{N-1}\{X_l^1.H_l^1.Q_{l-k}^1 + (X_l^1)^*.(H_l^1)^*.Q_{l-k}^{2*}\}$$

$$+ \sum_{l=0,l\neq k}^{N-1}\{X_l^2.H_l^2.Q_{l-k}^1 + (X_l^2)^*.(H_l^2)^*.Q_{l-k}^{2*}\} + N_k$$

$$= 2X_k + 2X_k^* + \sum_{l=0,l\neq k}^{N-1}\{X_l^1.Q_{l-k}^1 + (X_l^1)^*.Q_{l-k}^{2*}\} + \sum_{l=0,l\neq k}^{N-1}\{X_l^2.Q_{l-k}^1 + (X_l^2)^*.Q_{l-k}^{2*}\} + N_k \tag{3.24}$$

CPE component is expressed as,

$$CPE = 0 \tag{3.25}$$

ICI component is expressed as,

$$ICI = \sum_{l=0,l\neq k}^{N-1}\{X_l^1.Q_{l-k}^1 + (X_l^1)^*.Q_{l-k}^{2*}\} + \sum_{l=0,l\neq k}^{N-1}\{X_l^2.Q_{l-k}^1 + (X_l^2)^*.Q_{l-k}^{2*}\} \tag{3.26}$$

CIR is expressed as,

$$CIR = \frac{4}{2\sum_{l=1}^{N-1}\left|Q_l^1\right|^2 + \left|Q_l^{2*}\right|^2} \tag{3.27}$$

The desired received signal power can be represented by

$$\sigma_{DRS(SCDC)}^2 = E[\left|X_k\right|^2].E[\left|H_k^1\right|^2].\left|Q_0^1\right|^2 + E[\left|X_k\right|^2].E[\left|H_k^{2*}\right|^2].\left|Q_0^{2*}\right|^2$$

$$= \left|X\right|^2.\left|Q_0^1\right|^2 + \left|X\right|^2.\left|Q_0^{2*}\right|^2 \tag{3.28}$$

Hence, the ICI power is

$$\sigma_{ICI(SCDC)}^2 = E\left[\left|I_{ICI}\right|^2\right]$$

$$= \sum_{l=0,l\neq k}^{N-1} E[\left|X_l^1\right|^2].E[\left|H_l^1\right|^2].\left|Q_{l-k}^1\right|^2 + \sum_{l=0,l\neq k}^{N-1} E[\left|X_l^{1^*}\right|^2].E[\left|H_l^{1^*}\right|^2].\left|Q_{l-k}^{2*}\right|^2$$

$$+ \sum_{l=0,l\neq k}^{N-1} E[\left|X_l^2\right|^2].E[\left|H_l^2\right|^2].\left|Q_{l-k}^1\right|^2 + \sum_{l=0,l\neq k}^{N-1} E[\left|X_l^{2^*}\right|^2].E[\left|H_l^{2^*}\right|^2].\left|Q_{l-k}^{2*}\right|^2$$

$$= 2\sum_{l=1}^{N-1}\left|X\right|^2.\left|Q_l^1\right|^2 + \left|X\right|^2.\left|Q_l^{2*}\right|^2 \tag{3.29}$$

BER of QPSK modulated SCDC method in 2x2 MIMO-OFDM system is given

$$BER = \frac{1}{2}Q\left(\sqrt{\frac{\sigma_{DRS(SCDC)}^2}{N_0 + \sigma_{ICI(SCDC)}^2}}\right)$$

$$= \frac{1}{2}Q\left(\sqrt{\frac{\left|X\right|^2.\left|H\right|^2.\left|Q_0^1\right|^2 + \left|X\right|^2.\left|H\right|^2.\left|Q_0^{2*}\right|^2}{N_0 + 2\sum_{l=1}^{N-1}\left|X\right|^2.\left|H\right|^2.\left|Q_l^1\right|^2 + \left|X\right|^2.\left|H\right|^2.\left|Q_l^{2*}\right|^2}}\right)$$

$$= \frac{1}{2}Q\left(\sqrt{\frac{\frac{\left|X\right|^2.\left|H\right|^2}{N_0}\{\left|Q_0^1\right|^2 + \left|Q_0^{2*}\right|^2\}}{1 + 2\sum_{l=1}^{N-1}\frac{\left|X\right|^2.\left|H\right|^2}{N_0}\{\left|Q_l^1\right|^2 + \left|Q_l^{2*}\right|^2\}}}\right)$$

$$= \frac{1}{2}Q\left(\sqrt{\frac{\frac{E_b}{N_0}\{\left|Q_0^1\right|^2 + \left|Q_0^{2*}\right|^2\}}{1 + 2\sum_{l=1}^{N-1}\frac{E_b}{N_0}\{\left|Q_l^1\right|^2 + \left|Q_l^{2*}\right|^2\}}}\right) \tag{3.30}$$

3.3.3 Convolution coding in SCDC of 2x2 MIMO-OFDM

In Fig. 3.1, convolution encoder is placed after modulation. At the receiver side, viterbi decoder is recovered the transmitted date before demodulation. If convolution coding rate=1/2. BER of QPSK modulated in OFDM system is given [16]

$$BER = \frac{1}{2} Q\ (\sqrt{\frac{E_b}{N_0 C_r}}) \tag{3.31}$$

C_r = coding rate=1/2

$$BER = \frac{1}{2} Q\ (\sqrt{\frac{2E_b}{N_0}}) \tag{3.32}$$

BER of QPSK modulated in 2x2 MIMO-OFDM system is given

$$BER = \frac{1}{2} Q\ (\sqrt{\frac{2\sigma_{DRS}^2}{N_0 + \sigma_{ICI}^2}})$$

$$= \frac{1}{2} Q\ (\sqrt{\frac{4.\frac{E_b}{N_0}.\{|Q_0^1|^2 + |Q_0^2|^2\}}{1 + 2\sum_{l=1}^{N-1} \frac{E_b}{N_0}.\{|Q_l^1|^2 + |Q_l^2|^2\}}}) \tag{3.33}$$

BER of QPSK modulated SCDC with convolution coding in 2x2 MIMO-OFDM system is given

$$BER = \frac{1}{2} Q\ (\sqrt{\frac{2.\sigma_{DRS(SCDC)}^2}{N_0 + \sigma_{ICI(SCDC)}^2}})$$

$$= \frac{1}{2} Q\ (\sqrt{\frac{2.\frac{E_b}{N_0}\{|Q_0^1|^2 + |Q_0^{2*}|^2\}}{1 + 2\sum_{l=1}^{N-1} \frac{E_b}{N_0}\{|Q_l^1|^2 + |Q_l^{2*}|^2\}}}) \tag{3.34}$$

3.3.4 Space frequency block code (SFBC) in 2x2 MIMO-OFDM

In the SFBC method, signals are remapped as the form of

$$X_l^1 = X_k or - X_{k+1}^*, X_l^2 = X_{k+1} or X_k^*$$

The received signal at RX1 can be expressed as,

$$Y_k^1 = \sum_{l=0}^{N-1} X_l^1 \cdot H_l^1 \cdot Q_{l-k}^1 + \sum_{l=0}^{N-1} X_l^2 \cdot H_l^2 \cdot Q_{l-k}^1 + N_{1k}$$

$$= X_k.H_k^1.Q_0^1 + \sum_{l=0,l\neq k}^{N-1} X_l^1.H_l^1.Q_{l-k}^1 + X_{k+1}.H_k^2.Q_0^1 + \sum_{l=0,l\neq k}^{N-1} X_l^2.H_l^2.Q_{l-k}^1 + N_{1k} \tag{3.35}$$

$$Y_{k+1}^1 = \sum_{l=0}^{N-1} X_l^1 \cdot H_l^1 \cdot Q_{l-k-1}^1 + \sum_{l=0}^{N-1} X_l^2 \cdot H_l^2 \cdot Q_{l-k-1}^1 + N_{k+1}$$

$$= -X_{k+1}^*.H_{k+1}^1.Q_0^1 + \sum_{l=0,l\neq k+1}^{N-1} X_l^1.H_l^1.Q_{l-k-1}^1 + X_k^*.H_{k+1}^2.Q_0^1 + \sum_{l=0,l\neq k+1}^{N-1} X_l^2.H_l^2.Q_{l-k-1}^1 + N_{k+1} \tag{3.36}$$

Similarly, the received signal at RX2 can be expressed as,

$$Y_k^2 = \sum_{l=0}^{N-1} X_l^1 \cdot H_l^1 \cdot Q_{l-k}^2 + \sum_{l=0}^{N-1} X_l^2 \cdot H_l^2 \cdot Q_{l-k}^2 + N_{2k}$$

$$= X_k.H_k^1.Q_0^2 + \sum_{l=0,l\neq k}^{N-1} X_l^1.H_l^1.Q_{l-k}^2 + X_{k+1}.H_k^2.Q_0^2 + \sum_{l=0,l\neq k}^{N-1} X_l^2.H_l^2.Q_{l-k}^2 + N_{2k} \tag{3.37}$$

$$Y_{k+1}^2 = \sum_{l=0}^{N-1} X_l^1 \cdot H_l^1 \cdot Q_{l-k-1}^2 + \sum_{l=0}^{N-1} X_l^2 \cdot H_l^2 \cdot Q_{l-k-1}^2 + N_{2(k+1)}$$

$$= -X_{k+1}^*.H_{k+1}^1.Q_0^2 + \sum_{l=0,l\neq k+1}^{N-1} X_l^1.H_l^1.Q_{l-k-1}^2 + X_k^*.H_{k+1}^2.Q_0^2 + \sum_{l=0,l\neq k+1}^{N-1} X_l^2.H_l^2.Q_{l-k-1}^2 + N_{2(k+1)} \tag{3.38}$$

In the receiver, the decision variable $Z_k^{'}$ of the kth and k+1th symbol is found as,

$$Z_k^{'} = Y_k^1 + Y_{k+1}^{2^*}$$

$$= X_k.H_k^1.Q_0^1 + \sum_{l=0,l\neq k}^{N-1} X_l^1.H_l^1.Q_{l-k}^1 + X_{k+1}.H_k^2.Q_0^1 + \sum_{l=0,l\neq k}^{N-1} X_l^2.H_l^2.Q_{l-k}^1$$

$$- X_{k+1}.(H_{k+1}^1)^*.Q_0^{2^*} + \sum_{l=0,l\neq k+1}^{N-1} (X_l^1)^*.(H_l^1)^*.Q_{l-k-1}^{2^*}$$

$$+ X_k.(H_{k+1}^2)^*.Q_0^{2^*} + \sum_{l=0,l\neq k+1}^{N-1} (X_l^2)^*.(H_l^2)^*.Q_{l-k-1}^{2^*} + N_k$$

$$= X_k\{H_k^1.Q_0^1 + (H_{k+1}^2)^*.Q_0^{2^*}\} + X_{k+1}\{H_k^2.Q_0^1 - (H_{k+1}^1)^*.Q_0^{2^*}\}$$

$$+ \sum_{l=0,l\neq k}^{N-1} X_l^1.H_l^1.Q_{l-k}^1 + X_l^2.H_l^2.Q_{l-k}^1$$

$$+ \sum_{l=0,l\neq k+1}^{N-1} (X_l^1)^*.(H_l^1)^*.Q_{l-k-1}^{2^*} + (X_l^2)^*.(H_l^2)^*.Q_{l-k-1}^{2^*} + N_k \tag{3.39}$$

$$
\begin{aligned}
Z'_{k+1} &= Y_k^2 - Y_{k+1}^{1^*} \\
&= X_k.H_k^1.Q_0^2 + \sum_{l=0,l\neq k}^{N-1} X_l^1.H_l^1.Q_{l-k}^2 + X_{k+1}.H_k^2.Q_0^2 \\
&\quad + \sum_{l=0,l\neq k}^{N-1} X_l^2.H_l^2.Q_{l-k}^2 + X_{k+1}.(H_{k+1}^1)^*.Q_0^{1*} \\
&\quad - \sum_{l=0,l\neq k+1}^{N-1} (X_l^1)^*.(H_l^1)^*.Q_{l-k-1}^{1*} - X_k.(H_{k+1}^2)^*.Q_0^{1*} \\
&\quad - \sum_{l=0,l\neq k+1}^{N-1} (X_l^2)^*.(H_l^2)^*.Q_{l-k-1}^{1*} + N_k \\
&= X_k\{H_k^1.Q_0^2 - (H_{k+1}^2)^*.Q_0^{1*}\} + X_{k+1}\{H_k^2.Q_0^2 + (H_{k+1}^1)^*.Q_0^{1*}\} \\
&\quad + \sum_{l=0,l\neq k}^{N-1} X_l^1.H_l^1.Q_{l-k}^2 + X_l^2.H_l^2.Q_{l-k}^2 \\
&\quad - \sum_{l=0,l\neq k+1}^{N-1} (X_l^1)^*.(H_l^1)^*.Q_{l-k-1}^{1*} + (X_l^2)^*.(H_l^2)^*.Q_{l-k-1}^{1*} + N_k
\end{aligned}
\tag{3.40}
$$

(i) Condition 1: Normalized frequency offset is not zero.

When $\varepsilon_\tau = \Delta f^\tau T \neq 0$, equations (3.39-3.40) can be written as,

$$
\begin{aligned}
Z'_k &= X_k + X_k\{H_k^1.Q_0^1 + (H_{k+1}^2)^*.Q_0^{2*} - 1\} + X_{k+1}\{H_k^2.Q_0^1 - (H_{k+1}^1)^*.Q_0^{2*}\} \\
&\quad + \sum_{l=0,l\neq k}^{N-1} \{X_l^1.H_l^1 + X_l^2.H_l^2\}Q_{l-k}^1 + \sum_{l=0,l\neq k+1}^{N-1} \{(X_l^1)^*.(H_l^1)^* + (X_l^2)^*.(H_l^2)^*\}Q_{l-k-1}^{2*} + N_k \\
&= X_k + X_k\{Q_0^1 + .Q_0^{2*} - 1\} + X_{k+1}\{Q_0^1 - Q_0^{2*}\} + \sum_{l=0,l\neq k}^{N-1} \{X_l^1 + X_l^2\}Q_{l-k}^1 \\
&\quad + \sum_{l=0,l\neq k+1}^{N-1} \{(X_l^1)^* + (X_l^2)^*\}.Q_{l-k-1}^{2*} + N_k
\end{aligned}
\tag{3.41}
$$

$$
\begin{aligned}
Z'_{k+1} &= X_{k+1} + X_k\{H_k^1.Q_0^2 - (H_{k+1}^2)^*.Q_0^{1*}\} + X_{k+1}\{H_k^2.Q_0^2 + (H_{k+1}^1)^*.Q_0^{1*} - 1\} \\
&\quad + \sum_{l=0,l\neq k}^{N-1} \{X_l^1.H_l^1 + X_l^2.H_l^2\}Q_{l-k}^2 - \sum_{l=0,l\neq k+1}^{N-1} \{(X_l^1)^*.(H_l^1)^* + (X_l^2)^*.(H_l^2)^*\}Q_{l-k-1}^{1*} + N_k \\
&= X_{k+1} + X_k\{Q_0^2 - Q_0^{1*}\} + X_{k+1}\{Q_0^2 + Q_0^{1*} - 1\} + \sum_{l=0,l\neq k}^{N-1} \{X_l^1 + X_l^2\}Q_{l-k}^2
\end{aligned}
$$

$$-\sum_{l=0,l\neq k+1}^{N-1}\{(X_l^1)^* + (X_l^2)^*\}Q_{l-k-1}^{1*} + N_k \tag{3.42}$$

CPE component is expressed as,

$$CPE_{Z_k^/} = X_k.(Q_0^1 + Q_0^{2*} - 1), for X_k date \tag{3.43}$$

$$CPE_{Z_{k+1}^/} = X_{k+1}.(Q_0^2 + Q_0^{1*} - 1), for X_{k+1} date \tag{3.44}$$

ICI component is expressed as,

$$ICI_{Z_k^/} = X_{k+1}\{Q_0^1 - Q_0^{2*}\} + \sum_{l=0,l\neq k}^{N-1}\{X_l^1 + X_l^2\}Q_{l-k}^1$$

$$+\sum_{l=0,l\neq k+1}^{N-1}\{(X_l^1)^* + (X_l^2)^*\}.Q_{l-k-1}^{2*}, for X_k data \tag{3.45}$$

$$ICI_{Z_{k+1}^/} = X_k\{Q_0^2 - Q_0^{1*}\} + \sum_{l=0,l\neq k}^{N-1}\{X_l^1 + X_l^2\}Q_{l-k}^2$$

$$-\sum_{l=0,l\neq k+1}^{N-1}\{(X_l^1)^* + (X_l^2)^*\}.Q_{l-k-1}^{1*}, for X_{k+1} data \tag{3.46}$$

CIR is expressed as,

$$CIR_{Z_k^/} = \frac{\left|Q_0^1 + Q_0^{2*}\right|^2}{\left|Q_0^1 - Q_0^{2*}\right|^2 + 2\sum_{l=0,l\neq k}^{N-1}\left|Q_{l-k}^1\right|^2 + 2\sum_{l=0,l\neq k+1}^{N-1}\left|Q_{l-k-1}^{2*}\right|^2}$$

$$= \frac{\left|Q_0^1 + Q_0^{2*}\right|^2}{\left|Q_0^1 - Q_0^{2*}\right|^2 + 2\sum_{l=1}^{N-1}\left|Q_l^1\right|^2 + 2\sum_{l=1}^{N-1}\left|Q_{l-1}^{2*}\right|^2} \tag{3.47}$$

$$CIR_{Z_{k+1}^/} = \frac{\left|Q_0^2 + Q_0^{1*}\right|^2}{\left|Q_0^2 - Q_0^{1*}\right|^2 + 2\sum_{l=1}^{N-1}\left|Q_l^2\right|^2 + 2\sum_{l=1}^{N-1}\left|Q_{l-1}^{1*}\right|^2} \tag{3.48}$$

(ii) Condition 2: Normalized frequency offset is zero.

When $\varepsilon_\tau = \Delta f^\tau T = 0$, equations (3.39-3.40) can be written as,

$$Z_k^{'} = 2X_k + \sum_{l=0,l\neq k}^{N-1}\{X_l^1 + X_l^2\}Q_{l-k}^1 + \sum_{l=0,l\neq k+1}^{N-1}\{(X_l^1)^* + (X_l^2)^*\}Q_{l-k-1}^{2*} + N_k$$

(3.49)

$$Z'_{k+1} = 2X_{k+1} + \sum_{l=0,l\neq k}^{N-1}\{X_l^1 + X_l^2\}Q_{l-k}^2 - \sum_{l=0,l\neq k+1}^{N-1}\{(X_l^1)^* + (X_l^2)^*\}Q_{l-k-1}^{1*} + N_k \tag{3.50}$$

CPE component is expressed as follows:

$$CPE_{Z'_k} = CPE_{Z'_{k+1}} = 0 \tag{3.51}$$

ICI component is expressed as follows:

$$ICI_{Z'_k} = \sum_{l=0,l\neq k}^{N-1}\{X_l^1 + X_l^2\}Q_{l-k}^1 + \sum_{l=0,l\neq k+1}^{N-1}\{(X_l^1)^* + (X_l^2)^*\}Q_{l-k-1}^{2*}, forX_k data \tag{3.52}$$

$$ICI_{Z'_{k+1}} = \sum_{l=0,l\neq k}^{N-1}\{X_l^1 + X_l^2\}Q_{l-k}^2 - \sum_{l=0,l\neq k+1}^{N-1}\{(X_l^1)^* + (X_l^2)^*\}Q_{l-k-1}^{1*}, forX_{k+1} data \tag{3.53}$$

CIR is expressed as

$$CIR_{Z'_k} = \frac{4}{2\sum_{l=0,l\neq k}^{N-1}\left|Q_{l-k}^1\right|^2 + 2\sum_{l=0,l\neq k+1}^{N-1}\left|Q_{l-k-1}^{2*}\right|^2}$$

$$= \frac{4}{2\sum_{l=1}^{N-1}\left|Q_l^1\right|^2 + 2\sum_{l=1}^{N-1}\left|Q_{l-1}^{2*}\right|^2} \tag{3.54}$$

$$CIR_{Z'_{k+1}} = \frac{4}{2\sum_{l=1}^{N-1}\left|Q_l^1\right|^2 + 2\sum_{l=1}^{N-1}\left|Q_{l-1}^{2*}\right|^2} \tag{3.55}$$

The desired received signal power can be represented by

$$\sigma_{DRS(SFBC)}^2 = E[\left|X_k\right|^2].E[\left|H_k^1\right|^2].\left|Q_0^1\right|^2 + E[\left|X_k\right|^2].E[\left|H_{k+1}^2\right|^2].\left|Q_0^{2*}\right|^2$$

$$= \left|X\right|^2.\left|H\right|^2.\left|Q_0^1\right|^2 + \left|X\right|^2.\left|H\right|^2.\left|Q_0^{2*}\right|^2$$

$$= \left|X\right|^2.\left|Q_0^1\right|^2 + \left|X\right|^2.\left|Q_0^{2*}\right|^2 \tag{3.56}$$

Hence, the ICI power is:

$$\sigma_{ICI(SFBC)}^2 = E\left[\left|I_{ICI}\right|^2\right] = E[\left|X_{k+1}\right|^2].E[\left|H_k^2\right|^2].\left|Q_0^1\right|^2 - E[\left|X_{k+1}\right|^2].E[\left|H_{k+1}^{1^*}\right|^2].\left|Q_0^{2*}\right|^2$$

$$+\sum_{l=0,l\neq k}^{N-1}\{E[|X_l^1|^2].E[|H_l^1|^2].|Q_{l-k}^1|^2+E[|X_l^2|^2].E[|H_l^2|^2].|Q_{l-k}^1|^2\}$$

$$+\sum_{l=0,l\neq k+1}^{N-1}\{E[|X_l^{1^*}|^2].E[|H_l^{1^*}|^2].|Q_{l-k-1}^{2*}|^2+E[|X_l^{2^*}|^2].E[|H_l^{2^*}|^2].|Q_{l-k-1}^{2*}|^2\}$$

$$=|X|^2.|H|^2.|Q_0^1|^2-|X|^2.|H|^2.|Q_0^{2*}|^2+\sum_{l=1}^{N-1}\{|X|^2.|H|^2.|Q_l^1|^2+|X|^2.|H|^2.|Q_l^1|^2\}$$

$$+\sum_{l=1}^{N-1}\{|X|^2.|H|^2.|Q_{l-1}^{2*}|^2+|X|^2.|H|^2.|Q_{l-1}^{2*}|^2\}$$

$$=|X|^2.|H|^2\{|Q_0^1|^2-|Q_0^{2*}|^2\}+2\sum_{l=1}^{N-1}|X|^2.|H|^2.|Q_l^1|^2+2\sum_{l=1}^{N-1}|X|^2.|H|^2.|Q_{l-1}^{2*}|^2$$

$$=|X|^2.\{|Q_0|^2-|Q_0^*|^2\}+2\sum_{l=1}^{N-1}|X|^2.|Q_l^1|^2+2\sum_{l=1}^{N-1}|X|^2.|Q_{l-1}^{2*}|^2 \qquad (3.57)$$

BER of QPSK modulated SFBC in 2x2 MIMO-OFDM system is given

$$BER=\frac{1}{2}Q\ (\sqrt{\frac{\sigma^2_{DRS(SFBC)}}{N_0+\sigma^2_{ICI(SFBC)}}})$$

$$=\frac{1}{2}Q\ (\sqrt{\frac{|X|^2.|H|^2.|Q_0^1|^2+|X|^2.|H|^2.|Q_0^{2*}|^2}{N_0+|X|^2.|H|^2\{|Q_0^1|^2-|Q_0^{2*}|^2\}+2\sum_{l=1}^{N-1}|X|^2.|H|^2.|Q_l^1|^2+2\sum_{l=1}^{N-1}|X|^2.|H|^2.|Q_{l-1}^{2*}|^2}})$$

$$=\frac{1}{2}Q\ (\sqrt{\frac{\frac{|X|^2.|H|^2}{N_0}\{|Q_0^1|^2+|Q_0^{2*}|^2\}}{1+\frac{|X|^2.|H|^2}{N_0}\{|Q_0^1|^2-|Q_0^{2*}|^2\}+2\sum_{l=1}^{N-1}\frac{|X|^2.|H|^2}{N_0}\{|Q_l^1|^2\}+2\sum_{l=1}^{N-1}\frac{|X|^2.|H|^2}{N_0}\{|Q_{l-1}^{2*}|^2\}}})$$

$$=\frac{1}{2}Q\ (\sqrt{\frac{\frac{E_b}{N_0}\{|Q_0^1|^2+|Q_0^{2*}|^2\}}{1+\frac{E_b}{N_0}\{|Q_0^1|^2-|Q_0^{2*}|^2\}+2\sum_{l=1}^{N-1}\frac{E_b}{N_0}\{|Q_l^1|^2\}++2\sum_{l=1}^{N-1}\frac{E_b}{N_0}\{|Q_{l-1}^{2*}|^2\}}})$$

(3.58)

CHAPTER 4

RESULTS AND DISCUSSION

According to the theoretical analysis presented in chapter 3, performance results of MIMO-OFDM system for different configuration are presented in the following section. In order to compare the seven different schemes (*i.e.*, OFDM with SCDC, 2x2 MIMO-OFDM without SCDC, 2x2 MIMO-OFDM with SCDC, 2x2 MIMO-OFDM-SCDC with CC, 2x2 MIMO-OFDM with SC, 2x1 MISO-OFDM with SFBC and 2x2 MIMO-OFDM with SFBC), the performance of MIMO-OFDM system in the presence of normalized frequency offset and phase noise has been evaluated in terms of ICI, CIR and BER. The simulation is performed for 2 transrecivers configuration. Plots are obtained at same normalized frequency offset and phase noise variance for two received signal. The system has been examined with 64 subcarriers using BPSK, QPSK subcarrier modulation and transmitted signal to noise ratio E_b/N_0 (E_b is energy per bit and N_0 is the spectral density coefficient).

4.1 Real and Imaginary Parts of ICI Coefficients

We have derived the ICI coefficients in previous chapter and it is given by equation (3.5). As the coefficient is small, this results in a substantial reduction in ICI. The ICI components are the interfering transmitted signals on k^{th} subcarriers. Q_{l-k}^{τ} is the complex coefficients for the ICI components in the received signal. The sequence Q_{l-k}^{τ} is defined as the ICI coefficient between l^{th} and k^{th} subcarriers between transmitter and receiver.

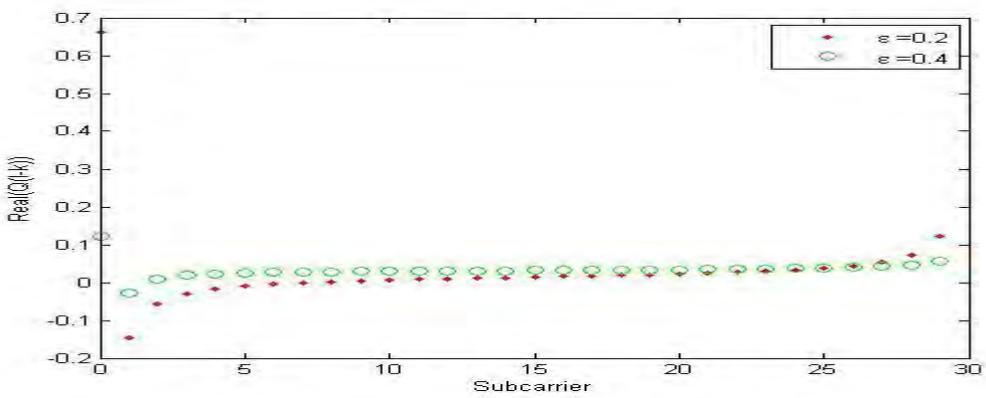

Fig. 4.1: (a) Plots of Real part of Q_{l-k}^{τ}

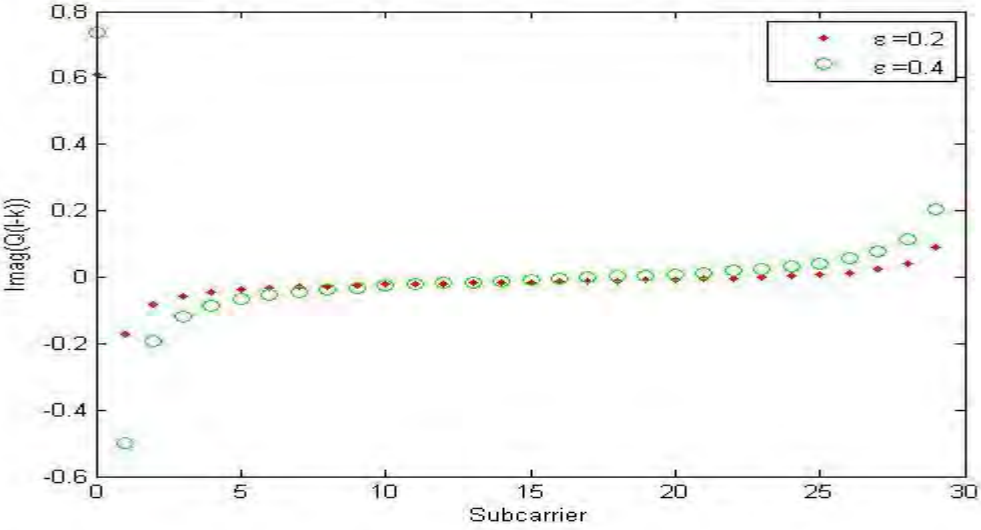

Fig. 4.1: (b) Plots of Imaginary part of Q_{l-k}^{τ}

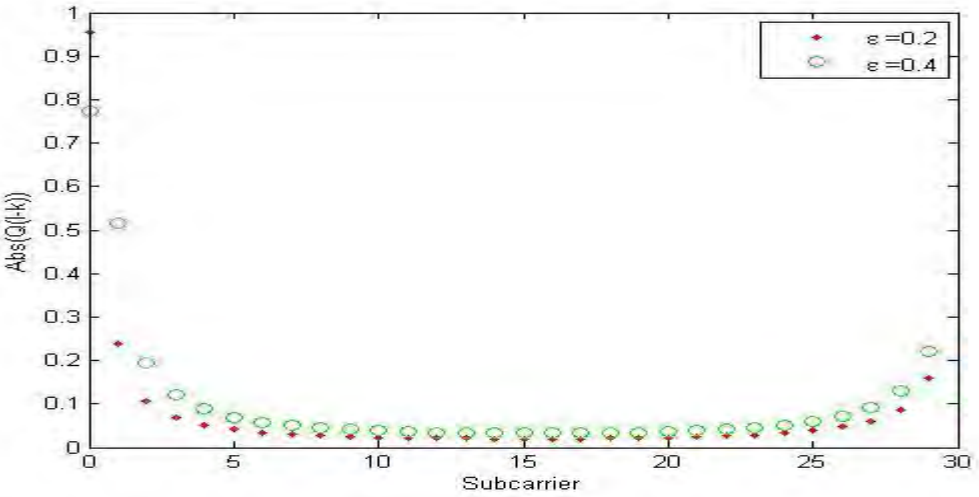

Fig. 4.1: (c) Plots of Amplitude of Q_{l-k}^{τ}

Fig. 4.1 (a), Fig. 4.1 (b) and Fig. 4.1 (c) are the plots of ICI coefficient for subcarrier N = 30. When normalized frequency offset (ε=0) and phase noise (φ=0) are zero, Q_0^{τ} takes the maximum value $Q_0^{\tau} = 1$. To analyze the effect of ICI on the received signal, l is taken as 0. We have used the normalized frequency offset of 0.2 and 0.4 and constant phase noise. It is seen that the real and imaginary parts of the ICI coefficients change gradually with respect to the subcarrier. From the Fig. 4.1, it is found that the normalized frequency offset (ε) increases; the weights of real and imaginary part of the ICI coefficients are also increased.

4.2 ICI Cancellation during Modulation and Demodulation

The combined modulation and demodulation method is called the ICI-SC scheme. The reduction of the ICI signal levels in the ICI-SC scheme leads to improve the system performance.

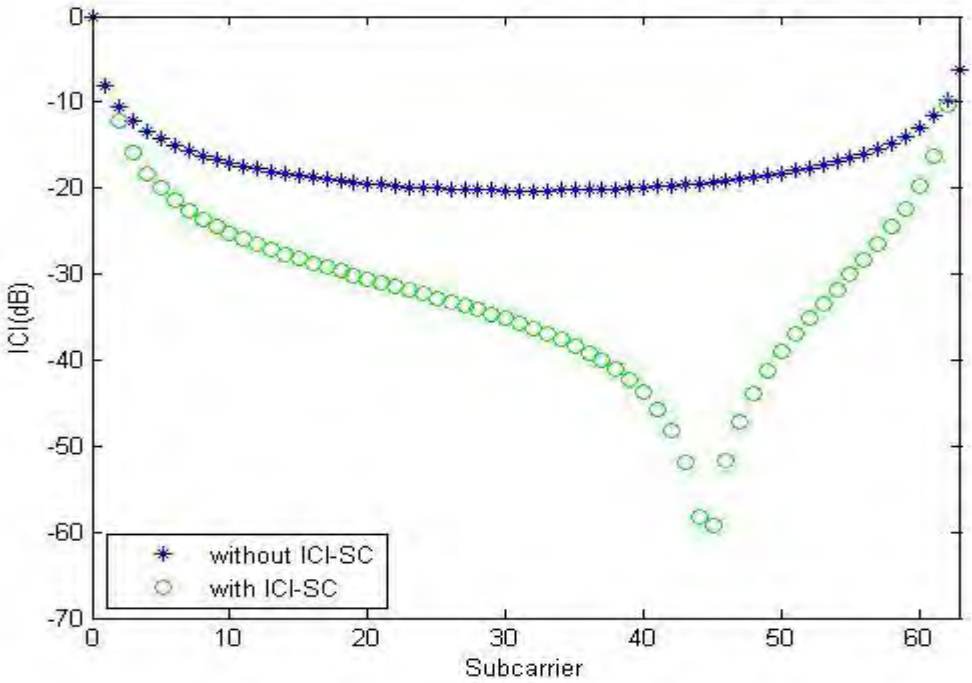

Fig. 4.2: Plots of ICI without SC and with SC in OFDM using DC

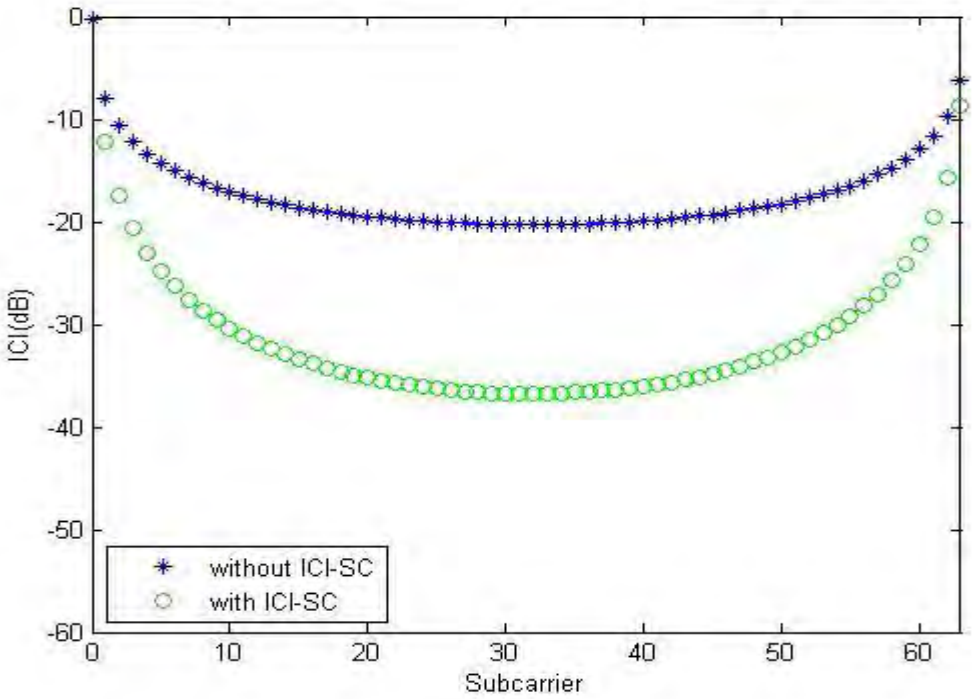

Fig. 4.3: Plots of ICI without SC and with SC in 2x2 MIMO-OFDM without DC

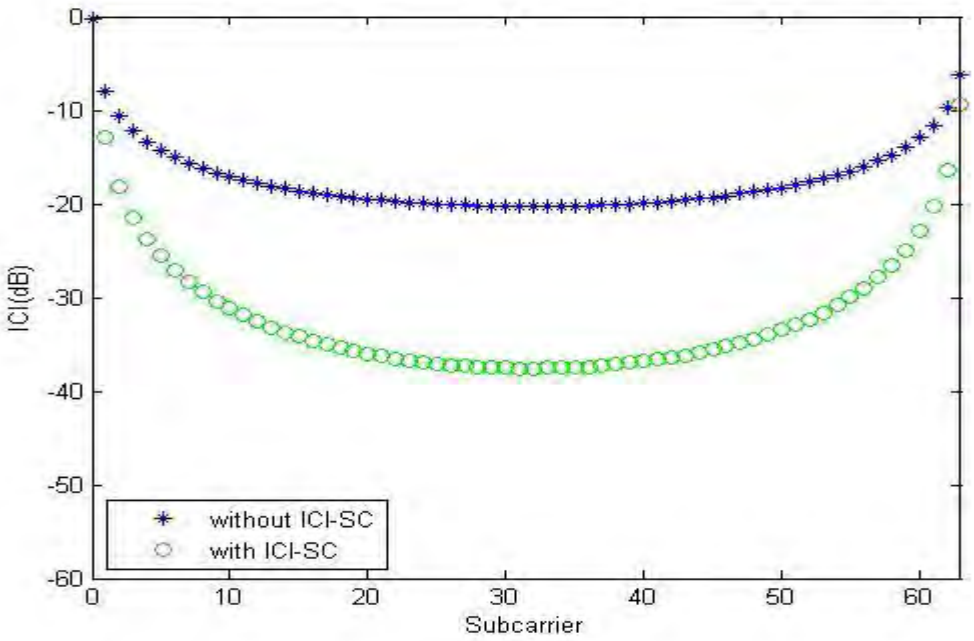

Fig. 4.4: Plots of ICI without SC and with SC in 2x2 MIMO-OFDM using DC

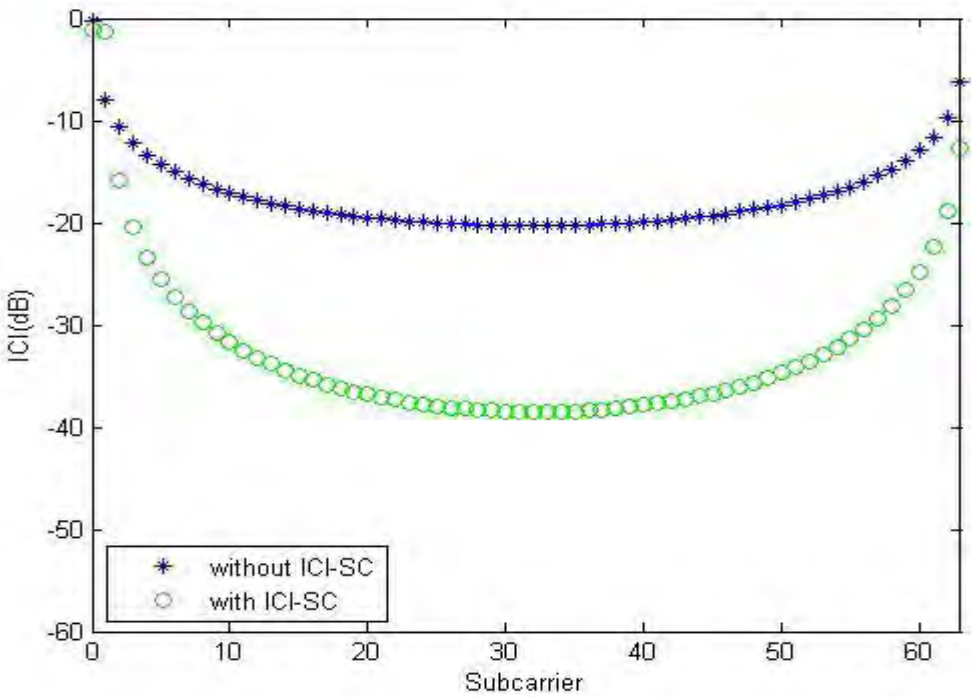

Fig. 4.5: Plots of ICI without SC and with SC in 2x2 MIMO-OFDM using SFBC

From Fig. 4.2 to Fig. 4.5, depict a comparison among SCDC-OFDM, 2x2 MIMO-OFDM (without SCDC and with SCDC) and SFBC. Here, we have assumed the number of subcarriers, N= 64, normalized frequency offset, ε = 0.2 and phase noise variance, σ_{ϕ}^{2} = 0.2 rad^2. It is found that ICI crosstalk is much smaller in SC than

without SC among four methods. It is also seen that ICI decreases at a certain range of subcarrier and then increases with the increasing number of subcarriers. For example, N = 45, the value of ICI for SCDC-OFDM is approximately -59.23dB, which is the lowest ICI crosstalk among the 4-different methods and then it increases again. At N = 33, the values of ICI for 2x2 MIMO-OFDM without SCDC, with SCDC and SFBC are approximately -36.75dB, -37.55dB and -38.55dB respectively. Thus, the ICI effects become smaller with ICI cancelling modulation and demodulation.

4.3 Effect of Frequency Offset/Phase Noise on ICI

The frequency offset and phase noises are important variables in the communication system. At higher values of normalized frequency offset and phase noise variance ICI performance degrades significantly. Equations (3.11), (3.26) and (3.52) are used here to evaluate the effect of ICI in communication system. When the normalized frequency offset is varying, the phase noise variance is constant. At the constant value of normalized frequency offset, the phase noise variance is varying. It is noted that to observe the effect of frequency offset on ICI, we have assumed constant phase noise.

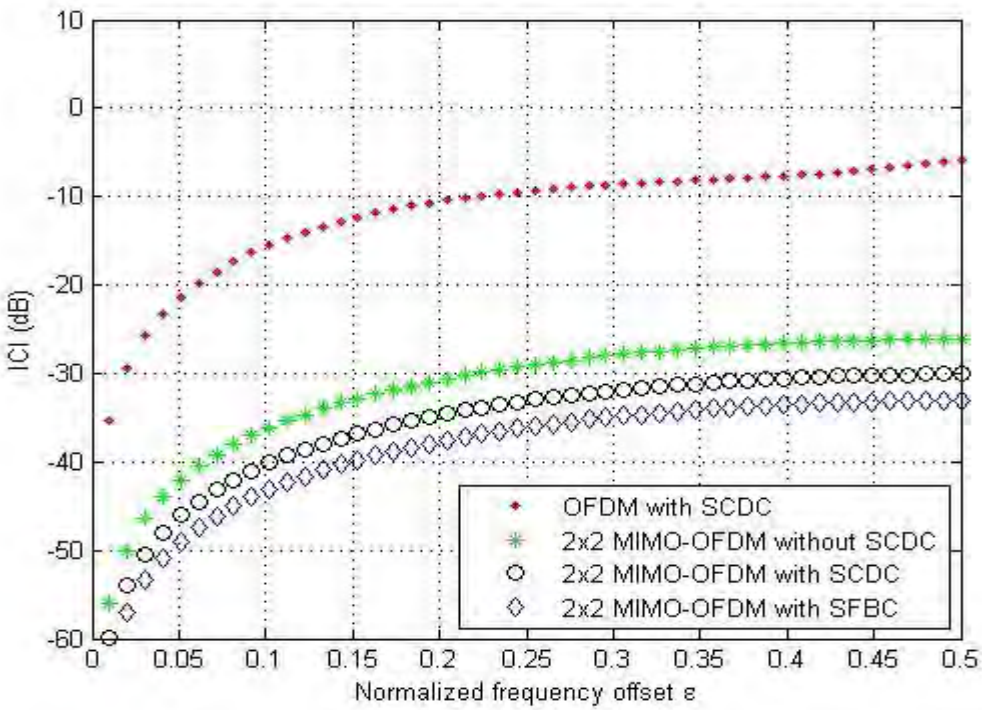

Fig. 4.6: Plots of ICI vs. normalized frequency offset

Fig. 4.6 shows an illustration the effect of normalized frequency offset on ICI. From the Fig. 4.6, it is found that SFBC in 2x2 MIMO-OFDM has lower ICI (dB) than other methods. For ε = 0.25, SFBC and SCDC in 2x2 MIMO-OFDM have the value of ICI approximately -35.97dB and -32.97dB respectively.

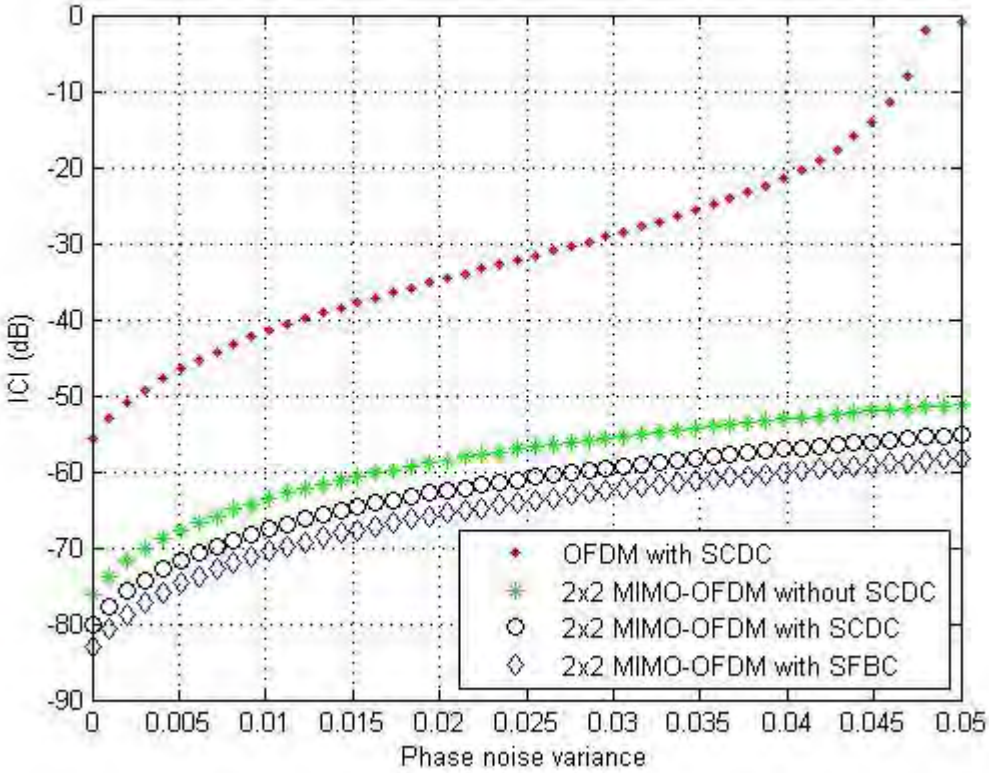

Fig. 4.7: Plots of ICI vs. phase noise variance

Fig. 4.7 shows the effect of phase noise on ICI and also comparison among four different methods. It is found that SFBC scheme has lower ICI effect significantly. The ICI of SFBC can be reduced by 2 - 26dB for $0 < \varepsilon < 0.5$.

4.4 Effect of Frequency Offset/Phase Noise on CIR

The effects of normalized frequency offset on CIR are plotted in Fig. 4.8 using equations (3.12), (3.27) and (3.54). It is observed that 2x2 MIMO-OFDM with SFBC has better performance than OFDM with SCDC, 2x2 MIMO-OFDM (without and with SCDC) and 2x1 MISO-OFDM systems. For example, at ε = 0.25, SFBC and SCDC in 2x2 MIMO-OFDM value of CIR approximately are 39.11 dB and 34.86 dB. Whereas 2x1 MISO-OFDM has the least CIR about of 5dB.

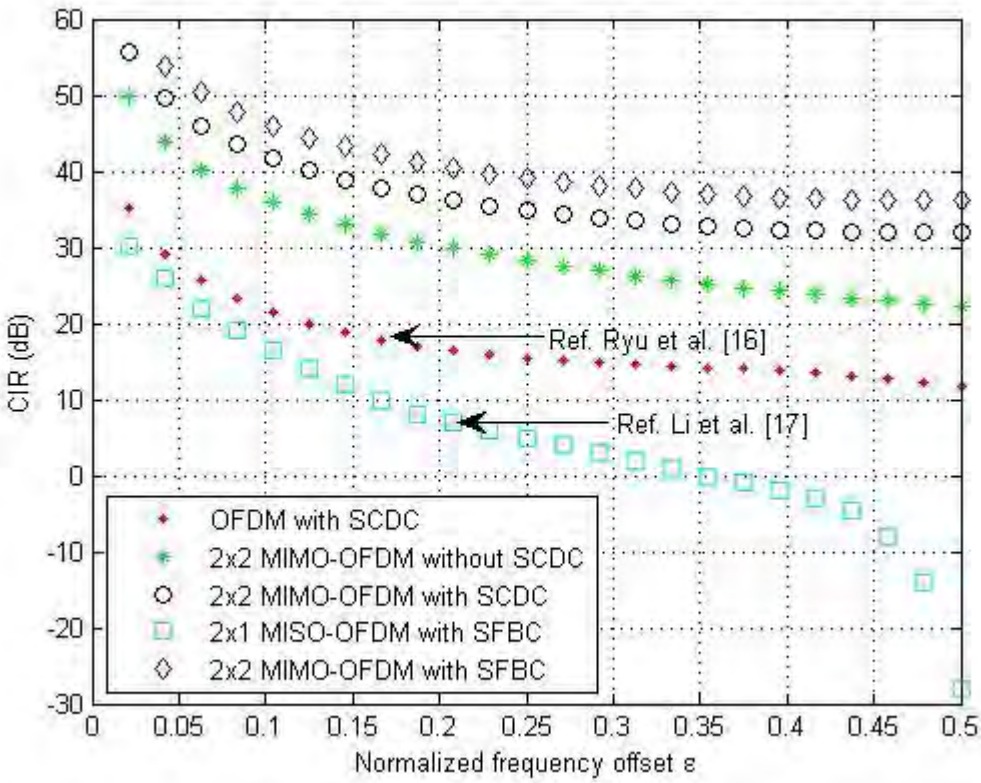

Fig. 4.8: Plots of CIR vs. normalized frequency offset

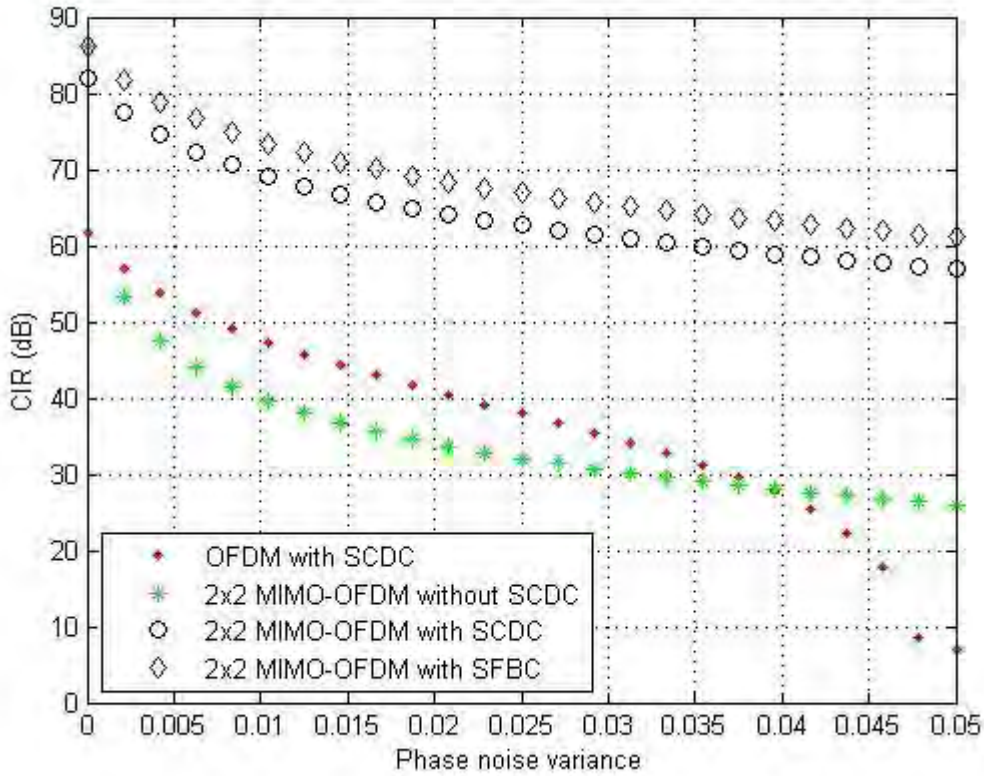

Fig. 4.9: Plots of CIR vs. phase noise variance

The effect of phase noise variance on CIR is shown in Fig. 4.9 using equations (3.12), (3.27) and (3.54). It is seen that 2x2 MIMO-OFDM with SCDC and SFBC show better performance than SCDC-OFDM. Again, SCDC-OFDM has better CIR when $\sigma_\phi^2 \leq 0.037\,\text{rad}^2$ than 2x2 MIMO without SCDC. But, for $\sigma_\phi^2 \geq 0.037\,\text{rad}^2$, 2x2 MIMO-OFDM without SCDC performs better. For instance, σ_ϕ^2 = 0.025 rad^2, the values of CIR are about 66.75dB and 62.50dB in SFBC and SCDC in 2x2 MIMO-OFDM respectively. Especially for small phase noise variance in the range from 0 - 0.05, the CIR improvement can be greater than 2 - 35dB.

4.5 BER Performance of BPSK MIMO-OFDM System

Binary phase shift keying (BPSK) and quadrature phase shift keying (QPSK) modulation schemes are chosen for subchannel modulation as they are used many standards. In BPSK, the symbol size is 1, that's why it is easy to detection. Larger symbol sizes are more sensitive to ICI.

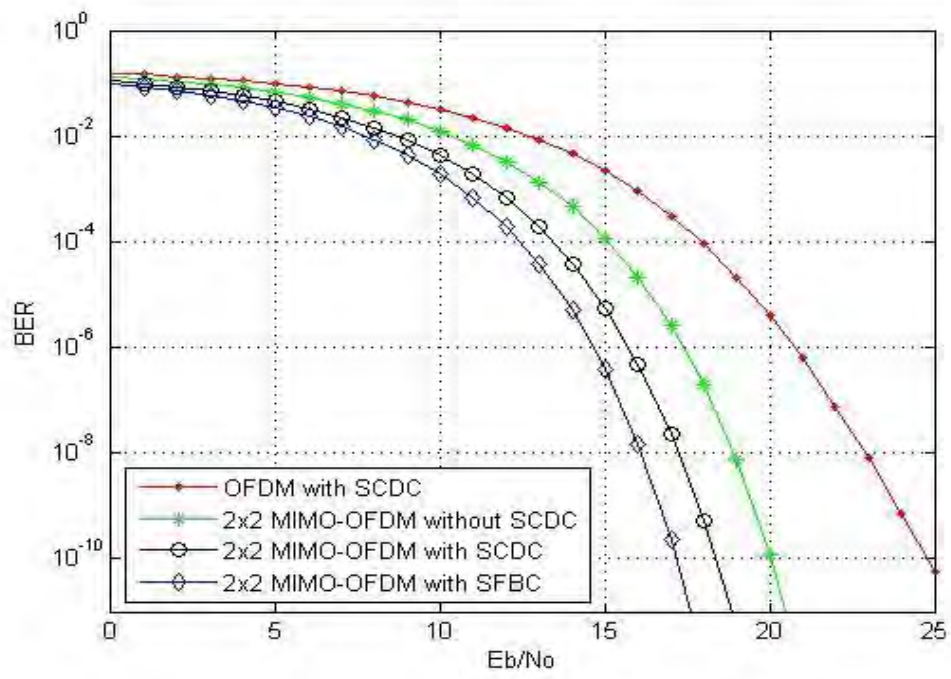

Fig. 4.10: Plots of bit error rate vs. E_b/N_0 at ε = 0.1

Here, Fig. 4.10 shows BER performance of BPSK for normalized frequency offset with ε = 0.1 and phase noise variance with σ_ϕ^2 = 0.02 rad^2. From the Fig. 4.10, it is found that 2x2 MIMO-OFDM with SFBC results lower BER than other methods. For

example, at E_b/N_0 = 15dB, the values of BER for SCDC-OFDM and 2x2 MIMO-OFDM with SFBC are approximately 2.169×10^{-3} and 3.866×10^{-7} respectively.

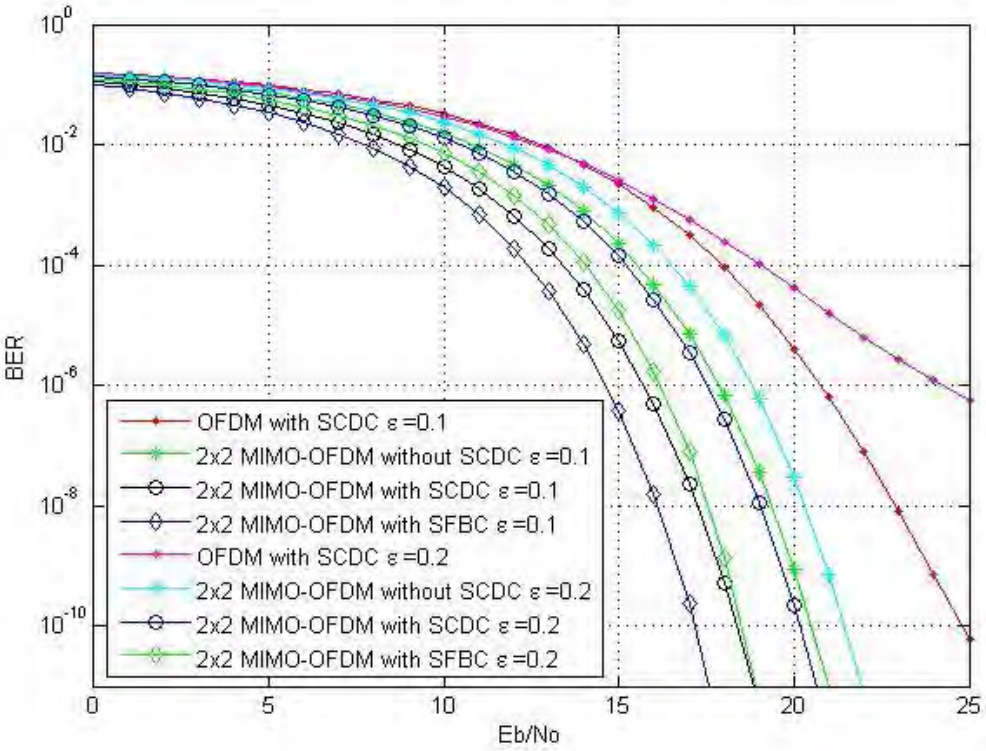

Fig. 4.11: Plots of bit error rate vs. E_b/N_0 at ε = 0.1 or 0.2

Fig. 4.11 shows the comparison among four different techniques for various values of normalized frequency offset for BPSK. From the Fig. 4.11, we observe that as the value of normalized frequency offset ε increases, the BER increases. It is also noticed that SFBC has less BER compared to other methods. For normalized frequency offset 0.2, the values of BER for SCDC-OFDM and 2x2 MIMO-OFDM with SFBC are approximately 2.52×10^{-3} and 1.78×10^{-5} respectively at E_b/N_0 = 15dB.

Table 4.1: BER of different normalized frequency offset for E_b/N_0 = 15dB

Normalized frequency offset	ε = 0.1	ε = 0.2
OFDM-SCDC	2.169×10^{-3}	2.252×10^{-3}
2x2 MIMO-OFDM	0.116×10^{-3}	7.304×10^{-4}
2x2 MIMO-OFDM-SCDC	5.530×10^{-6}	1.401×10^{-4}
2x2 MIMO-OFDM-SFBC	3.866×10^{-7}	1.782×10^{-5}

4.6 BER Performance of QPSK MIMO-OFDM System

In order to compare the six different schemes using equations (3.16), (3.30) and (3.58), BER curves are plotted for QPSK modulation. It is seen that BER performance in QPSK degradation more quickly than BPSK. For example, at E_b/N_0 = 15dB, the values of BER for 2x2 MIMO-OFDM with SC, 2x2 MIMO-OFDM with SCDC, 2x1 MISO-OFDM with SFBC and 2x2 MIMO-OFDM with SFBC are approximately 5.7×10^{-4}, 2.279×10^{-5}, 9.465×10^{-6} and 2.329×10^{-6} respectively.

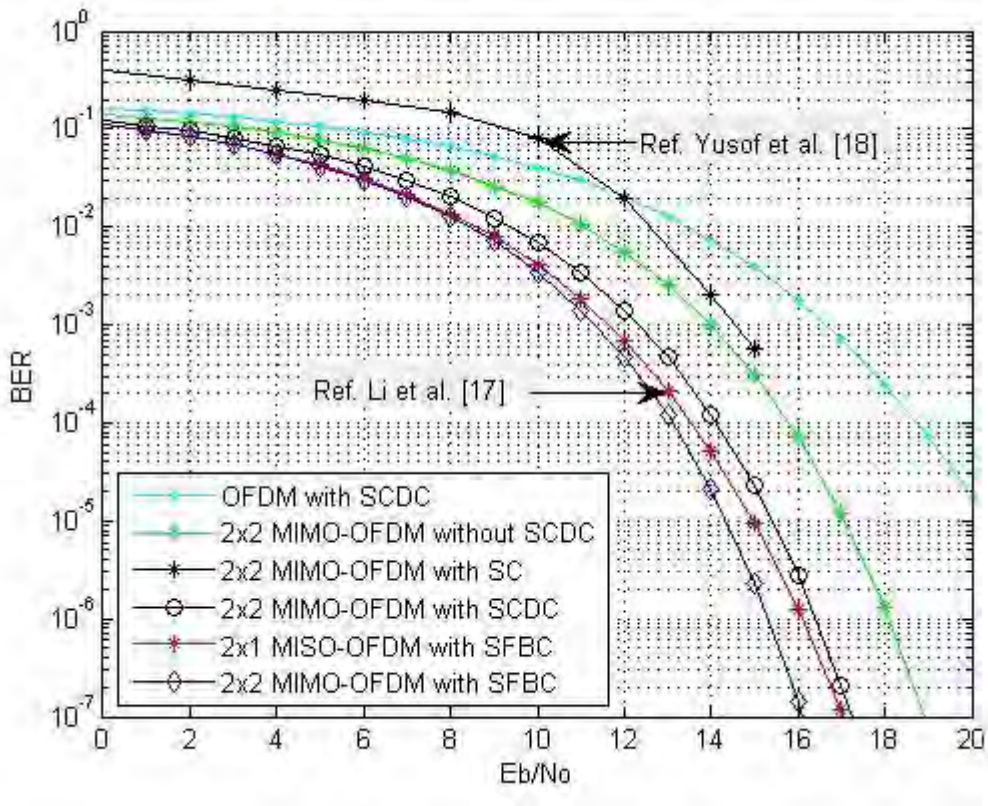

Fig. 4.12: Plots of bit error rate vs. E_b/N_0 at $\varepsilon = 0.1$

Fig. 4.13 compares the performance BER of QPSK with different normalized frequency offset. As normalized frequency offset increases BER increases dramatically. These results show that degradation of performance increases with normalized frequency offset. In normalized frequency offset 0.2, the values of BER for SCDC and SFBC in 2x2 MIMO-OFDM with are approximately 3.65×10^{-4} and 6.209×10^{-5} respectively at same E_b/N_0.

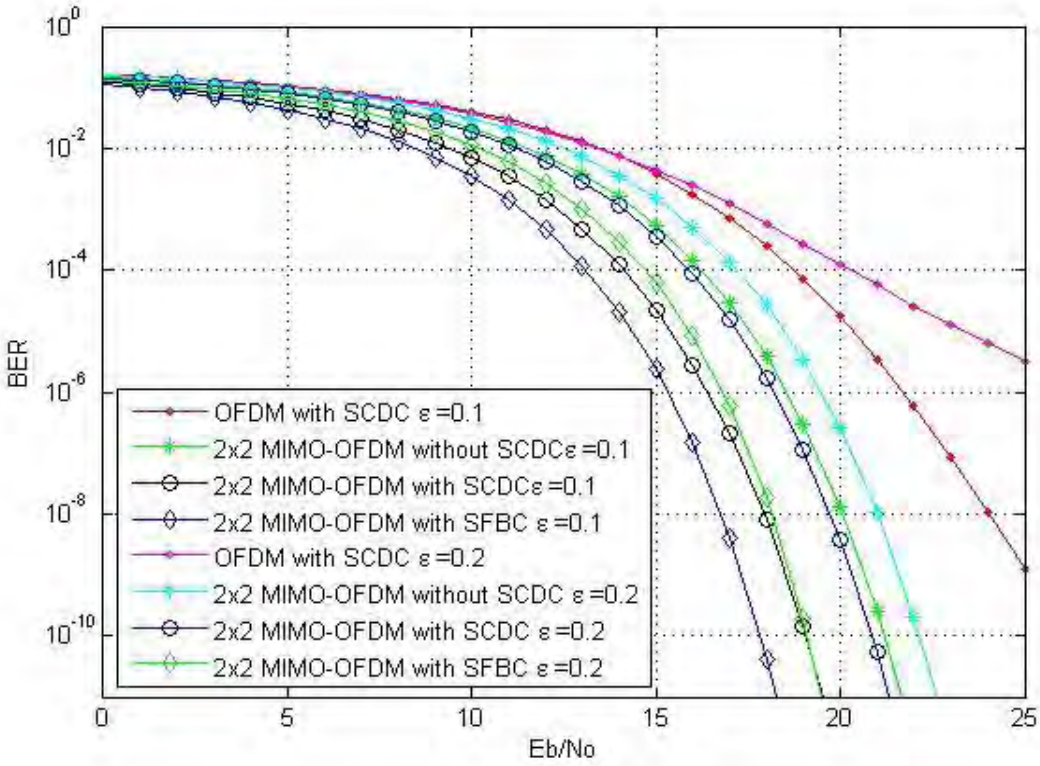

Fig. 4.13: Plots of bit error rate vs. E_b/N_0 at ε = 0.1 or 0.2

4.7 Comparison of BER Performance of QPSK, BPSK MIMO-OFDM System

A comparison between BPSK and QPSK modulation is shown in Fig 4.14 at ε = 0.1. For constant ε value, BER of BPSK is less than that of QPSK. It can be seen that QPSK results in high BER degradation than BPSK. At E_b/N_0 = 15 dB, the BER of BPSK is 3.866×10^{-7} and that of QPSK is 2.329×10^{-6} respectively in 2x2 MIMO-OFDM with SFBC.

Table 4.2: BER of BPSK and QPSK at ε = 0.1 for E_b/N_0 = 15dB

Schemes	BPSK	QPSK
OFDM-SCDC	2.169×10^{-3}	3.869×10^{-3}
2x2 MIMO-OFDM	0.116×10^{-3}	0.312×10^{-3}
2x2 MIMO-OFDM-SCDC	5.530×10^{-6}	2.270×10^{-5}
2x2 MIMO-OFDM-SFBC	3.866×10^{-7}	2.329×10^{-6}

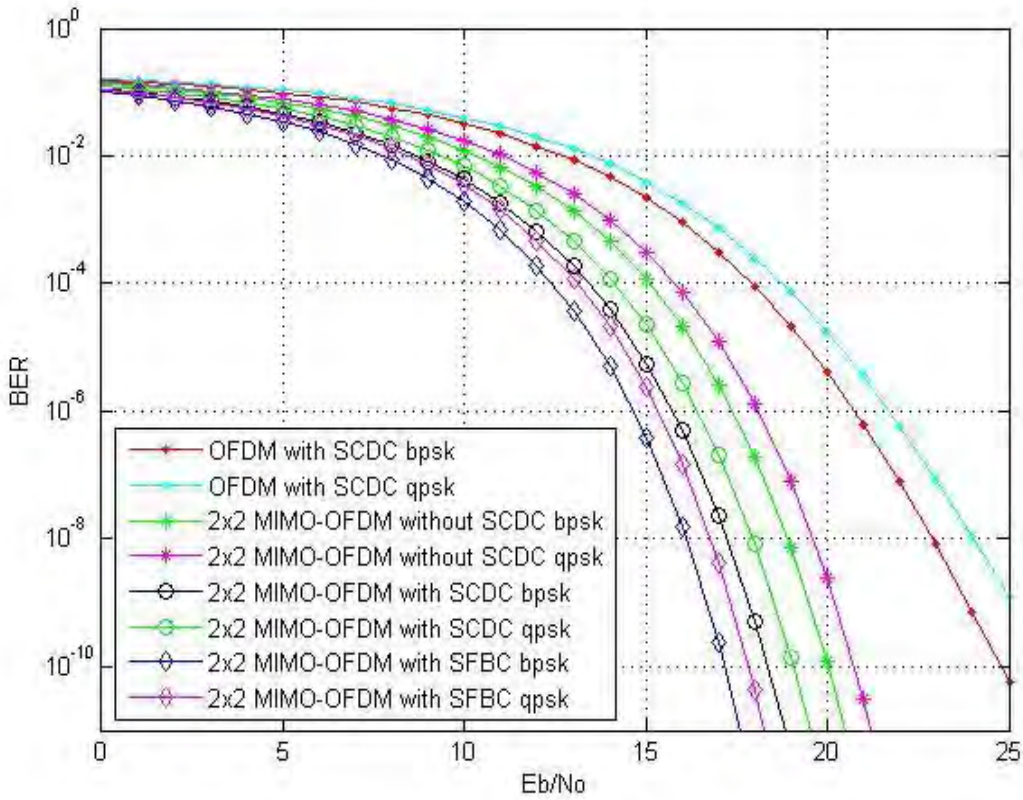

Fig. 4.14: Plots of bit error rate vs. E_b/N_0 at $\varepsilon = 0.1$

4.8 Effect of Convolution Coding on MIMO-OFDM System

The effect of convolution coding (CC) on performance is depicted in Fig 4.15 on different system. It is found that coded system has shown better performance than uncoded system. As seen from Fig. 4.15, the graph of BER vs E_b/N_0 for coded BPSK modulated AWGN channel. The curve for the uncoded BER is worse than the coded one because at the E_b/N_0 of 15 dB, its BER is very high giving a value of 5.53×10^{-6} while that of coded channel is 4.96×10^{-10} in 2x2 MIMO-OFDM with SCDC. This shows a very significant improvement coding on the channel.

From the Fig. 4.16, it is shown that QPSK results in high BER degradation than BPSK modulation. For QPSK modulation, the values of BER for convolution coding and without coding are approximately 7.833×10^{-9} and 2.279×10^{-5} respectively in 2x2 MIMO-OFDM with SCDC at $E_b/N_0 = 15$dB. Convolution coding

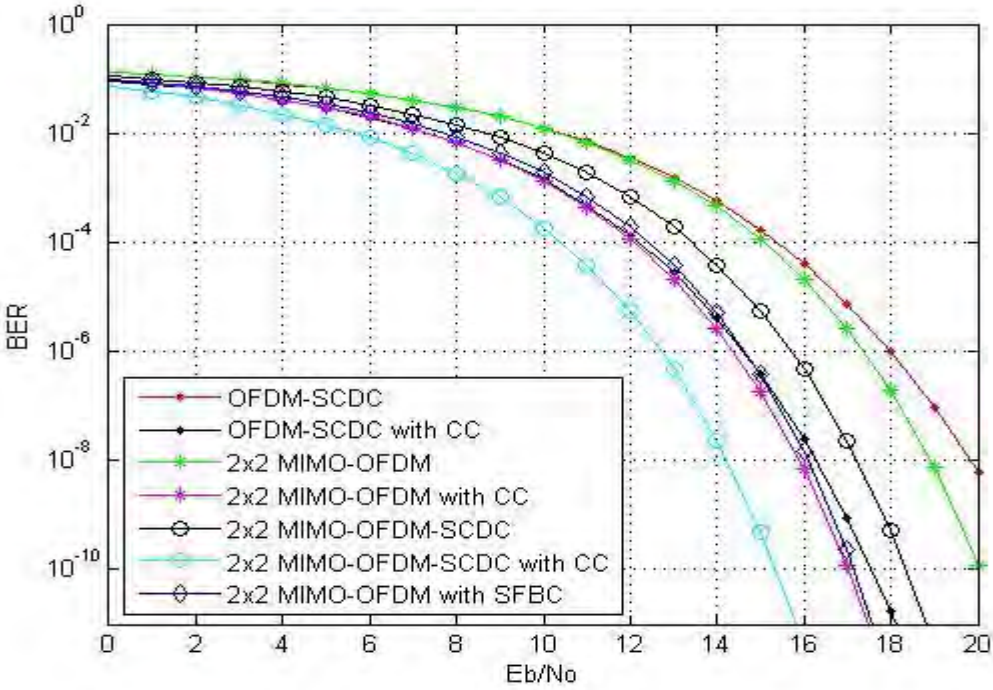

Fig. 4.15: Plots of bit error rate vs. E_b/N_0 at ε = 0.1 using BPSK

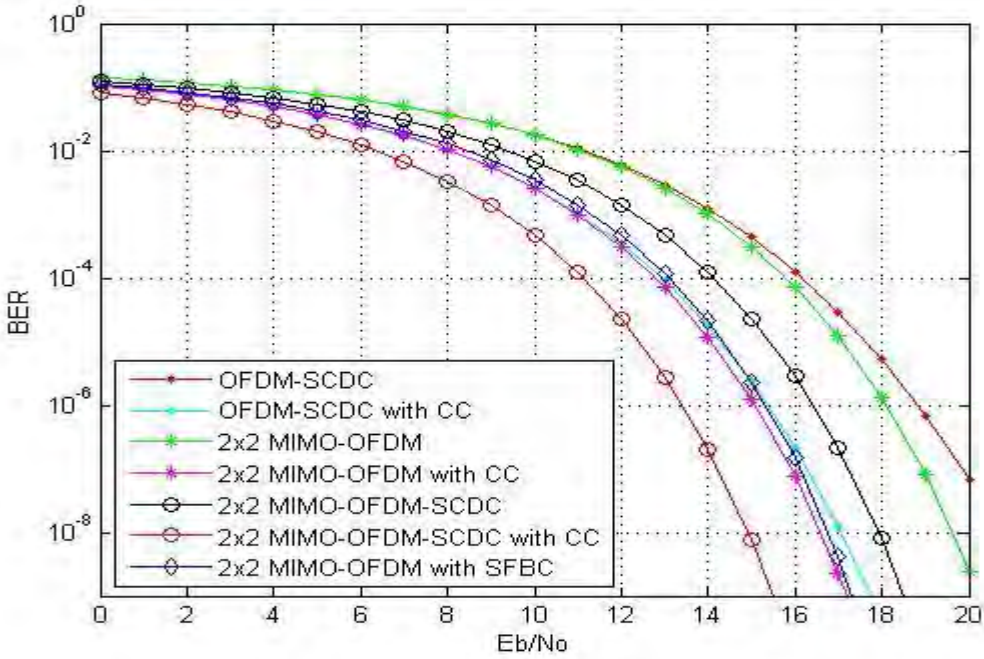

Fig. 4.16: Plots of bit error rate vs. E_b/N_0 at ε = 0.1 using QPSK

in SCDC-OFDM is better when $E_b / N_0 \leq 15$ dB. But $E_b / N_0 \geq 15$ dB, SFBC has better performance. As seen from Fig. 4.17, the values of BER for 2x2 MIMO-OFDM with SC, 2x1 MISO-OFDM with SFBC, 2x2 MIMO-OFDM with SFBC and 2x2 MIMO-OFDM-SCDC with CC are approximately 5.7×10^{-4}, 9.465×10^{-6}, 2.329×10^{-6}

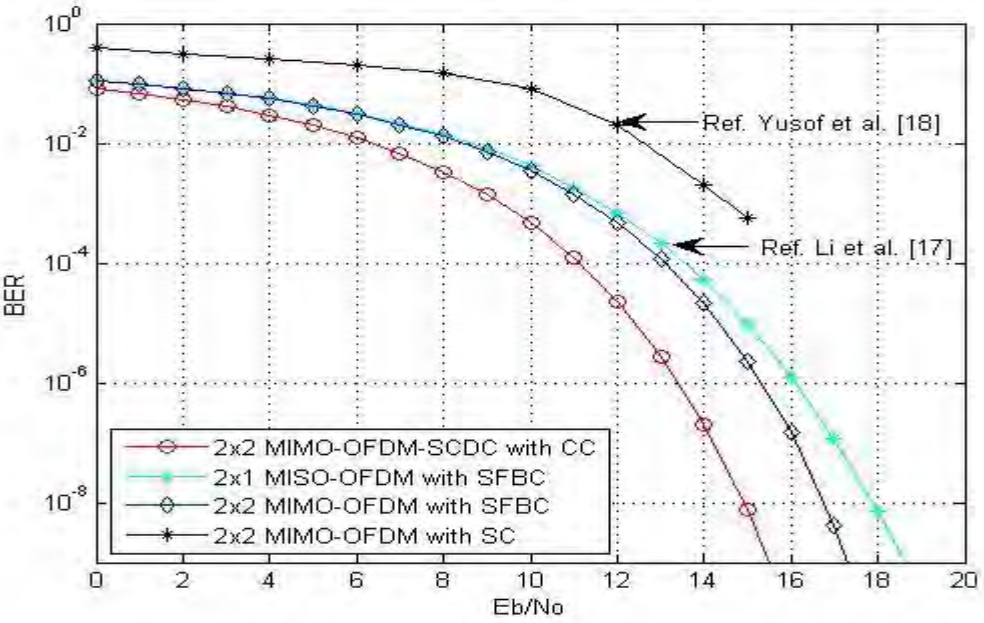

Fig. 4.17: Plots of bit error rate vs. E_b/N_0 at $\varepsilon = 0.1$

and 7.833×10^{-9} respectively at E_b/N_0 = 15dB. It is established that BER depends on the modulation type. It is found that coding leads to a substantial improvement in terms of BER.

4.9 Comparison of CIR and E_b/N_0 with Published Results

From the Fig. 4.8, 4.12 and 4.17, it is found that CIR and E_b/N_0 are improved using SCDC with CC and SFBC in 2x2 MIMO-OFDM system. A relative comparison is established with the published result and shown in Table 4.3.

Table 4.3: Comparison of CIR and E_b/N_0 with published results

Methods	CIR (dB) at $\varepsilon = 0.25$	E_b/N_0 (dB) at BER$=5.7\times10^{-4}$	Authors/ Ref.
2x2 MIMO-OFDM with SC	Not applicable	15	Yusof *et al.* [18]
2x1 MISO-OFDM with SFBC	5	12.2	Li *et al.* [17]
2x2 MIMO-OFDM with SFBC	39.11	11.8	Our work
2x2 MIMO-OFDM with SCDC	34.86	12.8	Our work
2x2 MIMO-OFDM-SCDC with CC	Not applicable	9.8	Our work

CHAPTER 5

CONCLUSION AND FUTURE WORK

5.1 Conclusion

A detailed theoretical analysis is carried out to evaluate the detrimental effects of phase noise and frequency offset on ICI and its reduction scheme in 2x2 MIMO-OFDM systems using SCDC with convolution coding (CC) and SFBC. In this thesis, at first we have derived an analytical model to reduce the ICI effect using SCDC with CC and SFBC scheme combining the effects of phase noise and frequency offset. Analytical expressions of CPE, ICI, CIR and BER are derived for both cases following the developed model. The salient features of our work are summarized below:

i) In the case of normalized frequency offset, SFBC method has significantly lower ICI compared with OFDM-SCDC, without SCDC and with SCDC in 2x2 MIMO-OFDM. The ICI of SFBC in 2x2 MIMO-OFDM can be reduced by 2 - 26 dB for $0 < \varepsilon < 0.5$. In the phase noise variance aspect, ICI gives almost similar result.

ii) In terms of phase noise variance, SFBC in 2x2 MIMO-OFDM has better CIR than other scheme. It is also worth to mention that OFDM with SCDC is better when phase noise variance is less than 0.037 rad^2. But above the 0.037 rad^2, MIMO-OFDM without SCDC gives better. Especially for small phase noise variance in the range from 0 to 0.05, the CIR of SFBC improvement can be greater than 2 - 35 dB. In the normalized frequency offset characteristic, SFBC in 2x2 MIMO-OFDM has performed better result.

iii) As the value of normalized frequency offset (ε) increases, the BER also increases and thus degradation of performance increases with normalized frequency offset. For instance, in the BPSK modulation, the values of BER for 2x2 MIMO-OFDM with SFBC are approximately 3.866×10^{-7} at $\varepsilon = 0.1$ and 1.782×10^{-5} at $\varepsilon = 0.2$ respectively at $E_b/N_0 = 15$dB.

iv) The comparison between two modulation techniques (BPSK and QPSK) are same normalized frequency offset. For constant ε value, BER of BPSK is less than BER of QPSK. It is found that QPSK results in high BER degradation than BPSK. For example, BPSK modulation of normalized frequency offset 0.2, the values of BER for SCDC-OFDM and 2x2 MIMO-OFDM with SFBC are approximately 2.52×10^{-3} and 1.78×10^{-5} respectively at E_b/N_0 = 15dB. The BER performance of QPSK with normalized frequency offset 0.2; the values of BER for SCDC-OFDM and 2x2 MIMO-OFDM with SFBC are approximately 4.405×10^{-3} and 6.209×10^{-5} respectively at same E_b/N_0.

v) Finally, Convolution coding is introduced in the system to improve the performance and it showed better performance than uncoded signal. For instance, the values of E_b/N_0 for 2x1 MISO-OFDM with SFBC, 2x2 MIMO-OFDM with SFBC and 2x2 MIMO-OFDM-SCDC with CC are approximately 12.2dB, 11.8dB and 9.8dB respectively at BER=5.7×10^{-4}.

5.2 Future Work

The MIMO-OFDM system is a promising technique in high data rate wireless communication. In this thesis, two techniques for ICI cancellation have been proposed to improve the system performance. There are still many issues for MIMO-OFDM systems that need to be investigated and some of them are discussed as below:

- We have analyzed the performance of frequency offset and phase noise in flat fading channel. This SCDC and SFBC in 2x2 MIMO-OFDM technique can also be applied under frequency selective Rayleigh and Rician fading channel.

- The pulse shaping, maximum likelihood (ML) and extended kalman filtering (EKF) method can also be designed for flat fading and frequency selective fading channel.

- Reed Solomon code, Turbo code, Walsh code and Gold code can be used in proposed system.

- The SFBC scheme can be extended to double polarized SFBC (DP-SFBC).

- Optimum combination of error correction code can be investigated with STBC and SFBC or Quasi Orthogonal Space Time Block Codes (QSTBC) in MIMO-OFDM systems.

APPENDIX A

DERIVATION OF ICI COEFFICIENT

$$Q_L^{\tau} = \frac{1}{N}\sum_{n=0}^{N-1} e^{j[(\frac{2\pi}{N})(L+\varepsilon^{\tau})n+\varphi^{\tau}(n)]}$$

$$= \frac{1}{N}.\frac{1-\exp\{j2\pi(L+\varepsilon^{\tau})+\varphi^{\tau}\}}{1-\exp[\{j2\pi(L+\varepsilon^{\tau})+\varphi^{\tau}\}/N]}$$

$$= \frac{1}{N}.\frac{\exp[\{j2\pi(L+\varepsilon^{\tau})+\varphi^{\tau}\}/2].\exp[\{-j2\pi(L+\varepsilon^{\tau})+\varphi^{\tau}\}/2]-\exp\{j2\pi(L+\varepsilon^{\tau})+\varphi^{\tau}\}}{\exp[\{j2\pi(L+\varepsilon^{\tau})+\varphi^{\tau}\}/2N]\exp[-\{j2\pi(L+\varepsilon^{\tau})+\varphi^{\tau}\}/2N]-\exp[\{j2\pi(L+\varepsilon^{\tau})+\varphi^{\tau}\}/N]}$$

$$= \frac{1}{N}.\frac{\exp[\{j2\pi(L+\varepsilon^{\tau})+\varphi^{\tau}\}/2].\{\exp[\{-j2\pi(L+\varepsilon^{\tau})+\varphi^{\tau}\}/2]-\exp[\{j2\pi(L+\varepsilon^{\tau})+\varphi^{\tau}\}/2]\}}{\exp[\{j2\pi(L+\varepsilon^{\tau})+\varphi^{\tau}\}/2N].\{\exp[-\{j2\pi(L+\varepsilon^{\tau})+\varphi^{\tau}\}/2N]-\exp[\{j2\pi(L+\varepsilon^{\tau})+\varphi^{\tau}\}/2N]\}}$$

$$= \frac{1}{N}.\frac{\exp[\{j2\pi(L+\varepsilon^{\tau})+\varphi^{\tau}\}/2].\sin\{2\pi(L+\varepsilon^{\tau})+\varphi^{\tau}\}/2]}{\exp[\{j2\pi(L+\varepsilon^{\tau})+\varphi^{\tau}\}/2N]\sin[\{2\pi(L+\varepsilon^{\tau})+\varphi^{\tau}\}/2N]}$$

$$= \frac{1}{N}.\exp[\{j2\pi(L+\varepsilon^{\tau})+\varphi^{\tau}\}(1/2-1/2N)]\frac{\sin\{2\pi(L+\varepsilon^{\tau})+\varphi^{\tau}\}/2]}{\sin[\{j2\pi(L+\varepsilon^{\tau})+\varphi^{\tau}\}/2N]}$$

$$= \exp[\{j2\pi(L+\varepsilon^{\tau})+\varphi^{\tau}\}(1/2-1/2N)]\frac{\sin\{2\pi(L+\varepsilon^{\tau})+\varphi^{\tau}\}/2]}{N.\sin[\{2\pi(L+\varepsilon^{\tau})+\varphi^{\tau}\}/2N]}$$

Using formula:

$$S = \sum_{n=0}^{N-1} a^n$$

$$= a^o + a^1 + a^2 + a^3 + a^4 + ...$$

$$= 1 + a^1 + a^2 + a^3 + a^4 + ...$$

$$a > 1, ...S = \frac{a^N - 1}{a - 1}$$

$$a < 1, ...S = \frac{1-a^N}{1-a}$$